UNIVERSITY OF CALGARY

Architecture of the Asthmatic Lung

by

Stacey Boser

A THESIS

SUBMITTED TO THE FACULTY OF GRADUATE STUDIES

IN PARTIAL FULFILLMENT OF THE REQUIREMENTS FOR THE

DEGREE OF MASTER OF SCIENCE

DEPARTMENT OF CARDIOVASCULAR/RESPIRATORY SCIENCES

CALGARY, ALBERTA

OCTOBER, 1999

Abstract

The purpose of this study was to determine whether airway wall remodelling was best described by euclidean or fractal geometry, and if asthma involved small airways and parenchyma. The study population consisted of three groups: fatal asthma (FA), non-fatal asthma (NFA) and non-asthma control (NAC).

Airway dimensions were determined on silicone casts and a fractal dimension (D) from digital images using a box counting method. A point counting technique determined the proportion of smooth muscle in small airways and parenchyma on tissue sections.

Average lengths and diameters of airways were not significantly altered in asthma. By contrast, FA had a significantly lower D (1.61) compared to NAC (1.78) ($p < 0.05$). Morphometric studies revealed greater amounts of smooth muscle in small airways and parenchyma of asthmatics compared with NAC.

We conclude that airway remodelling is better described in fractal than euclidean terms and asthma involves the smallest airways and parenchyma.

Acknowledgements

I would like to acknowledge my supervisor, Dr. Francis Green, as well as my committee members, Dr. Ian Mitchell, Dr. Gordon Ford and Dr. Sam Schurch for all of their help and guidance.

This work was supported in part by the Herron Study of Childhood Asthma (Alberta Children's Hospital and University of Calgary) and the Alberta Lung Association.

Dedications

I would like to dedicate this thesis to Harvey Hawes and to my mother and father, Dianne and Ed Boser, for always being there when I needed them (and to Sheba).

Table of Contents

List of Tables

List of Figures

List of Abbreviations

A – Alveoli
AD – Alveolar Duct
bmi – Basement Membrane Intersections
BR – Branching Ratio (length or diameter of generation n+1 / generation n)
CV – Coefficient of Variation
D – Fractal Dimension
D1 – Fractal Dimension of one side of a cast
D2 – Fractal Dimension of the other side of a cast
F – Female
FA – Fatal Asthma
L – Length
LAB – Lower Anterior Bronchus
LLAB – Left Lower Anterior Bronchus
LLPB – Left Lower Posterior Bronchus
LPB – Lower Posterior Bronchus
LUAB – Left Upper Anterior Bronchus
M – Male
mgd – Mucous Gland Duct
NAC – Non-Asthma Control
NFA – Non-Fatal Asthma
PAR – Parenchyma
PPAS – Prairie Provinces Asthma Study
RB1 – Respiratory Bronchiole generation 1
RB2 – Respiratory Bronchiole generation 2
RB3 – Respiratory Bronchiole generation 3
TB – Terminal Bronchiole
UAB – Upper Anterior Bronchus
Z – Magnification Factor (the distance between two points on a grid)

Chapter 1: Introduction

Asthma is a disease involving narrowing of the airways in response to a wide variety of stimuli that have little or no effect on the normal lung. It is increasing in prevalence worldwide with the majority occurring in children and adolescents (Woolcock et.al, 1997; von Mutius, 1998). Moreover, the severity of the disease appears to be worsened as hospitalization and morbidity have also increased in the last decades (von Mutius et.al, 1998). These increases may be due to a greater incidence of asthma diagnosis by the medical profession and / or environmental factors resulting from new technology and lifestyle changes. Risk factors for fatal asthma in the Prairie Provinces include a history of severe or life threatening attacks requiring systemic corticosteroids, previous hospital admissions, failure to seek medical care and complications associated with the over reliance or under use of medications (Tough et.al, 1996). In addition, risk of death was also asscciated with gender, season, employment and region (Tough et.al, 1996).

One of the cardinal features of asthma is reversible airflow obstruction. Yet increased severity or chronicity leads to an irreversible component (Brown et.al., 1984). Abnormalities observed in both autopsy and bronchial biopsy that may contribute to the fixed obstruction include basement membrane thickening (Unger, 1945; Bullen, 1952; Houston et.al, 1953; Messer et.al, 1960; Roche et.al, 1989; Dunnill, 1960; Salvato, 1968; Cutz et.al, 1978; Jeffery et.al, 1989), inflammation and oedema of the wall (Dunnill, 1960; Cutz et.al, 1978; Carroll

et.al, 1997), enlargement of the mucous glands (Takizawa et.al, 1971, Dunnill et.al, 1969; Glynn et.al, 1960), smooth muscle hypertrophy and/or hyperplasia in both large (Heard et.al, 1972; Hossain, 1973; Cutz et.al, 1978; Carroll et.al, 1993; James et.al, 1989; Takizawa et.al, 1971; Dunnill et.al, 1969) and small airways (Saetta et.al, 1991, Carroll et.al, 1993) and hypertrophy of the airway mucosal longitudinal elastic bundles (Carroll et.al, in press). These pathologic changes are associated with thickening of the airway wall (James et.al, 1989, Carroll et.al, 1993). This has functional implications due to uncoupling of the distending forces of parenchymal recoil from the narrowing forces on the airway (Moreno et.al, 1986). In addition, the same or even less smooth muscle shortening results in increased airway narrowing (Moreno et.al, 1986).

Lung casting and morphometry have previously been used to measure changes in the airways. Our lab is in a unique position to use both of these techniques as excellent pathologic specimens are available from the Prairie Provinces Asthma Study (PPAS).

Measures of changes in the architecture of the airways in asthma are important for modeling particle deposition in diseased airways. Moreover, knowing the specific sites of disease will facilitate the development of new inhalant devices for asthma therapy, capable of targeting diseased lung and minimizing drug dose.

This study will begin with an introduction to lung casting and its uses, followed by a detailed study utilizing these lung casts involving measuring

lengths, diameters and fractal dimensions in order to better understand branching patterns of the airways. Finally, a histopathological morphometric study of smooth muscle in asthma will be described in which the focus will be on changes in smooth muscle in the smaller airways and lung parenchyma. There is increasing recognition of the physiologic importance of the peripheral lung in asthma (ATS, 1998); however there have been very few morphologic studies of this region. Specifically the anatomy of the respiratory bronchioles, alveolar ducts and alveolar interstitium have not been studied.

Lung Casting

Silicone casts have been employed for studies of the contiguity and dimensions of airways in man and in other mammals (Yeh et.al, 1979; Yeh et.al, 1980; Haefeli-Bleuer et.al, 1988; Horsfield, 1990; Phillips et.al, 1994; Phillips et.al, 1994; Graham et.al, 1995). Positive pressure has frequently been used (Frank et.al, 1966; Phalen et.al, 1973; Wang et.al, 1988; Smith et.al, 1990; Nettum et.al, 1993), which presents danger of distortion of the airways or possibly even rupture, because of the high pressures involved.

Negative-pressure techniques have been employed for silicone-rubber filling of the avian respiratory tract, which includes delicate air sacs as well as non-collapsible pneumatic spaces in the bones (Duncker et.al, 1964; Duncker et.al, 1964). This technique, to our knowledge, has not been applied to mammalian lungs. The advantages of using negative pressure in producing casts of the airways in obstructive disease are numerous. It applies the greatest pressure difference to the distal regions of the bronchial tree, where the resistance to flow is greatest, and therefore should result in good filling of the distal airways at lower applied pressures and should show less tendency to rupture or distort proximal airways.

We have developed a technique using low-viscosity Silastic (734RTV, Dow Corning Inc.), with added silicone oil to lower viscosity even more, to study airways of fixed human lungs, including those with asthma, obtained at autopsy. After polymerization of the silicone, microdissection of four lung casts in situ were

performed. This allowed for airway sections to be taken and then correlated with the surface of the cast, in order to determine how accurately the casts represented the structure of the airways. Our results indicate that silicone casts faithfully reproduce airway contours in obstructive lung disease with minimal distortion or shrinkage, and would therefore be a good technique to use for morphometry of asthmatic airways. Further details of this technique are described in detail in materials and methods.

Euclidean and Fractal Geometry of the Airways in Asthma

Benoit Mandelbrot, a mathematician, was the first to introduce the term fractal (Mandelbrot, 1983; Editorial, 1991), and it means irregular or fragmented. One of the fundamental properties of a fractal structure is self-scaling similarity over a wide range of scales. As a result, small portions of the object are similar in shape to the entire object, with more detail unfolding at higher magnifications. Many objects in nature including trees, cumulous clouds, coastlines and coral formations are fractal. The more conventional method used to measure biological structures is euclidean geometry. Although this method has been useful, it is now thought that many biological structures bear only passing resemblance to euclidean forms, such as cubes, pyramids or spheres. Euclidean geometry is limited to describing dimensions only as integers: 1,2 or 3. Fractal geometry, on the other hand, admits to fractional dimensions and as a result describes structures as having a dimension greater than 1, but less than 2 (Weibel, 1991), which is an indication of its tendency to fill a region of space.

The branching patterns of human airways have already been described in detail utilizing the euclidean model (Weibel et.al, 1962; Weibel, 1963; Horsfield et.al, 1976; Yeh et.al, 1979; Yeh et.al, 1980; Schlesinger et.al, 1981; Horsfield et.al, 1987; Haefeli-Bleuer et.al, 1988; Phillips et.al, 1994; Phillips et.al, 1994). Studies done by Weibel, 1963, on the normal lung found that length and diameter vary considerably, but when they are averaged for each generation, the proportions remain constant. Length-to-diameter ratio is 3.25, and branching

ratios are 0.86 for diameter and 0.62 for length, irrespective of generation (Weibel, 1963). In addition, there was an exponential decay in the mean diameter of the airways in relation to generation. However, it was observed that exponential scaling did not apply beyond generation 10 in the bronchial tubes (Weibel et.al, 1962). If, however, the dichotomous branching of the airways were a fractal structure, there would be no one characteristic scale to describe it, but multiple scales to describe the variability in diameter and length at each generation (Goldberger et.al, 1992). The fractal model takes into consideration this variability that occurs in a structure, whereas the traditional model neglects variation at each generation and uses only average values for tube lengths and diameters (Goldberger et al, 1992).

There are also a number of other advantages to using fractal geometry over other forms of euclidean analysis. The fractal dimension remains constant over a wide range of scales, so the effects of variation in size due to magnification or processing artifacts are minimal and can be discounted (Cross et.al, 1994), whereas the classic measurements of length and diameter are very dependent on scales. Also, the fractal dimension is retained when projected from a three dimensional structure to a two dimensional image, and can consequently be analyzed in this form (Cross et.al, 1994). Any small changes in geometry or organizational variability that may occur as a result of transfer from a three dimensional to a two dimensional structure does not produce significant architectural or functional differences compared with the original object. This is a

result of the object being heterogeneous with variability present at all scales and in all dimensions (Nelson, 1990).

In this study, we measured branching patterns in asthma and controls utilizing both the euclidean and fractal method. The box counting method, used in this study to measure fractal dimension, has been reviewed as a very accurate and reliable technique, with errors less than 1.5% for objects with known fractal dimensions (Cross et.al, 1994). In addition we also determined if these casts were composed of multiple fractal structures. This is due to the fact that at different resolution levels in the lung, there are entirely different structures with different self-similarity patterns, such as alveoli, which are pouches and airways, which are tubes (Weibel, 1991). Our observations demonstrate that fractal geometry may offer a better model of measuring differences in asthmatic airways compared to other methods.

Small Airway Disease in Asthma

The importance of small airways in asthma have perhaps been underestimated due to the difficulty of in vivo sampling and lack of specificity of physiologic measurements (Howarth, 1998). Yet, there is increasing histopathological evidence for inflammation and bronchial smooth muscle hypertrophy within the small airways in asthma (Saetta et.al, 1991; Carroll et.al, 1993; Hamid et.al, 1997). Although the changes in individual components of the airway wall are adequately described in the conducting airways the studies have only measured up to the terminal bronchioles. As a result, very little is known about the changes in the respiratory bronchioles and parenchyma in asthma. Measurements of these changes would give a complete picture of the distribution of histopathological remodeling within the lung.

There is evidence that smooth muscle distribution in asthma is not uniform. Recent studies have shown variability in smooth muscle hypertrophy along an axial pathway, with the presence of two possible populations of asthmatics: a "fatal" phenotype, with a bimodal distribution of smooth muscle increase involving segmental airways and terminal bronchioles; and a "non-fatal" phenotype, with a unimodal distribution primarily involving membranous bronchioles (Green et.al, 1998). Other investigators have also found two groups of asthmatics; one with a unimodal increase of smooth muscle in the central airways, the other showing involvement of both central and small airways (Ebina et.al, 1990).

Functional heterogeneity is also observed. Recent studies using Technegas®, a remarkable substance with properties between those of a gas and an aerosol, have revealed inhomogeneity in gas trapping in asthma (King et.al, in press). In asthmatic patients, Technegas® inhalation revealed wedge-shaped areas of nonventilated lung indicating large airway closure. In contrast, other asthmatic patients showed a nonsegmental or disperse appearance of the Technegas® in the nonventilated lung, indicating small airway closure.

The role of the small airways in asthma was recently reviewed by the American Thoracic Society (ATS 1998). Small airway obstruction is characterized by abnormal ventilation distribution, combined with normal elastic and flow resistive properties, independence of maximal expiratory flow, and gas trapping (Macklem, 1998). Many studies have shown that the peripheral or small airways are a major site of airflow obstruction in asthma (Despas et.al, 1972; Hogg et.al, 1972; King et.al, in press; Wagner et.al, 1990; Yanai et.al, 1992). In mild asthma, the obstruction has little effect on the overall mechanical properties of the lung, but does affect gas distribution. Furthermore, during remission there is still a maldistribution of ventilation (McFadden et.al, 1968).

The question as to why there is excessive closure of small airways in asthma is complex. Three broad mechanisms appear to be involved: constriction of airway smooth muscle (Macklem, 1998); alterations in surface forces (Macklem, 1970); and changes in mechanical properties of the lung parenchyma (Hoppin, 1995). Despite these new developments, the architecture of the

smallest airways, specifically the respiratory bronchioles, have not yet been systematically studied in asthma. Moreover, some very basic questions concerning the uniformity of the disease in the lung have never been addressed due to a lack of suitable case material. In this study we confirm that asthma involves the small membranous (terminal) bronchioles and extend these observations to demonstrate that the disease also affects all three generations of respiratory bronchioles.

Remodelling of Lung Parenchyma in Asthma

It has been shown in humans that Remodelling occurs in the large and small airways (Redington et.al, 1997; Kuwano et.al, 1993; Carroll et.al, 1993; Carroll et.al, 1996). Many of these studies have focused on the effect of smooth muscle hypertrophy and hyperplasia on the functional changes of the airways (Seow et.al, 1998). Recent physiological evidence has indicated that the parenchymal region of the lung also plays an important role in asthma and may contribute to airway dysfunction (Wagner et.al, 1990; Brown et.al, 1997; Hoppin, 1995; Ingram, 1995).

Drug delivery to the peripheral lung has not been studied in detail (Woolcock, 1998). The importance of peripheral airway smooth muscle elements was brought to light by the observation that isoproterenol formulated into small (2.5 μm) particles (which penetrate to the distal lung) relieved airway obstruction to a greater extent than did larger (5.0 μm) particles (Patel et.al, 1990). Peripheral smooth muscle elements consist of smooth muscle in the terminal bronchioles and blood vessels, smooth muscle in the openings of the alveolar ducts and the 'contractile interstitial cell' located in the walls of the alveoli (Kapanci et.al, 1974). These myofibroblasts have no proven function but are thought to play a role in matching ventilation to perfusion (Kapanci et.al, 1974). All of these cells contain smooth muscle actin which is easily demonstrated by immunohistochemistry. In normal dogs and rats, there is a heterogeneous response to histamine-induced constriction which involves parenchymal tissues

(Ludwig et.al, 1991; Ludwig et.al, 1989; Sakae et.al, 1997) as well as peripheral airways. There is thus experimental evidence that normal lung parenchyma can function as a contractile unit.

Despite these new developments, the architecture of the alveolar ducts and alveolar parenchyma have not yet been systematically studied in asthma. In addition, the distribution of smooth muscle in this region of the lung have never been addressed, due to a lack of suitable case material. In this study we show that asthma, in addition to being a disease of the airways, is also a parenchymal disease. Specifically, we demonstrate increased non vascular smooth muscle actin in the alveolar ducts and distal parenchymal tissues.

Chapter 2: Materials and Methods

Study Population

The study population consisted of three groups, which have all had autopsies either through the medical examiner and/or participating hospitals as part of the Prairie Provinces Asthma Study (PPAS). The first group is defined as individuals with Fatal Asthma (FA, n = 6) in that they had asthma and died as a result of it. There were two control groups, a Non-Fatal Asthma (NFA, n = 6) group which included individuals that had a history of asthma but died from other causes and a Non Asthma Control (NAC, n = 6) group who had no history of asthma and died of non-respiratory causes. All individuals were non-smokers. A medical history, including details of asthma history, asthma symptoms and severity, use of asthma medications, smoking, hospitalization due to asthma and basic demographic information were obtained from a questionnaire administered to the next of kin supplemented by medical examiner's notes and pharmacy records. The study had received ethical approval from the University of Calgary Conjoint Ethics Committee and informed consent was obtained from next of kin for pathologic studies of lung tissues.

Lung Pathology

The autopsy included assessment of the pathology grade of asthma severity from 1 to 4, corresponding to absent, mild, moderate and severe based upon histological evaluation of the lung sections. Subjective grading used in this study was a composite based on the overall severity of the changes for smooth

muscle hypertrophy, inflammation (lymphocytic infiltrates and eosinophils), thickening of the lamina reticularis, and mucous gland hyperplasia. Death from asthma was defined as histological evidence of asthma as defined by the above criteria, together with evidence of asphyxia, i.e., mucous plugging, hyperinflation and collapse, and petecheal hemorrhages of the serosal cavities. Other potential causes of death were eliminated with the use of a toxicology report and full autopsies.

Lung Casting

Human lungs were obtained at autopsy from patients with and without a history of cigarette smoking and bronchiectasis. The fresh left lung was inflated through the vasculature and airways with glutaraldehyde fixative (2.5% in 0.1 M phosphate buffer, pH 7.3) at a pressure of 30 cm of H_2O (Figure 1). The main bronchus to a lobe (or segment) was cannulated and repeatedly flushed with degassed saline. Cut airways through which casting material might escape during injection were located and tied off. If it was impossible to tie off an airway (those cut flush with the tissue), then excess tissue was glued over the open airway with tissue-adhesive glue (Vetbond, 3M Animal Care Products, St. Paul, MN).

For some specimens, the pleura was completely or partially removed. For others the pleura was left intact and punctured to allow escape of fluid.

For injection of a segmental bronchus, 50-100 ml of silicone elastomer was required. Dow Corning self-leveling 734 RTV (room temperature vulcanizing) industrial-grade sealant was used and made less viscous by the addition of 10% by volume silicone oil (polydimethylsiloxane, Dow Corning "200 fluid" of 20 cs viscosity).

A bubble-free mixture was obtained by introducing the components into an evacuated collapsible polyethylene "squeeze tube" (Coughlan's Ltd., Winnipeg, MB) (Figure 2), and kneading the closed tube until the contents formed a

homogeneous mass (approximately 20 minutes). The mixture remained stable for several weeks.

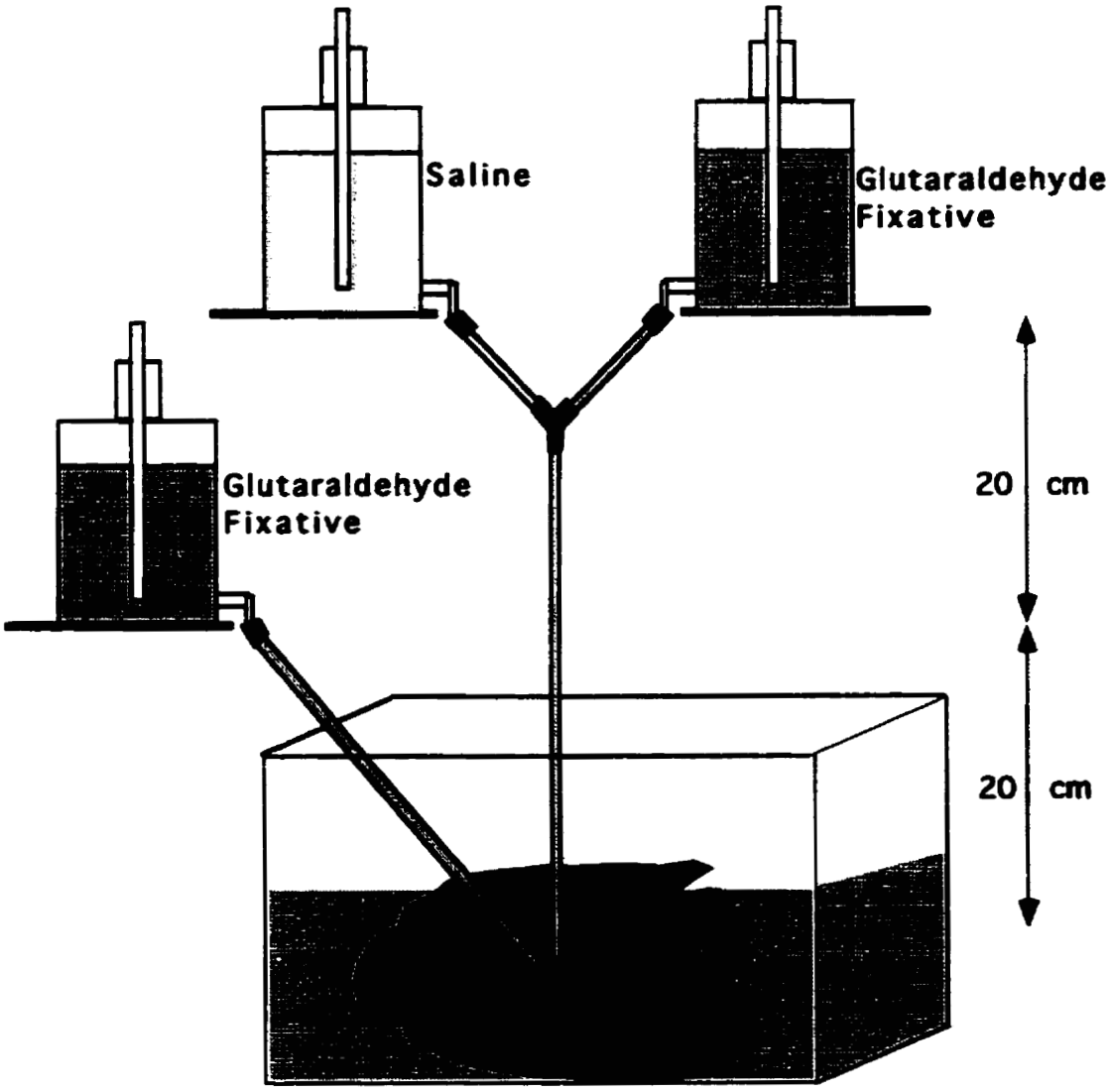

Figure 1. Apparatus for fixation by perfusion and inflation of left lung.

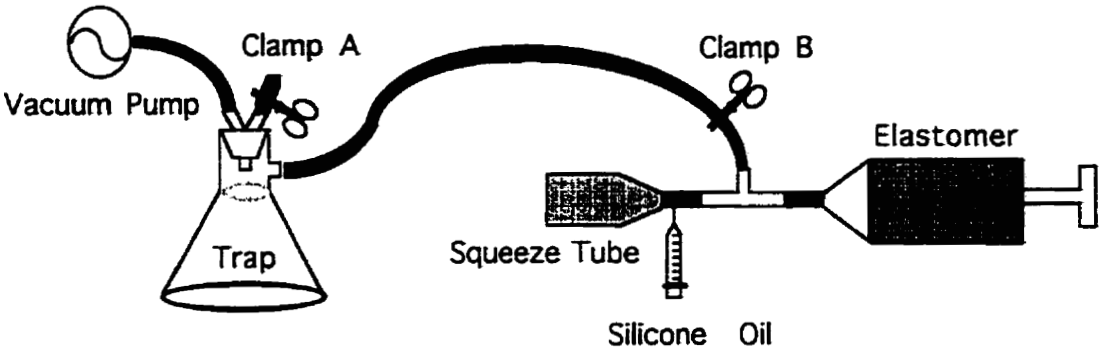

Figure 2. Apparatus for obtaining air-free mixture of elastomer and silicone oil.

The segmental bronchus was attached to Tygon tubing using metal connectors and size 0 surgical silk (Ethicon Company Ltd., Somerville, NJ) and sealed with tissue-adhesive glue (Vetbond, 3M Animal Care Products, St. Paul, MN). The tissue was then suspended in a modified plastic dessicator by attaching the tubing to a T-connector which extended through a rubber stopper at the top of the dessicator (Figure 3). A second T-connector, which also extended into the dessicator, was connected to the first with latex tubing, thus forming a bridge between the two connectors. The free end of the second connector led to

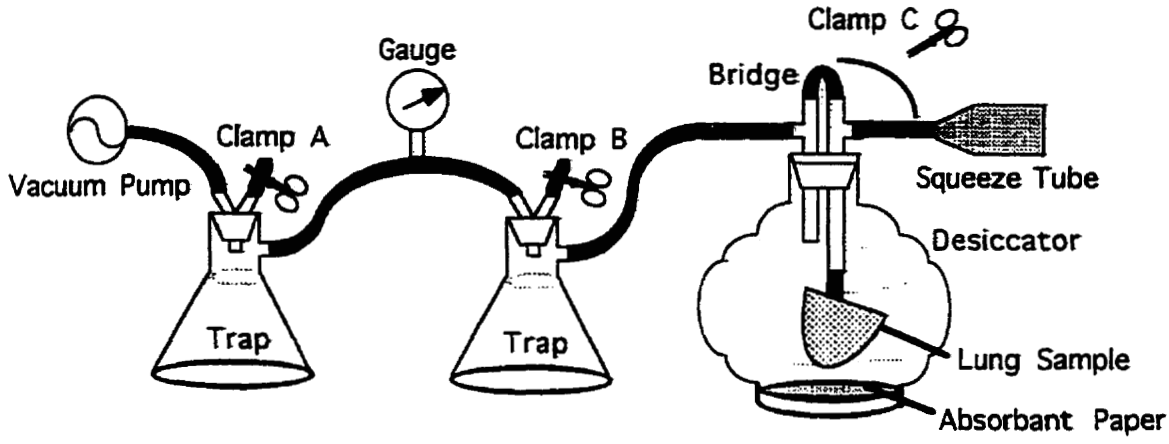

Figure 3. Apparatus for negative-pressure injection of airways.

a water trap, to a pressure gauge, to a second water trap and then to a venturi-type vacuum pump. Absorbent paper was placed in the bottom of the dessicator.

In order to inject the silastic mixture, the dessicator was closed, the vacuum pump activated, and the bridge between the two connectors was clamped (Figure 3, clamp C), thus drawing air in through the lung and removing excess moisture from the airways. Clamp C was then transferred from the bridge to the incoming air passage, and both the lung and chamber were evacuated. The lung and chamber were allowed to equilibrate for 10-15 mins. The squeeze tube containing the injection mass was then attached to the inlet, clamp C

(Figure 3) was moved again to the bridge, and the contents of the squeeze tube were allowed to flow into the lung for approximately 30 mins. The dessicator was then returned to atmospheric pressure by opening clamp B (Figure 3), and the injected lung tissue was left suspended for an additional 30 min. before being removed to saline to complete polymerisation.

Microdissection Technique

Following complete polymerisation of the silicone, four injected lungs, specifically one normal lung, two from cigarette smokers and one with bronchiectasis, were microdissected to reveal the lung casts within the airways. Once the casts were exposed, as much as possible without damaging them, 3 mm thick transverse blocks of the underlying airways were taken and processed for routine light microscopy through paraffin wax. The sample sites were marked on the cast for future correspondence with the airway sections.

The tissue on the lungs was then macerated in 5.25% sodium hypochlorite (household bleach) for 2-3 days. Linear shrinkage of the silicone was less than 1% in the fixative and between 1% and 2% in bleach.

Euclidean and Fractal Geometry

The left lungs were obtained at autopsy and fixed by inflation through both the vasculature and airways with glutaraldehyde fixative (2.5% in 0.1 M phosphate buffer, pH 7.3) at a pressure of 25 cm H_2O (Figure 1). After fixing overnight, the apical portion of the left lower lobe was removed from the rest of the lung and the pleura was punctured to allow fixative fluid and trapped gas to escape. It was suspended by the segmental bronchus to tygon tubing using size 0 surgical silk (Ethicon Company Ltd., Somerville, NJ) and sealed with tissue-adhesive glue, in a modified plastic dessicator which was connected to a vacuum pump (Figure 3). Casts were then prepared using a negative pressure injection technique as described above (Perry et.al, 1999).

Euclidean Analysis

Length and diameter of the larger airways (generation 4-12) were measured using sharp pointed digital calipers. Diameter and length were recorded to the nearest 0.01mm. Smaller airways (< 1mm in diameter or > generation 13) were measured with a dissecting microscope at a magnification of 10X, by means of an ocular micrometer with a distance of 100μm between divisions. In the transitional zone (generation 10-12) two generations of airways were measured by both methods (digital calipers and dissecting microscope with ocular ruler) to assess differences in measurement accuracy. The differences in the values obtained from each method were compared utilizing a t-test.

The axial path to the periphery was measured. This was defined by at least two of the following three characteristics; 1) the largest diameter of the two branches, 2) the straightest path (smallest branching angle) towards the periphery of the two branches, and 3) the longest in length of the two branches. The minor daughter, or the first generation branching directly off of the major daughter was also measured (Figure 4).

Dimensions of the airways were measured on the casts by carefully spreading the branches with forceps and needles (0.63 mm diameter), in order to fix the branchings in position on a foam piece. The length (L) of a branch was considered to begin at the intersection of its central axis with that of its parent branch, and end at the intersection of its central axis with that of its daughter branch (Schlesinger et.al, 1981) (Figure 4). Diameter measurements were taken for each generation at a point proximal (30% L), central (50% L) and distal (90% L). Measurements were then taken at a 90° angle at the same points for a total of 6 measures taken for each generation (Figure 4).

The coefficient of variation (CV = Standard Deviation / Mean * 100%) in diameter in each generation was calculated for each group. Lengths and diameters and log length and diameter were plotted against generation for both major and minor daughters. The overall slopes were compared between groups. In addition, average length-to-diameter ratio for all generations were plotted for each group for both major and minor daughters, as well as branching ratios (BR), which is the reduction factor with each successive generation, for both length and

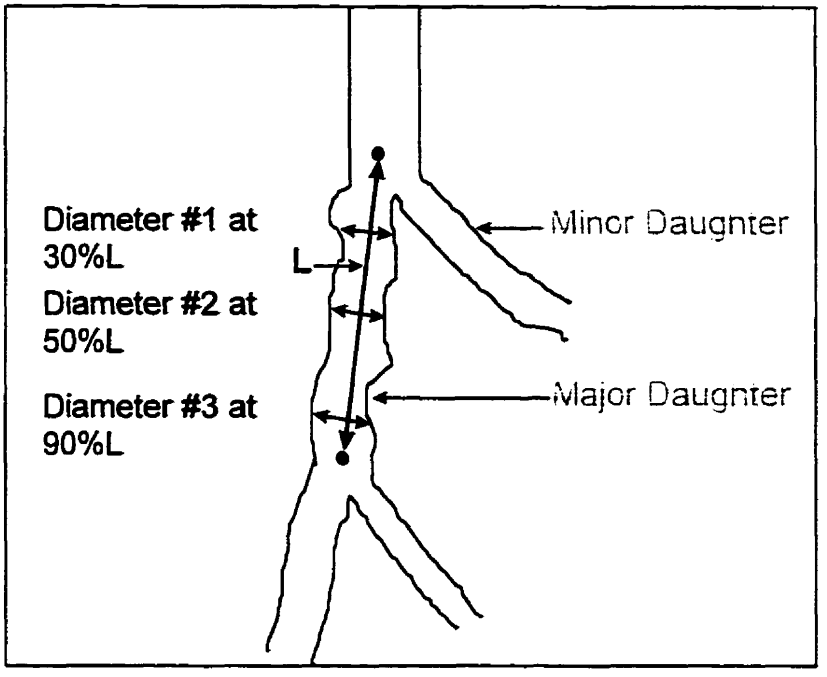

Figure 4. Diagram defines major daughter, minor daughter, generation length (L), and diameter #1,2 and 3.

diameter (BR = length or diameter generation n + 1 / generation n). The ratio of minor daughter/major was plotted for both length and diameter, as well. One way analysis of variance with Tukey-Kramer multiple comparison post hoc tests were used for group comparisons. A value of $p < 0.05$ was considered significant.

Fractal Analysis

Black and white images of both sides of whole lung casts were digitized at a resolution of 1280 X 960 pixels utilizing a digital camera (AGFA ePhoto 1280). A constant illumination was used, and the settings of focus, zoom and aperture on the camera were held constant. The images were all edge sharpened by 5%. The fractal analysis software (Benoit 1.1, TruSoft Int'l Inc., St. Petersburg, FL.)

measured the fractal dimension utilizing the box counting method. The solid image was converted to an outline of single pixels and then square grids with side lengths (s) from 1 to 240 pixels were placed over this image. The number of squares containing the outline of the image were counted. Log-log graphs were plotted of the reciprocal of the side length of the squares (1/s) against the number of outline containing squares (N(s)), according to the equation: log (N(s)) = D log (1/s), as s increases (Figure 5). The fractal dimension (D) is given by the slope of the graph. These log-log curves were then divided into three portions, with a new D calculated for each, to determine if fractal dimension changes for 3 groups of box sizes (small, medium and large) (Figure 6).

Many tests were done in order to measure the accuracy of the method used. The first (test 1) involved ten sets of measurements taken on images of a circle, square, Koch curve (with known D of 1.0, 1.0 and 1.26) and one representative lung cast from each group. The second (test 2) involved measuring the fractal dimension on 1 cast from each group that was rotated by 45° increments. Consequently 8 measures were taken from each of the three casts. The third (test 3) was a light test to measure any effects lighting may have on the fractal analysis of the lung cast images. Five variations of lighting were used. The fourth (test 4) was a positioning test of the casts, where the airways were spread out as much as possible, and then put as close together as possible. This was done on one cast from each of the three groups. The fifth (test 5) involved analyzing the casts both before and after trimming of as much of

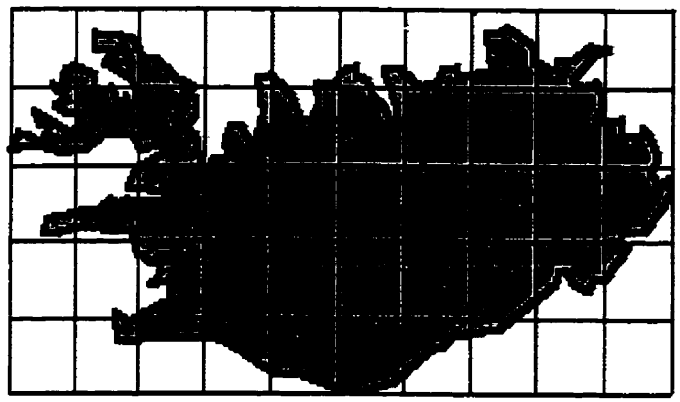

$r = 50$
$N = 35$

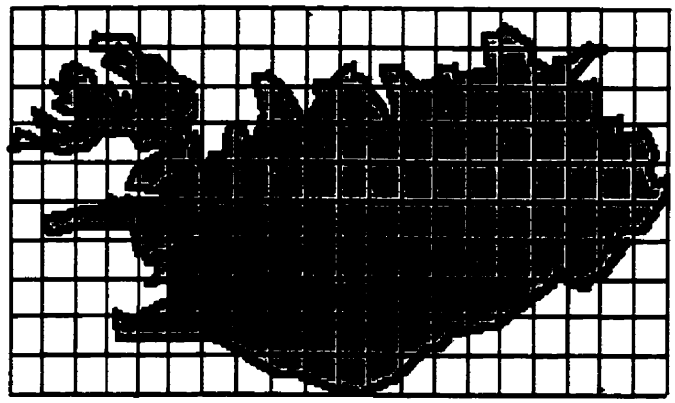

$r = 25$
$N = 76$

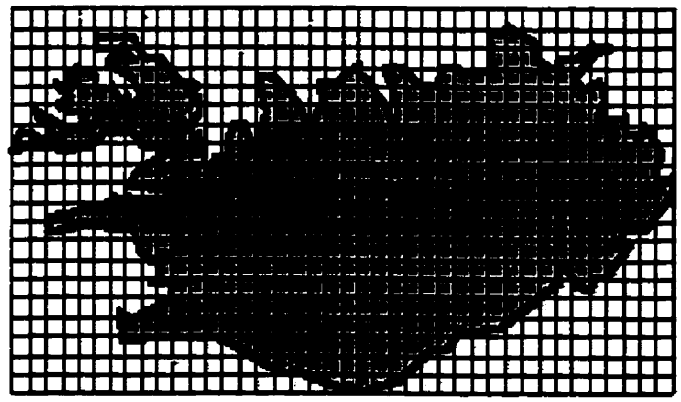

$r = 12.5$
$N = 168$

Figure 5. Fractal box counting method utilizing the formula: D = log (1/r) / log (N(r)) (as r increases), where D is the fractal dimension, r is the size of one box, and N is the number of boxes containing the outline of the object. The box size (r) is continually decreased, with a new (N(r)) calculated for each.

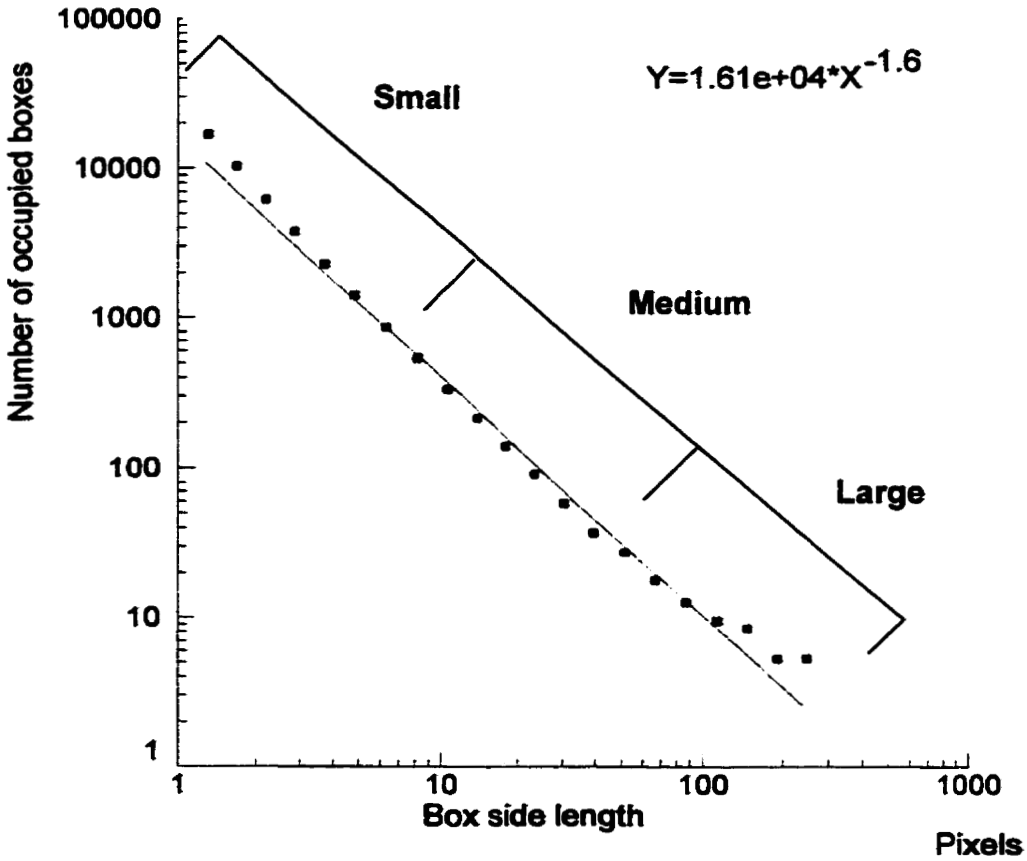

Figure 6. An example of a log-log graph plotted of the reciprocal of the side length of a square against the number of outline containing squares. The slope of the curve is the fractal dimension. The slope is recalculated for the small, medium and large box sizes, each containing 7 points on the curve, in order to determine if fractal dimension changes with different box sizes.

the alveolar ducts as possible, in order to reveal larger airways on the cast for the photographs. The sixth (test 6) involved changing the degrees of rotation of the grid during the analysis of fractal dimension on the computer program. Ten different rotations were measured. The last test (test 7) involved the measure of three randomly selected areas from 3 casts (1 from each group) with each area containing different generations.

The mean fractal dimension from the front (D1) and back (D2) image of the cast were used for group comparisons. Differences between D1 and D2 were determined using paired t-tests. Assessment of all of tests 1-7 were analyzed using the coefficient of variation (CV = Standard Deviation / Mean * 100%), as well as paired t-tests, where one variation of the test was set as the control and all other measures were compared to this control. For group comparisons (FA, NFA, NAC) and box size comparisons (small, medium, large) of fractal dimensions, one way analysis of variance with Tukey-Kramer multiple comparison post hoc tests were used. A value of $p < 0.05$ was considered significant.

Small Airway Disease in Asthma

Sampling

The fresh left lung, obtained at autopsy was inflated through the vasculature and airways with glutaraldehyde fixative (2.5% in 0.1 M phosphate buffer, pH 7.3) at a pressure of 25 cm of H_2O, and allowed to fix overnight (Figure 1). The lung was sampled systematically along the conducting airways supplying three segments; the upper anterior segmental bronchus (UAB), the lower anterior bronchus (LAB) and the lower posterior bronchus (LPB). The length of each of these airways was measured and then divided into 9 equal sections (Figure 7). The correlation between airway level and airway generation was determined on airway casts (Table 1) using the negative pressure casting technique (Perry et.al, 1999). A transverse block of the airway was taken at each of the 9 levels, with 9 being the largest (main bronchus) and 1 being the smallest (terminal bronchiole). Only levels 1 to 3 were used for this study in order to ensure that small airways in the periphery of the lung were counted, specifically generation 10 or higher. Five micrometer thick sections of paraffin-embedded blocks were stained with haematoxylin and eosin, a modified verhoefs elastic trichrome and for smooth muscle f-actin by immunohistochemistry.

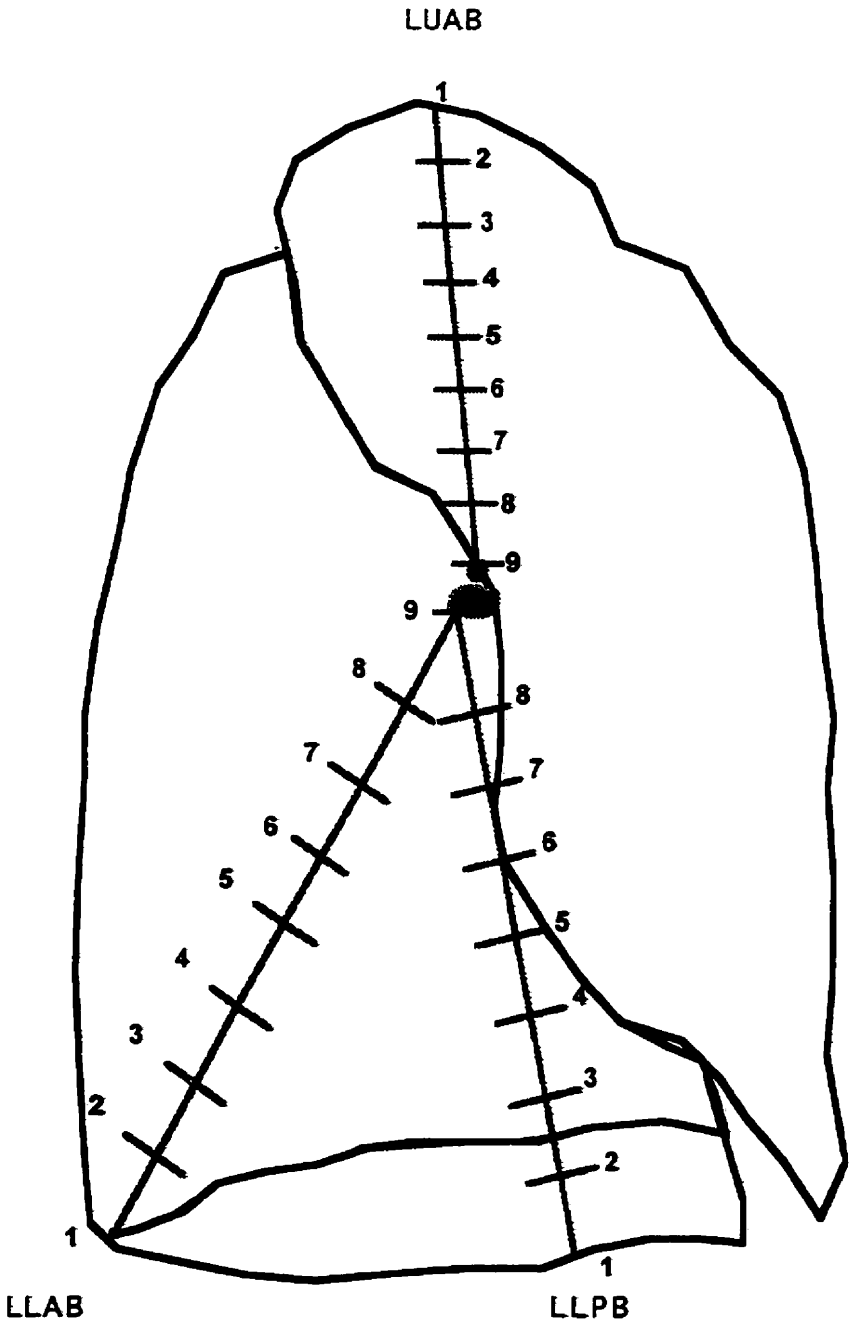

Figure 7. Method of sampling involving taking 9 equal sections from each of the left lower anterior bronchus (LLAB), the left lower posterior bronchus (LLPB) and the left upper anterior bronchus (LUAB).

Table 1. Correlation of airway level with airway generation in three airways, left lower anterior bronchus (LLAB), left lower posterior bronchus (LLPB) and left upper anterior bronchus (LUAB)

	Generation		
Level	**LLAB**	**LLPB**	**LUAB**
9	2 ± 0	2 ± 0	2 ± 0
8	3.8 ± 0.84	3.4 ± 0.55	3.75 ± 0.5
7	5.2 ± 1.1	5.2 ± 0.84	5.75 ± 0.96
6	6.6 ± 1.14	7.4 ± 1.52	7.75 ± 0.96
5	8.2 ± 1.3	9.6 ± 1.67	9.75 ± 0.96
4	9.6 ± 1.34	11.2 ± 1.64	11 ± 1.41
3	11.6 ± 2.07	12.8 ± 1.79	13.25 ± 1.71
2	14.6 ± 2.88	15.8 ± 2.59	16.33 ± 2.08
1	17.7 ± 2.99	19.5 ± 3.7	19.67 ± 3.21

Morphometry and Feature Identification

Terminal Bronchioles

Terminal bronchioles (TB) were only analyzed if seen in true cross section, and were free from branching. A true cross section was determined by the ratio of the diameter in its longest axis to the widest point perpendicular to this axis (Bosken et.al, 1990) being > 0.5. Only airways with a calculated diameter < 1.2 mm were included. The boundary of the TB was determined by the surrounding lung parenchyma. When two airways were in close proximity (for example, distal to a bifurcation) such that there was no lung parenchyma to separate them, an imaginary line was drawn between the two airways such that the dividing wall was equally distributed between the airways. Similarly, in the case of the accompanying pulmonary artery, the boundary was drawn between the airway and the vessel. The internal perimeter was defined by the inner

border of the basement membrane. The lumen was defined as points falling internal to the basement membrane.

The area fractions of selected features in the airway wall profile were determined by a point counting technique (Weibel et.al, 1962), using a Carl Zeiss Axioplan light microscope, model # 451888, drawing tube and square lattice grid containing 240 points, a Baxter Tally III Electronic Tabulator, model #008485. The point grid was superimposed onto a segment of the airway wall, and the number of points falling on each area of interest per grid were counted. The size of the airways varied, so it was necessary to adjust magnification according to airway size (the majority being counted at either 20 or 40X magnification). Under a magnification of 20, the distance between two points on the grid (Z) is 0.055mm, and under 40, Z is 0.0275mm. The features that were quantified were: smooth muscle, epithelium, mucus cells within the epithelium, basement membrane, blood vessels within the wall, and inflammatory cells.

Respiratory Bronchioles

The anatomy of the respiratory bronchiole is complex and although semi-quantitative grading systems exist, there are no quantitative morphometric studies in humans. Respiratory bronchioles, generation 1, 2 and 3 (RB1, RB2, RB3) were identified based on their anatomic relationships to each other and adjacent structures. Only longitudinally oriented airways with identifiable beginnings and ends were selected. The outer boundary of the respiratory bronchiole was determined by the border between the respiratory bronchiole

wall, and the adjacent lung parenchyma (Figure 8 - black line outlining airway). The airway length (l) was determined by the intersections of lines drawn through the center of the airways (Figure 8). The internal perimeter and the lumen were defined in the same manner as for terminal bronchioles. The features were also quantified in a similar manner as for terminal bronchioles.

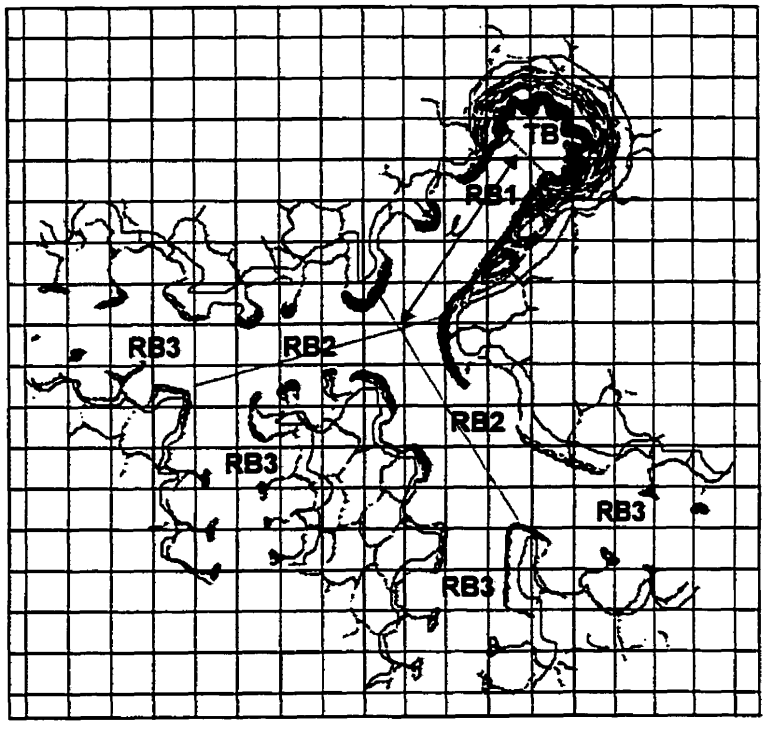

Figure 8. Diagrammatic representation of a longitudinal section of the three generations of respiratory bronchioles (RB1, RB2, RB3). Blue lines define segment length (l). Red line defines the outer boundary of the respiratory bronchiole.

Calculations

Using stereologic principles the area proportion occupied by the structures counted were calculated, using the formula: **(1)** Area (μm^2)= Z^2 n, where Z is the distance between two points on the grid (magnification factor), and n is the number of points that land on the structure of interest. It is important to note that a constricted airway increases the perceived area of smooth muscle. Studies by James et al. (James et.al, 1989) have shown that the internal perimeter of an airway remains constant at different lung volumes and degrees of smooth muscle shortening, despite changes in luminal area. Consequently, the internal perimeter (equation 2) was used to reconstruct the relaxed dimensions of the airway. Thus, smooth muscle area was appropriately normalized for all groups.

Luminal Surface Length (internal perimeter) was determined by using the formula: **(2)** Luminal Surface Length (μm) = bmi * Z * $\pi/4$, where bmi is the number of times the grid intersects with the basement membrane, and Z is the magnification factor (or the distance between two points on the grid). To determine thickness (smooth muscle, respiratory bronchiole wall, alveolar wall), the following formula was used: **(3)** Thickness (μm) = Area (μm^2) / Luminal Surface Length (μm).

The relaxed lumen area of a terminal bronchiole was calculated by assuming that it was a circle with a circumference equal to the lamina surface length ; thus **(4)** Relaxed lumen area (μm^2) = (Luminal Surface Length)^2 (μm^2) /

4π. For airways the measured luminal area calculated from the points falling over the lumen were subtracted from the expanded luminal area calculated from the perimeter. This gave an index of constriction.

Assessment of Error

Assessment of interobserver and intraobserver variability was calculated using the coefficient of variation (CV = Standard Deviation / Mean * 100%). Interobserver measurements were done on a subgroup of 15 airways. All of the airway measurements by both observers were performed on a different grid (i.e. the grid was moved in position, and as a result, the starting point was changed). Consequently, the interobserver variation includes variation due to grid position. Intraobserver measurements were done by performing 5 replicate measurements of 5 airway sections. These measures were taken both with the grid kept in the exact position for all repeated counts, as well as with the grid moved in position. As a result, there are two intraobserver variation's; one not including grid variation, and is therefore a measure of feature identification, and the other which does include grid variation. The measures of variation included all airway types (terminal bronchioles and respiratory bronchioles), and were made with the observer blinded to the case classification.

Analysis of Data

Three measurements of each category (TB, RB1, RB2, RB3) were randomly selected from the total population of acceptable fields, which included all three segments (UAB, LAB, and LPB) and were measured for each case.

For the assessment of variability (interobserver and intraobserver), coefficients of variation were calculated for each parameter. Intraobserver variation was calculated by dividing the standard deviation by the mean of 5 measurements made by the same observer. The results were expressed as the mean of the coefficient of variation. The coefficient of variability for interobserver error was calculated by dividing the standard deviation by the mean of the measurements of each of two observers.

For group comparisons (fatal asthma, non-fatal asthma, non-asthma control) and for interlobar comparisons for specific features, one-way analysis of variance with Tukey-Kramer multiple comparison post hoc tests were used. For interlobar comparisons, the mean smooth muscle thickness in UAB (identified as upper lobe) were compared to mean smooth muscle content in LPB and LAB combined (identified as lower lobe). A value of $p < 0.05$ was considered significant.

Remodelling of Lung Parenchyma in Asthma

Sampling

All of the sampling was done in the same manner as for the small airway study described above. Levels 1 to 3 were used for this study in order to ensure adequate sampling of lung parenchyma at generation 10 or higher. Five micron thick sections of paraffin-embedded blocks were stained with hematoxylin and eosin, a modified verhoefs elastic trichrome and for smooth muscle f-actin using immunohistochemistry (DAKO Immunostain ®).

Morphometry and Feature Identification

A Carl Zeiss Axioplan light microscope, model # 451888, drawing tube and square lattice grid containing 120 points and a Baxter Tally III Electronic Tabulator, model #008485 were used to determine the area fractions of selected features in the parenchyma utilizing a point counting technique previously described by Weibel et.al, 1962. Parenchymal smooth muscle was measured by placing the grid randomly over a section of lung tissue stained for f-actin. The field was accepted if it did not contain airways (terminal bronchioles), or blood vessels greater than 0.085mm in diameter. Minor degrees of alveolar collapse were accepted. If any alveolar walls were opposed to each other, the field was rejected. The outer boundary was determined by a grid containing 120 points and magnification was set at 20X objective, with a distance between two points on the grid (Z) of 0.055 mm. The area of lung parenchyma containing tissue with and without actin was measured, as well as the lumen area and intersections

with the alveolar wall. The actin positive features were further classified into alveolar duct, vascular and alveolar wall myofibroblast components.

Calculations

The area proportions were calculated for all structures measured by using stereologic principles based on the following formula: **(1)** Area (μm^2)= Z^2 n, where Z is the distance between two points on the grid (magnification factor), and n is the number of points that land on the structure of interest.

Alveolar surface length was determined by using the formula: **(2)** Luminal Surface Length (μm) = bmi * Z * $\pi/4$, where bmi is the number of times the grid intersects with the basement membrane, and Z is the magnification factor (or the distance between two points on the grid). The thickness of all structures (alveolar duct smooth muscle, alveolar wall smooth muscle, blood vessel smooth muscle and total wall) was determined using the following equation: **(3)** Thickness (μm) = Area (μm^2) / Luminal Surface Length (μm).

Assessment of Error

The coefficient of variation, **(4)** CV = Standard Deviation / Mean * 100%, was used to assess both interobserver and intraobserver variation. Interobserver measurements were done on a subgroup of 5 parenchymal areas. Intraobserver measurements were done by performing 5 replicate measurements of 5 parenchymal areas. Both measures of variability were done with the grid remaining in the exact position for all parenchymal areas. All measurements were made with the observer blinded to the case classification.

Analysis of Data

Three areas of lung were randomly selected and measured from each of the three segments (UAB, LAB, and LPB). For the assessment of variability, coefficients of variation were calculated for each parameter. One way analysis of variance were used for group comparisons (FA, NFA, NAC) and interlobar comparisons for specific features. For interlobar comparisons, the mean smooth muscle thickness in UAB (identified as upper lobe) were compared to mean smooth muscle content in LPB and LAB combined (identified as lower lobe). A value of $p < 0.05$ was considered significant.

Chapter 3: Results

Lung Casting

An example of the casting and microdissection of a normal bronchial tree from an adult who had never smoked is shown in Figure 9. A cured and partially dissected bronchial cast of the left lower lobe is shown in Figure 9A and at higher magnification in Figure 9B. There is complete filling of all the exposed airways and the silicone polymer abutts tightly against the airway walls without obvious distortion. Figures 9C and 9D show the same cast after maceration in bleach. The bronchial architecture has been maintained after maceration and there is no apparent shrinkage, which is consistent with the findings in the shrinkage tests. Casts from the normal (never smoker) lungs showed dichotomous branching into major and minor daughters, uniform diameter between segments and a relatively smooth contour to the wall. The main axis of the bronchial tree, shown at higher magnification in Figure 9D, shows small spiral irregularities corresponding to the spiral bands of bronchial smooth muscle. Figure 10 shows the terminal airways from an individual with normal lungs and reveals details of the respiratory bronchioles and proximal alveolar ducts. The contours of the airways and associated alveoli are faithfully reproduced.

In contrast, a bronchial cast from a case of bronchiectasis deviates from the normal in several aspects (Figure11A-D). There is marked distortion of the bronchial tree and many airways take on a sac-like appearance and end blindly due to luminal obstruction from mucous plugs. The diameter is no longer uniform

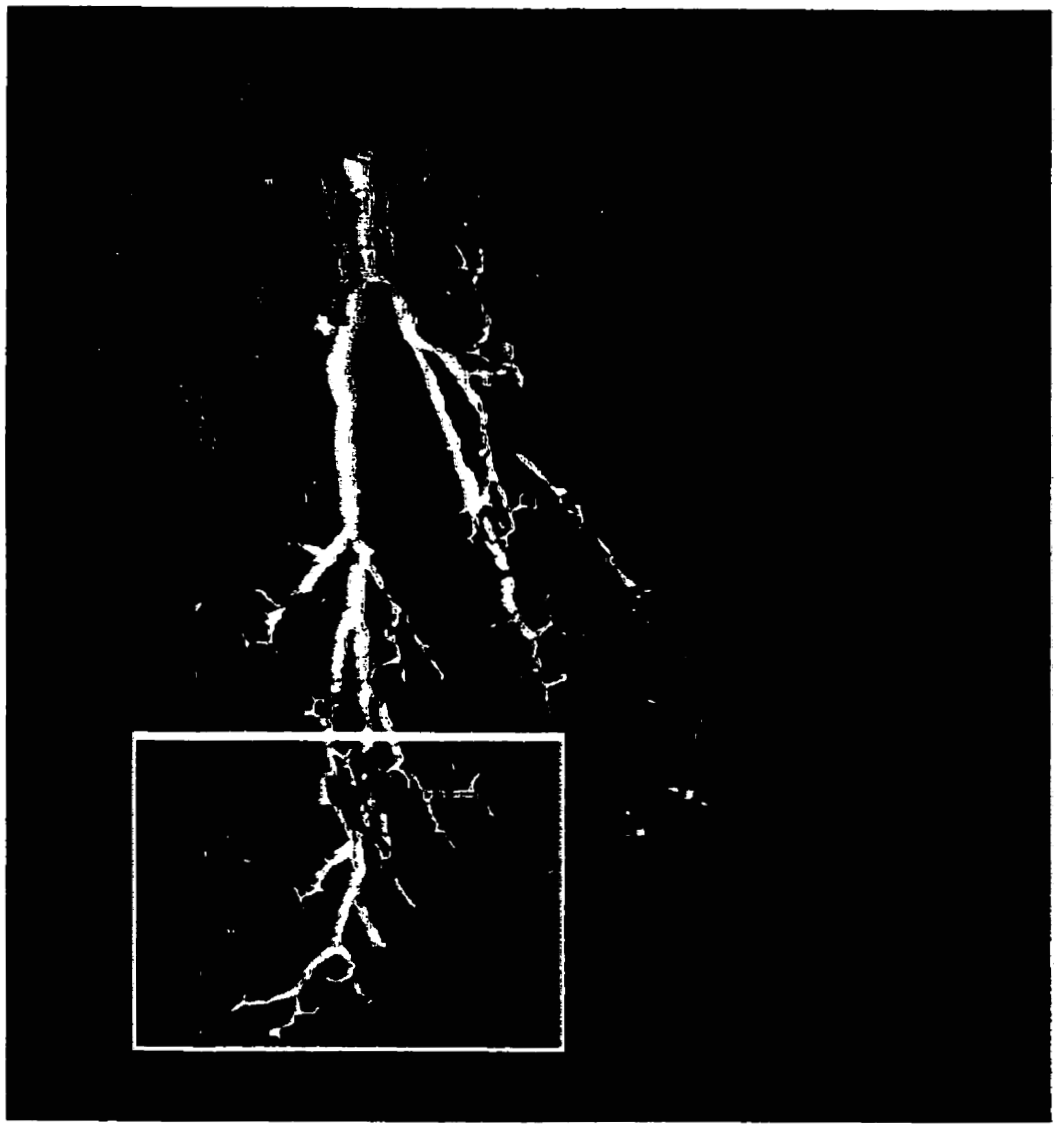

Figure 9A. Photograph of left lower lobe of adult never smoker with no history of lung disease. The main airway has been injected with silicone elastomer and allowed to cure. Parts of the silicone cast have been exposed by removing the overlying tissue and bronchial wall.

Figure 9B. This figure shows the boxed area in 9A at higher magnification. The silicone elastomer extends into the terminal bronchioles and is closely opposed to the bronchial wall without obvious distortion.

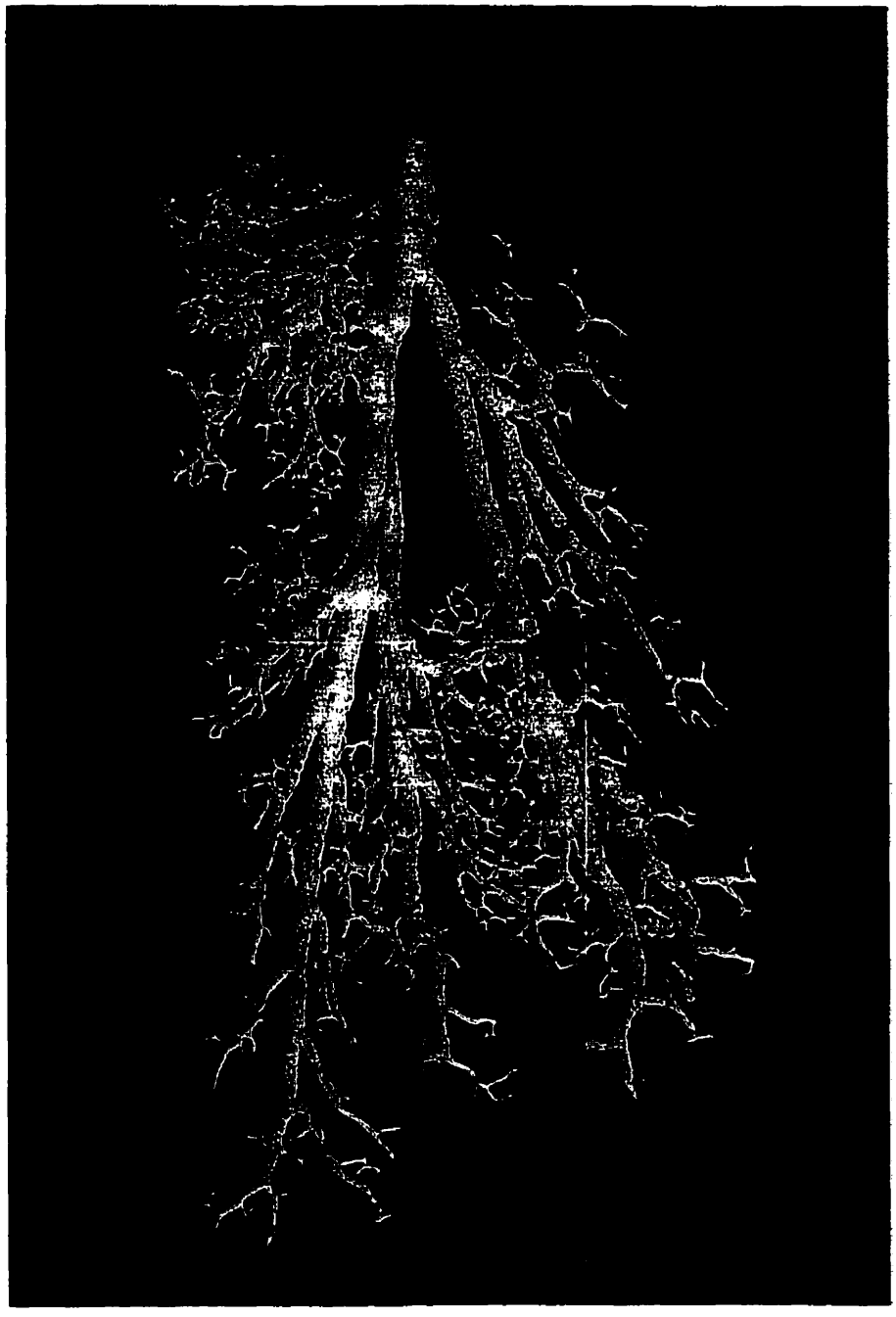

Figure 9C. Low power view of the same cast after complete maceration in sodium hypochlorite. There is no obvious distortion or shrinkage when compared with the cast within the lung prior to maceration. (see Figure 9A).

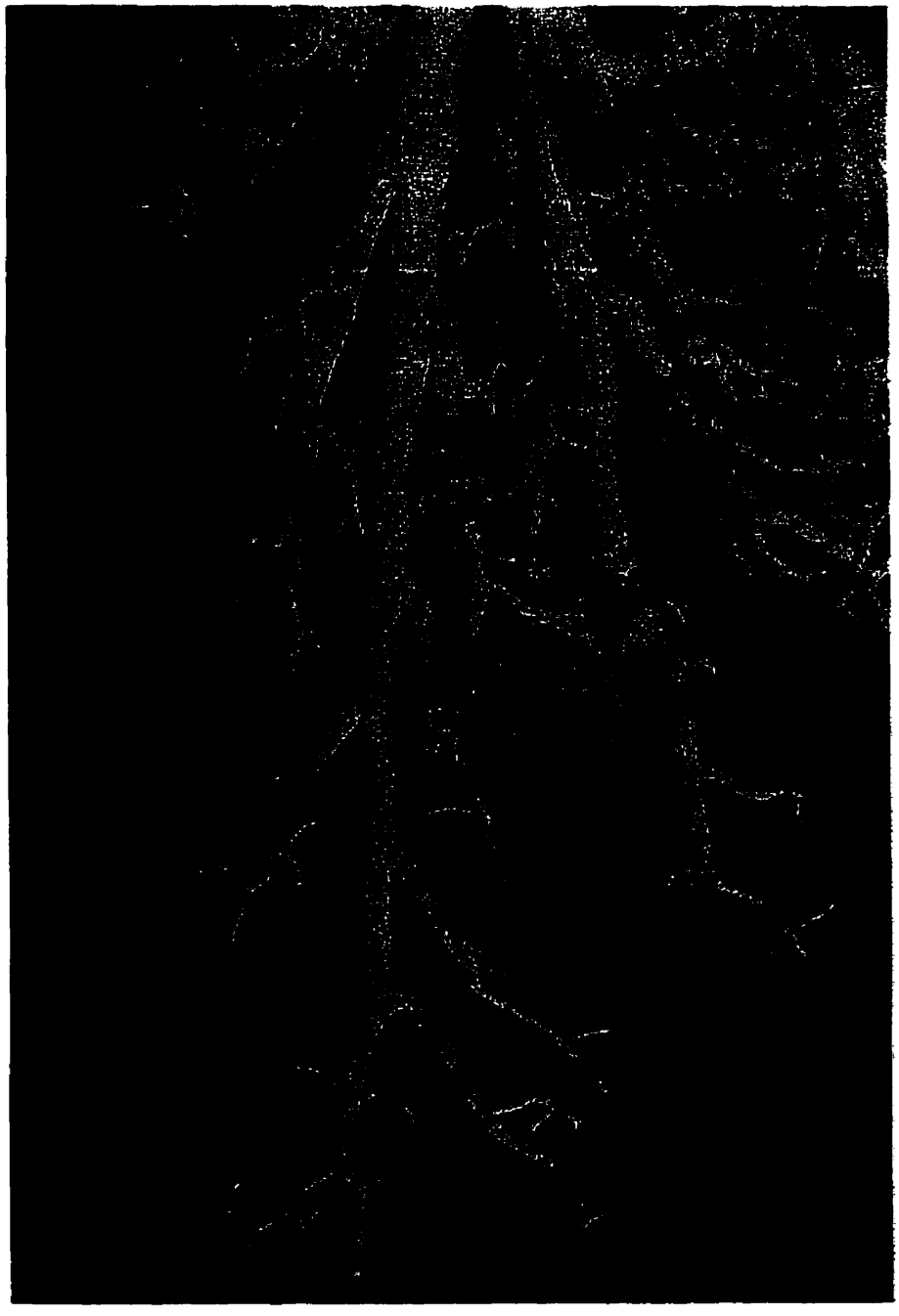

Figure 9D. At higher magnification, the characteristic dichotomous branching pattern of the human lung is seen with major and minor daughters, uniform diameter within a segment and fairly smooth contours. Faint spiral banding on the main axis of the cast correspond to smooth muscle bundles on histologic section.

Figure 10. Close up of cast from non-smoker showing details of the respiratory bronchioles (RB) and alveolar ducts (AD). Note that individual alveoli (A) arising from the respiratory bronchioles are filled by the silicone.

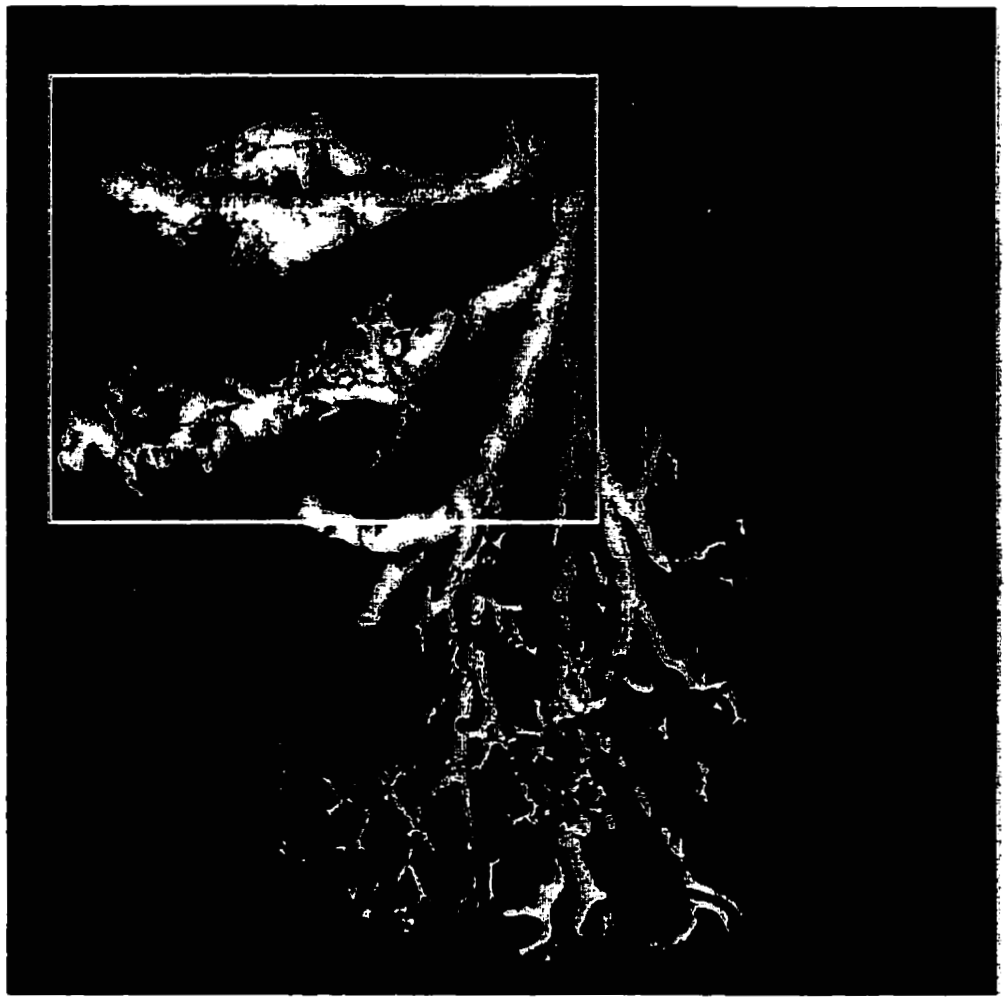

Figure 11A. Partially dissected silicone rubber cast from the left lower lobe of a case of bronchiectasis. The disease, which is characterized by irregularly dilated and ectatic bronchi, affected all lobes of the lung but appears more severe in the apical segment of the left lower lobe.

Figure 11B. This figure shows a partially microdissected area from the apical portion of the left upper lobe outlined by the box in Figure 5A. Note that there is complete filling of the airways, even when they are partially or completely obstructed distally. The arrowheads delineate the site sampled for histology (Fig 12)

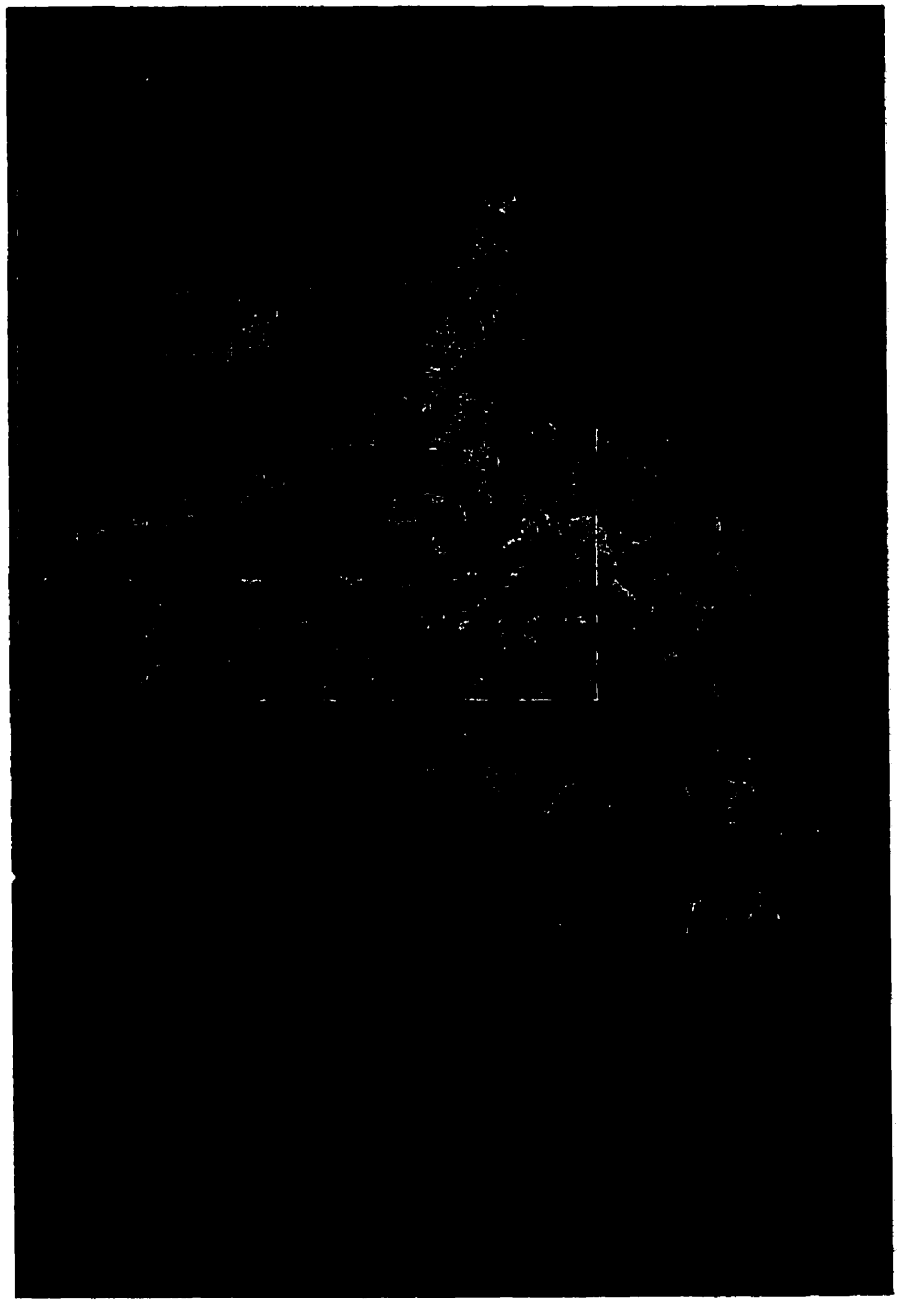

Figure 11C. This shows the specimen after complete maceration in sodium hypochlorite.

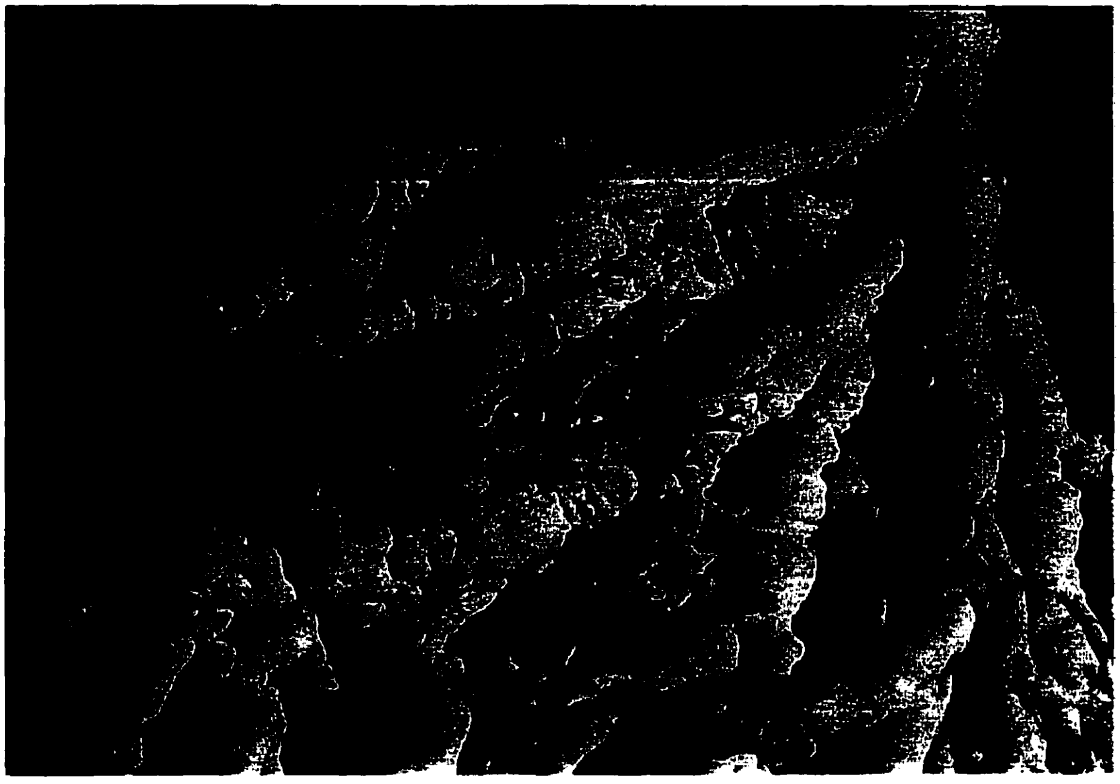

Figure 11D. This closeup shows details of the saccular bronchiectasis. The small diverticuli (arrows) arising from the proximal portions of the airways correspond to ectatic mucous gland ducts.

between branching parts, with areas of gross dilatation characteristic of disease. The small protrusions seen in the proximal portions of the cast (Figure 11D - arrows) correspond to ectatic mucous gland ducts on a histological section (Figure 12-mgd) which had been sampled prior to maceration from the region shown in Figure 11B (arrow heads). A bronchial cast from a heavy cigarette smoker also shows deviations from the normal airway structure (Figure 13A). The diameter of the airways is less uniform than seen in the never smoker and also shows regions of constriction and dilatation. Inspection at higher magnification (Figure 13B) also reveals many saccular diverticuli, corresponding to ectactic mucous gland ducts on histological examination.

Figure 12. H&E stained histologic section from the site indicated by the arrowhead in Figure 11B. The specimen shows fibrosis of the airway wall, chronic inflammatory cell infiltration, smooth muscle atrophy and ectatic mucous gland ducts (mgd). The latter correspond to the small protrusions (diverticuli) from the cast surface.

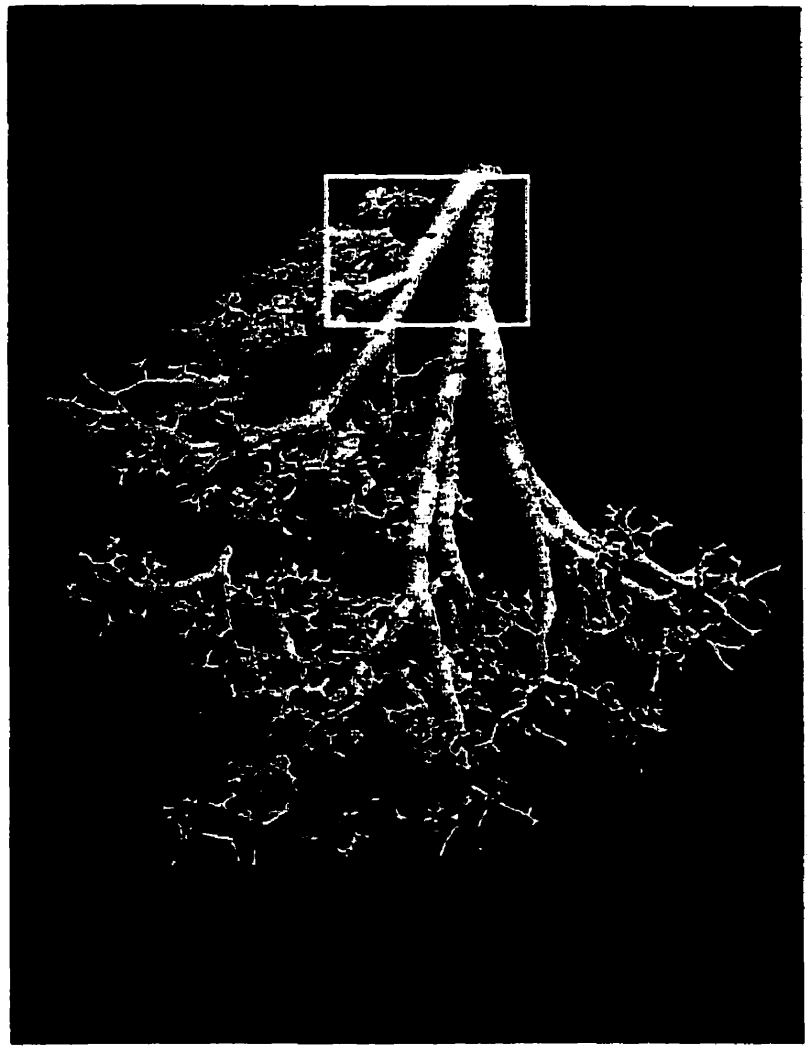

Figure 13A. Macerated cast of left lower lobe from adult current cigarette smoker. Note that the cast differs from that seen in the nonsmoker (Figure 9) in that the diameters of the segments are irregular and show banding and constrictions. There are numerous diverticuli originating in the proximal airways.

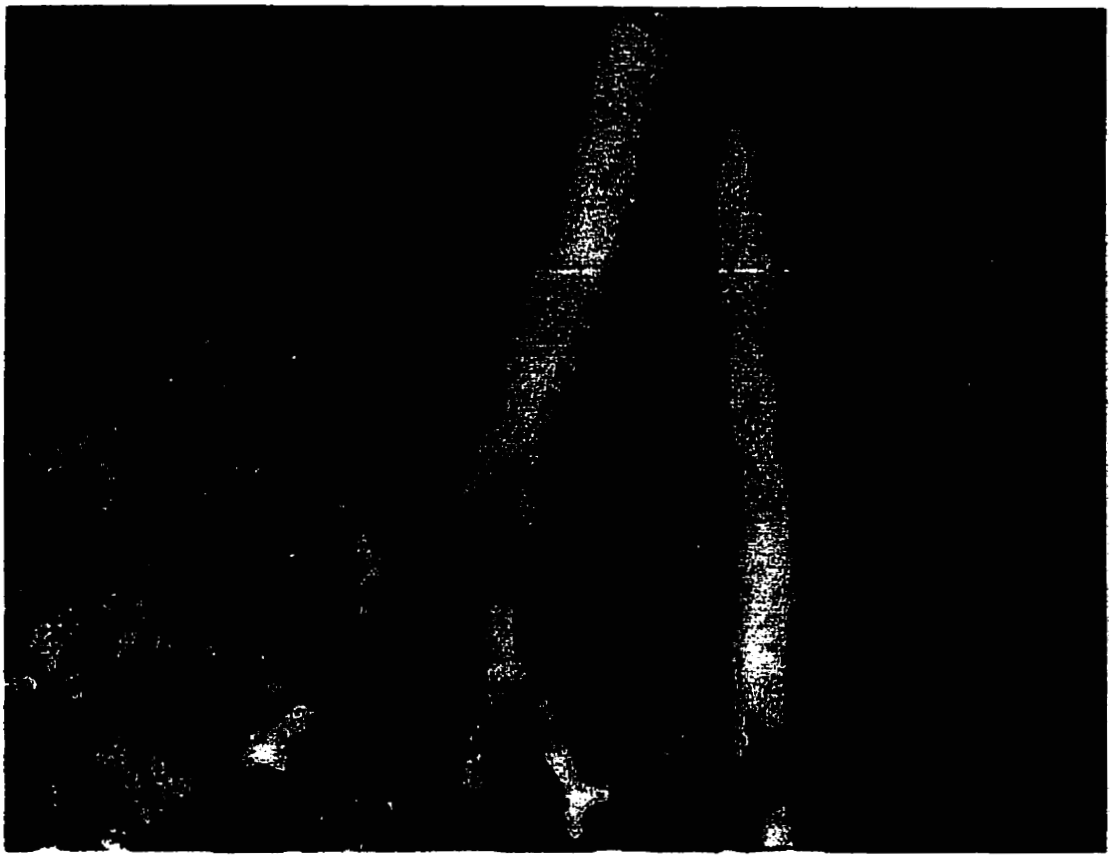

Figure 13B. High power view in a partially microdissected state of the diverticuli shown in Figure 13A. These correspond to ectatic mucous glands on histology.

Euclidean and Fractal Geometry

Six control cases (NAC), as well as six non-fatal (NFA) and six fatal asthmatics (FA) were used in this study. Table 2 describes subject characteristics, followed by Table 3 which describes causes of death for each case.

Table 2. Subject characteristics for the fractal and euclidean study, including age, sex, asthma duration, asthma grade (1-4), and treatment

	FA	*NFA*	*NAC*
Age, yr			
Mean	32.3	24.8	30.3
Range	18-59	18-33	18-50
Sex, M/F	3/3	3/3	3/3
Asthma Duration, yr			
Mean	11.5	13.75	0
Range	6-20	2-31	0
Asthma Grade			
Overall	3.7	0.83	0
Average	2-4	0-2	0
Treatment, % of subjects			
B-Agonists	100	66.7	0
In-Steroids	33.3	33.3	0
Oral Steroids	33.3	16.7	0

Table 3. Subject cause of death and age for both the fractal and euclidean study

Group	Case	Age	Cause of Death
FA	H253	55	Asthma
FA	H248	59	Asthma
FA	H296	18	Asthma
FA	H297	18	Asthma
FA	H316	24	Asthma
FA	H324	20	Asthma
NFA	H234	29	Intraventricular hemorrhage
NFA	H235	33	Drug toxicity, obecity
NFA	H236	21	Acute Ethanol Toxicity
NFA	H269	23	Asphyxia, suffocation in avalanche
NFA	H314	25	Morbid obesity, enlargement of heart and liver
NFA	H334	18	Diabetic ketoacidosis
NAC	H288	50	Leukemia
NAC	H330	21	Motor vehicle accident
NAC	H331	18	Brainstem tumor, acute bronchopneumonia
NAC	H332	33	Subarachnoid hemorrhage
NAC	H340	29	Seizure disorder
NAC	H343	31	Self inflicted gunshot wound to the head

Photographs of casts from each group are shown in Figure 14,15 and 16. Upon gross examination of the NAC cast, the airways appear uniform in diameter along each generation. The branching is regular, reaching the distal airways (respiratory bronchioles have been trimmed away) (Figure 14A). On closer examination, the airways appear smooth and uniform, with a slight decrease in diameter in each progressive generation (Figure 14B). The NFA cast begins to show some abnormalities with the presence of numerous saccular diverticuli, corresponding to ectatic mucous ducts on histological examination (Figure 15-large arrows). There are slight constrictions along each airway, resulting in non-uniform diameter along each generation. The casting material is still able to fill to

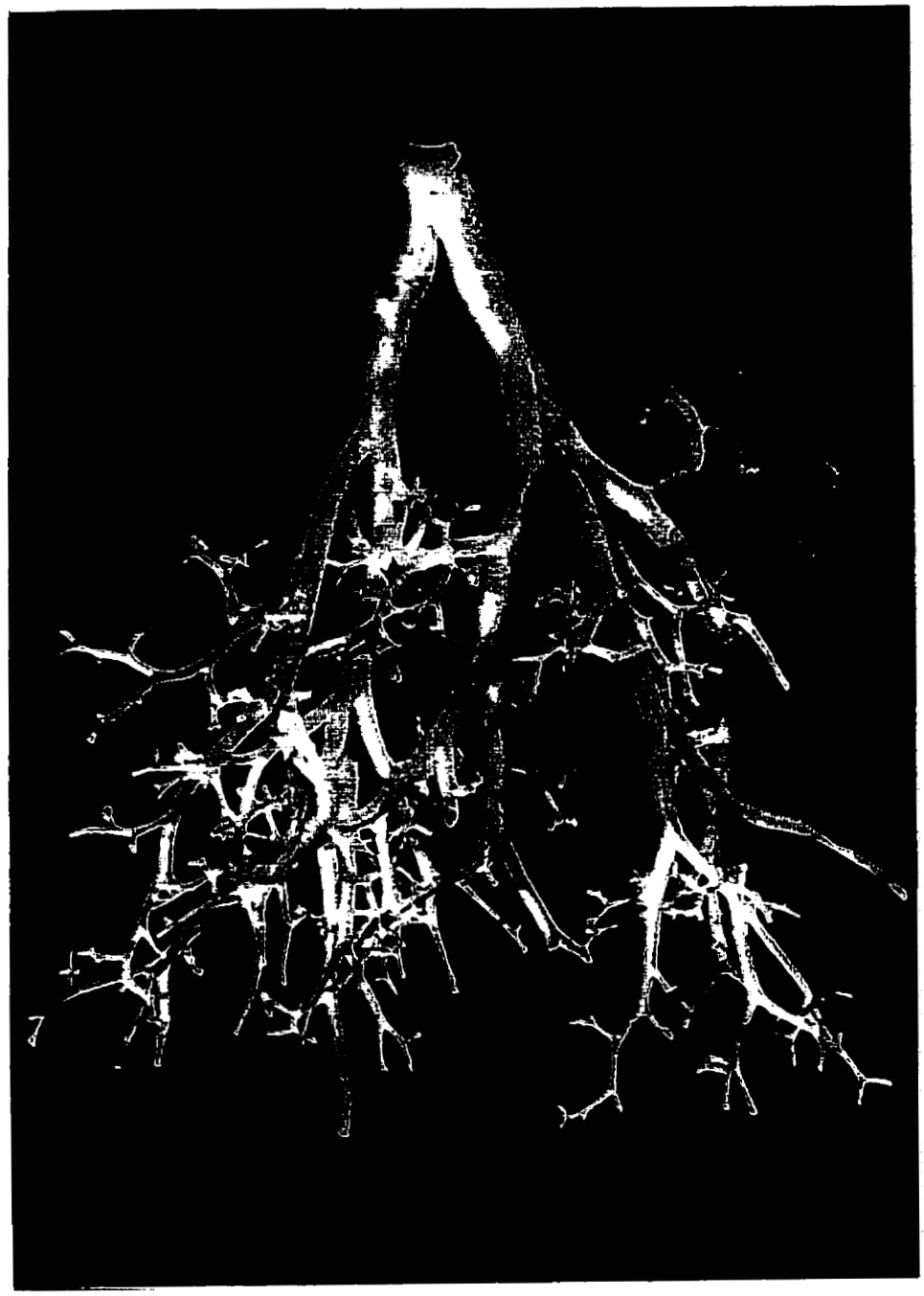

Figure 14A. Photograph of a Non-asthma control (NAC) cast. The branching is very regular, with no obvious distortions along each generation and reaches the distal airways. The respiratory bronchioles and alveolar ducts have been trimmed away.

Figure 14B. This figure shows a higher magnification of Figure 14A. Note again the regularity of the diameter along the airways in each generation.

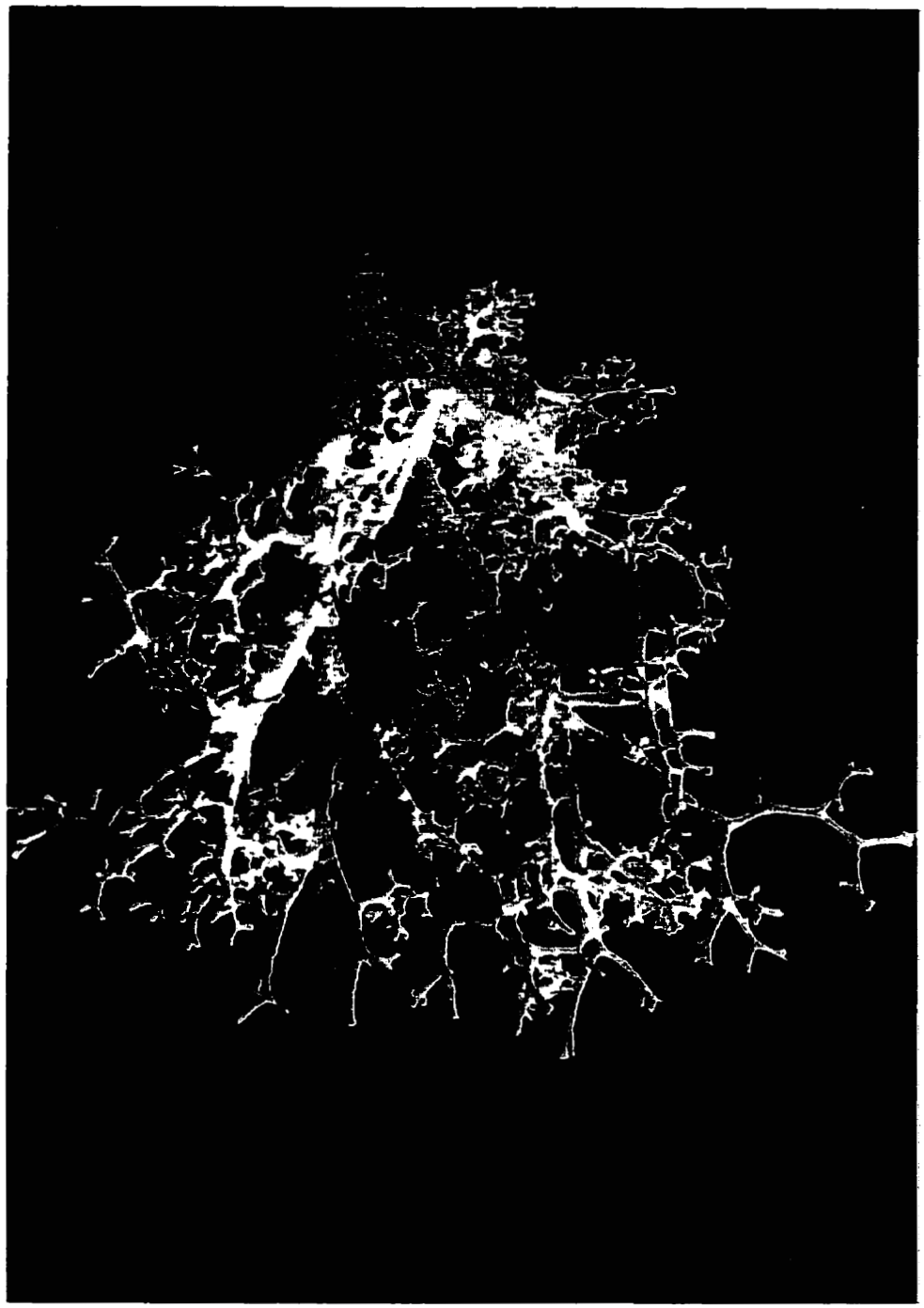

Figure 15. Photograph of a non-fatal asthma (NFA) cast. There are numerous saccular diverticuli present which correspond to ectatic mucous ducts on histological examination. Also present, are slight constrictions along each airway which results in a non-uniform diameter along each generation.

Figure 16A. Photograph of a fatal asthma (FA) cast. The airways are not uniform along each generation, with marked constrictions due to hypertrophied smooth muscle (arrow heads). The cast material was not able to reach the distal airways as in the NAC cast due to the presence of numerous mucous plugs. The FA cast also reveals numerous ectatic mucous ducts (arrow) as were seen in the NFA cast.

Figure 16B. This figure is a higher magnification of a FA cast. Once again the ectatic mucous ducts are very evident. Pronounced longitudinal ridges are visible due to the hypertrophy of longitudinal elastic bundles in asthma. Also more pronounced are the irregularities in diameter along each airway generation, as a result of smooth muscle constriction.

the distal airways as in NAC (Figure 15), resulting in numerous distal branches of the airways. A striking difference is seen in the cast of the fatal asthmatic compared to controls. The fatal asthmatic cast reveals ectatic mucous ducts (Figure 16A - large arrows), similar to those seen in NFA. Pronounced constrictions along the airways (arrow heads) are visible due to the constriction of hypertrophied smooth muscle in severe asthma. A close up reveals the irregular diameter along each generation, as a result of the smooth muscle constriction (Figure 16B). In addition, longitudinal ridges appear along the airways, which correspond to enlarged elastic bundles (Carroll et.al, 1999). Due to extensive mucous plugging of the airways in FA, the casting material is not able to penetrate to the distal airways, as in the NFA and NAC casts, resulting in a loss of the complex branching pattern normally seen in the airways.

Euclidean Dimensions

There were no significant differences found when comparing the two different methods of measurement (digital calipers and dissecting microscope with an ocular ruler) in the transitional zone (generation 11-12) of the airway casts.

The coefficient of variation (CV) of diameters of each generation revealed significantly greater variation in FA versus NAC as well as in NFA versus NAC in the major daughter (Table 4). The minor daughter measurements showed a significant difference in FA versus NAC (Table 4). The euclidean data for length and diameter vs generation for both major daughter and minor daughter are

Table 4. Average coefficient of variation (CV) in each group for diameters measured in each generation. Values are mean ± standard deviation.

Average CV	FA	NFA	NAC
Major Daughter	0.092 ± 0.055 *	0.100 ± 0.054 *	0.068 ± 0.038
Minor Daughter	0.115 ± 0.070 *	0.096 ± 0.06	0.082 ± 0.05

* $p < 0.05$; FA vs NAC; NFA vs NAC

shown in Figure 17A,B and 18A,B. Log length and log diameter vs generation are shown in Figure 19A,B and 20A,B. The slopes and Y intercepts of these curves were not significantly different between groups. For all calculations of branching patterns; length-to-diameter ratio (Figure 21A,B) and branch ratio for both length (Figure 22) and diameter (Figure 23), there were no significant differences between groups for both major daughter and minor daughter branches. In addition, the ratios of minor daughter/major daughter for both length (Figure 24) and diameter (Figure 25) revealed no significant differences between groups.

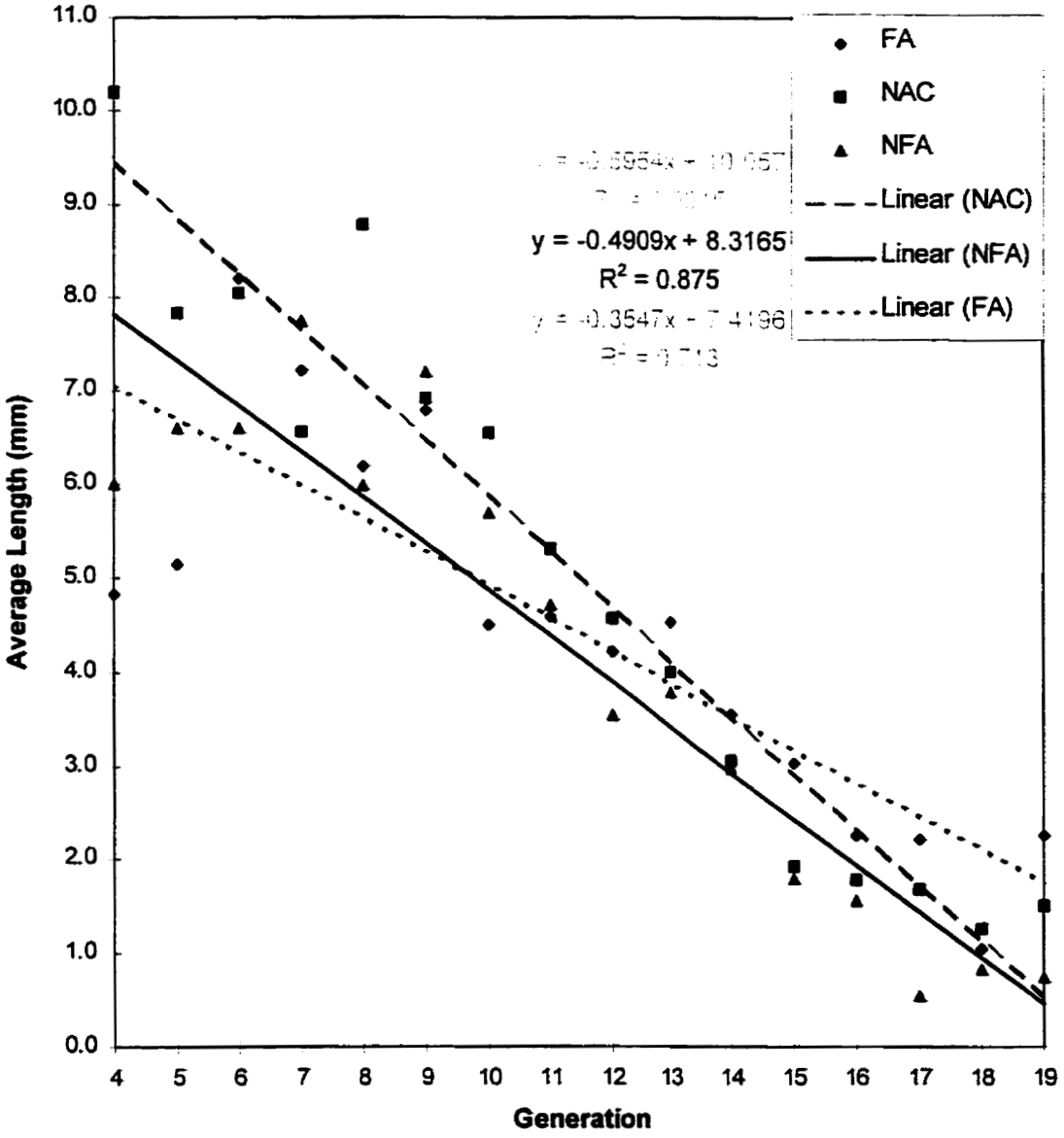

Figure 17A. Average change of major daughter airway length with increasing generation.

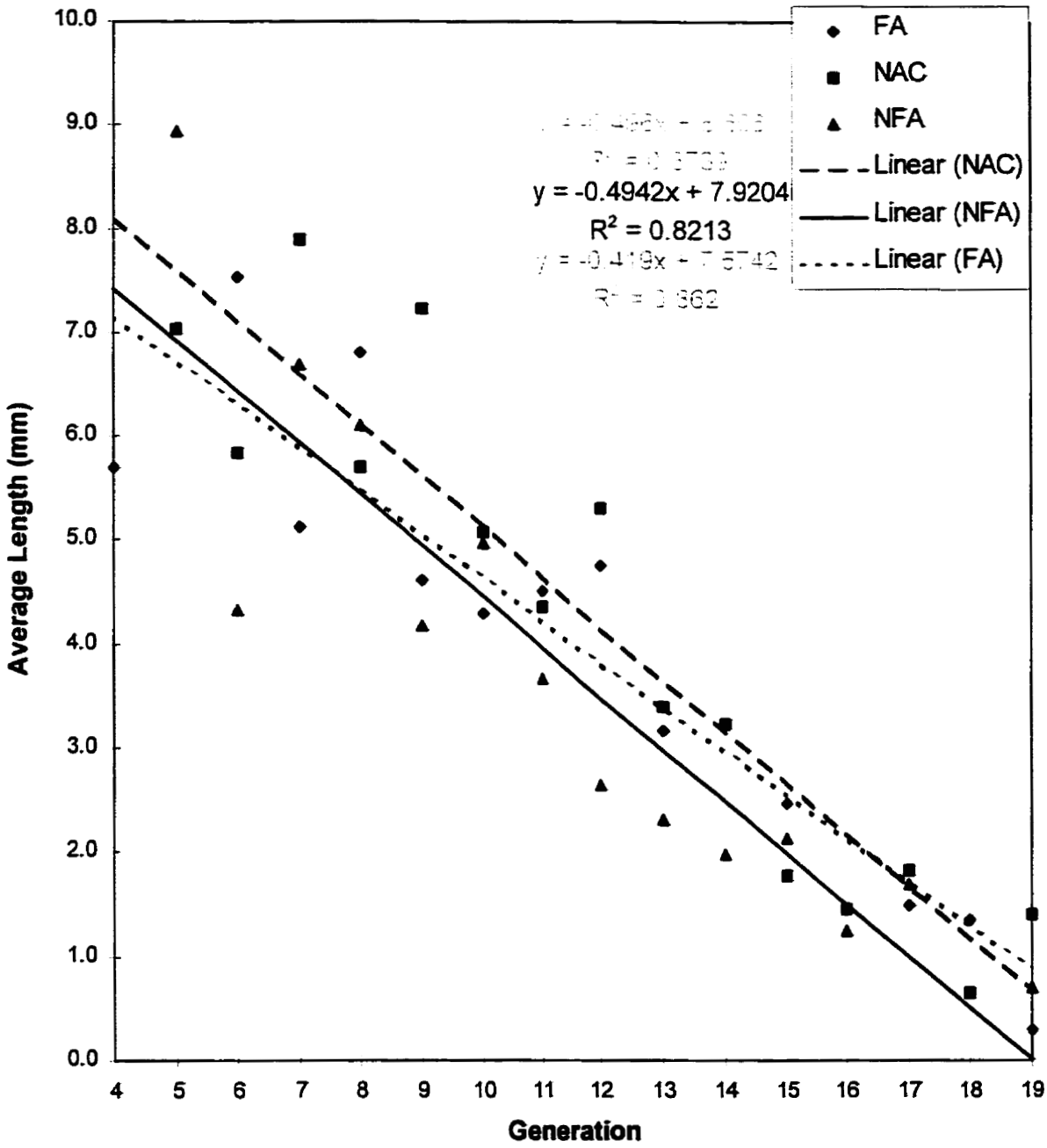

Figure 17B. Average change of minor daughter airway length with increasing generation.

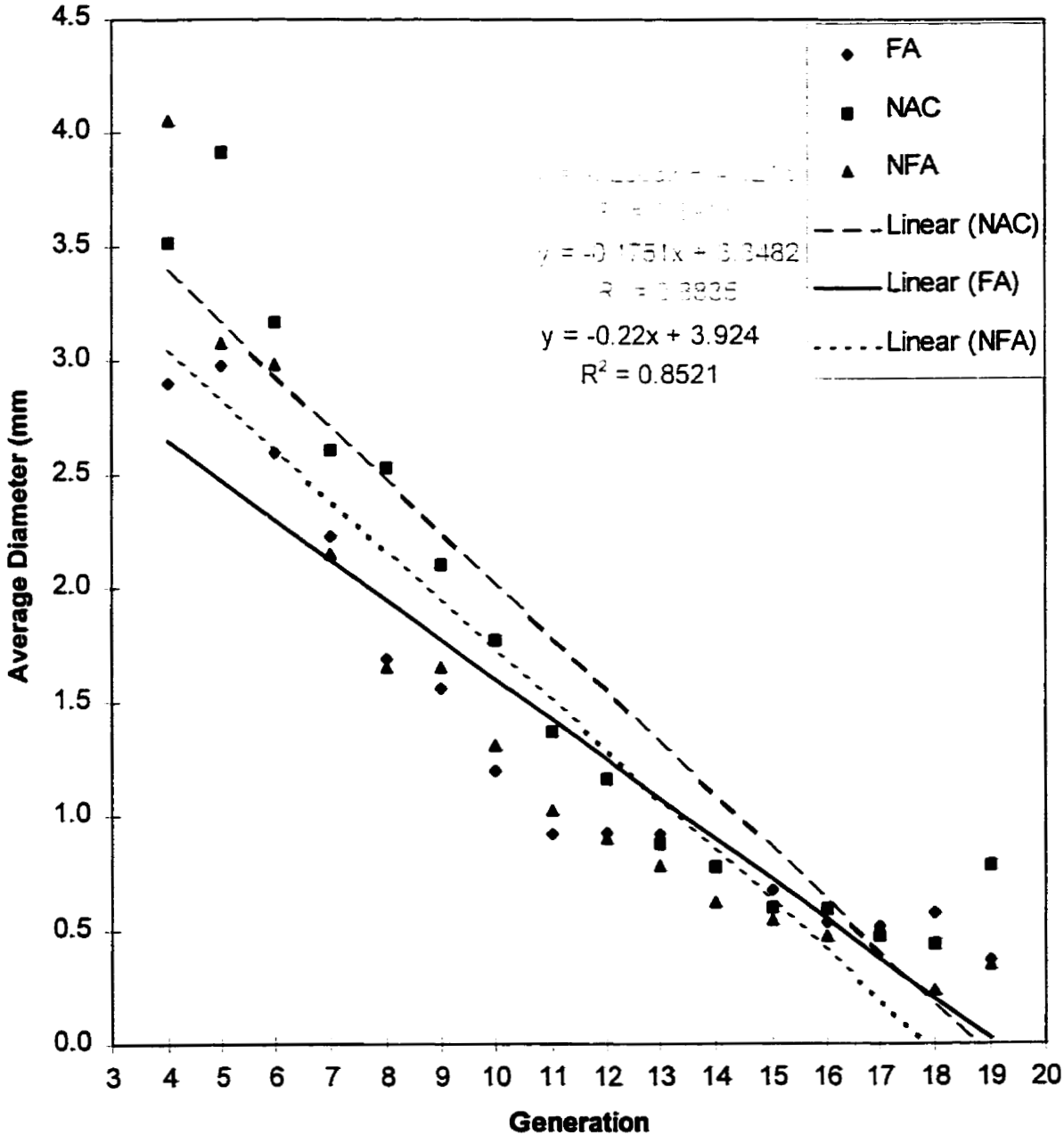

Figure 18A. Average change of major daughter airway diameter with increasing generation.

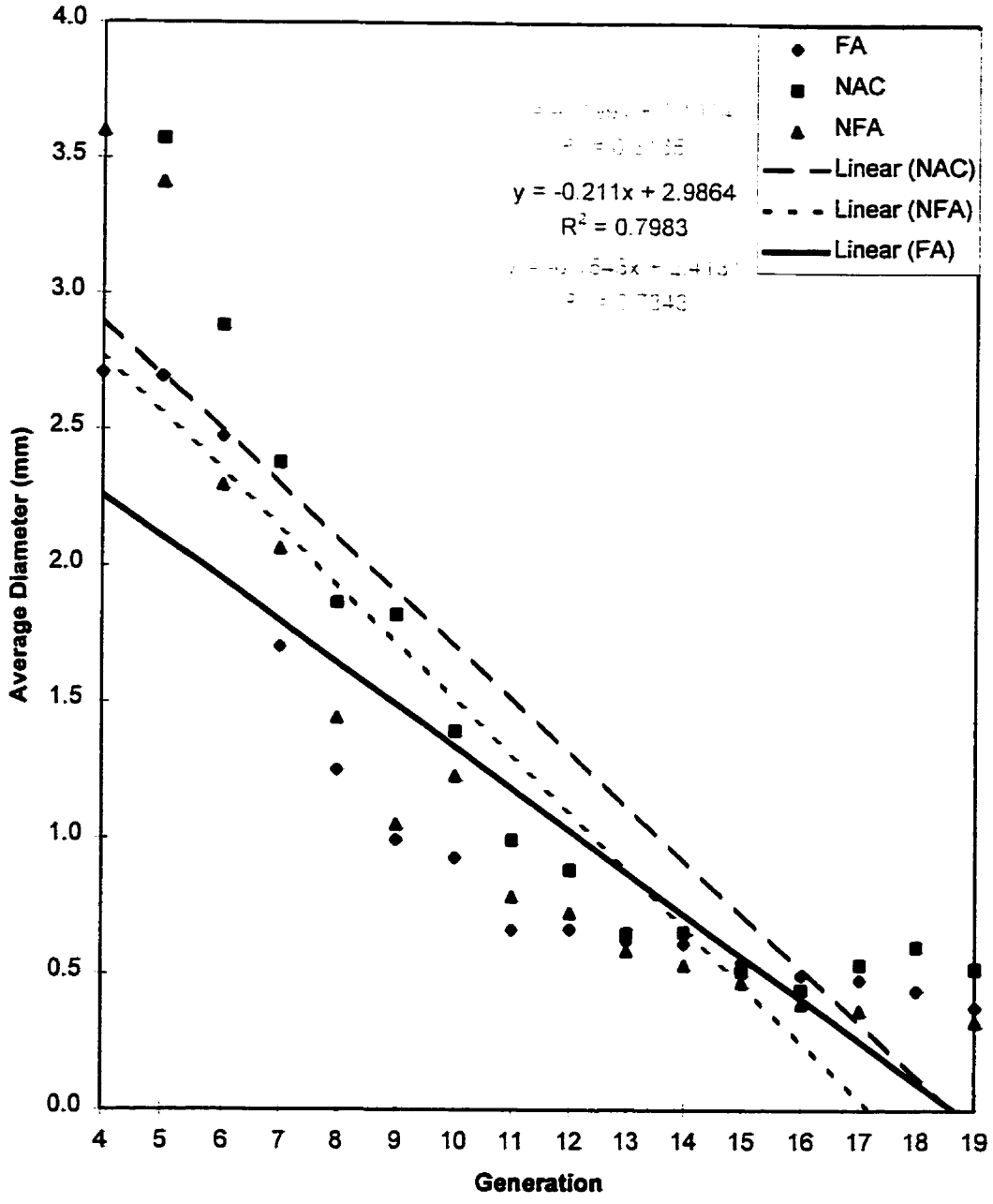

Figure 18B. Average change of minor daughter airway diameter with increasing generation.

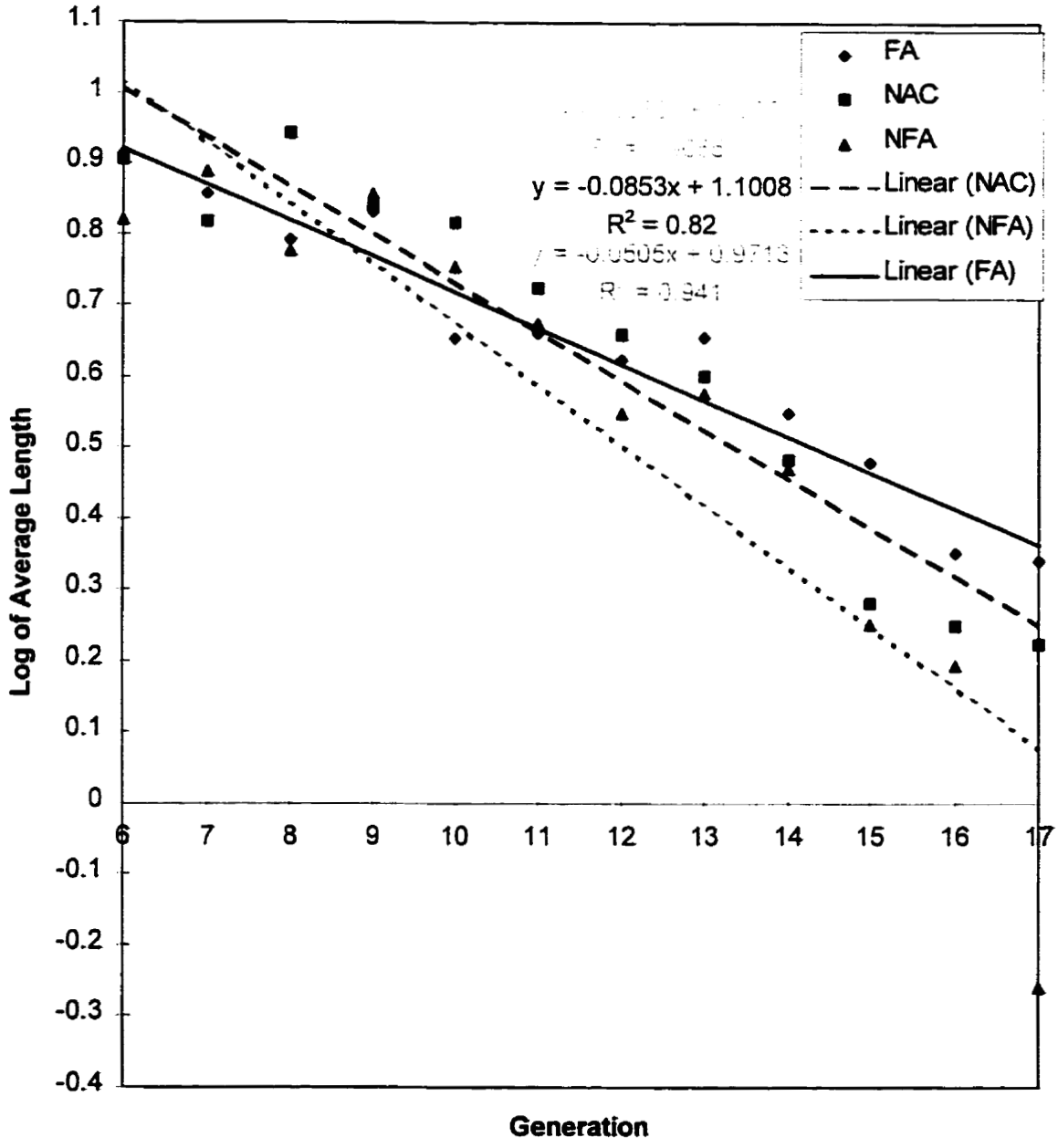

Figure 19A. Average change of major daughter airway log length with increasing generation.

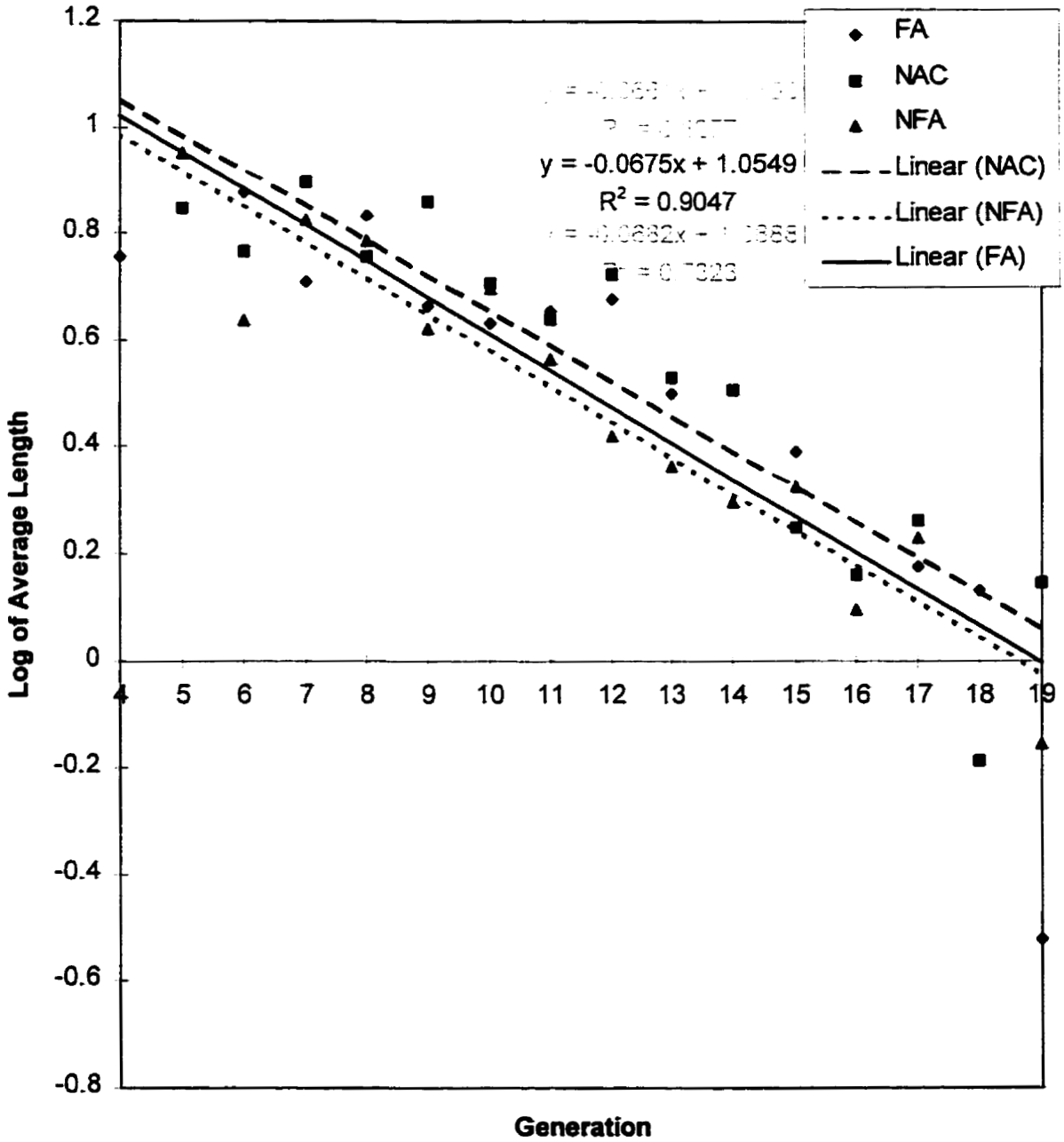

Figure 19B. Average change of minor daughter airway log length with increasing generation.

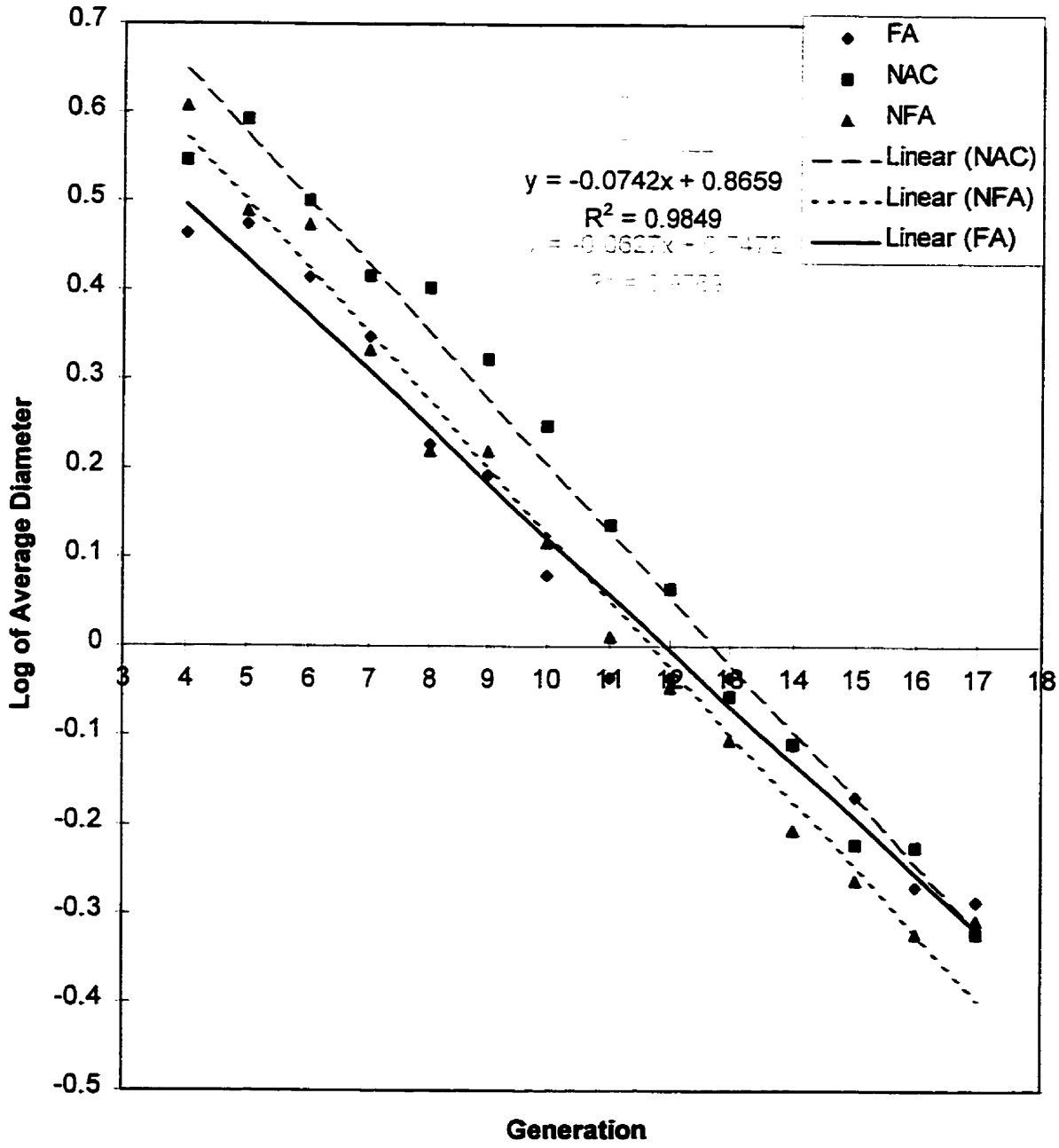

Figure 20A. Average change of major daughter airway log diameter with increasing generation.

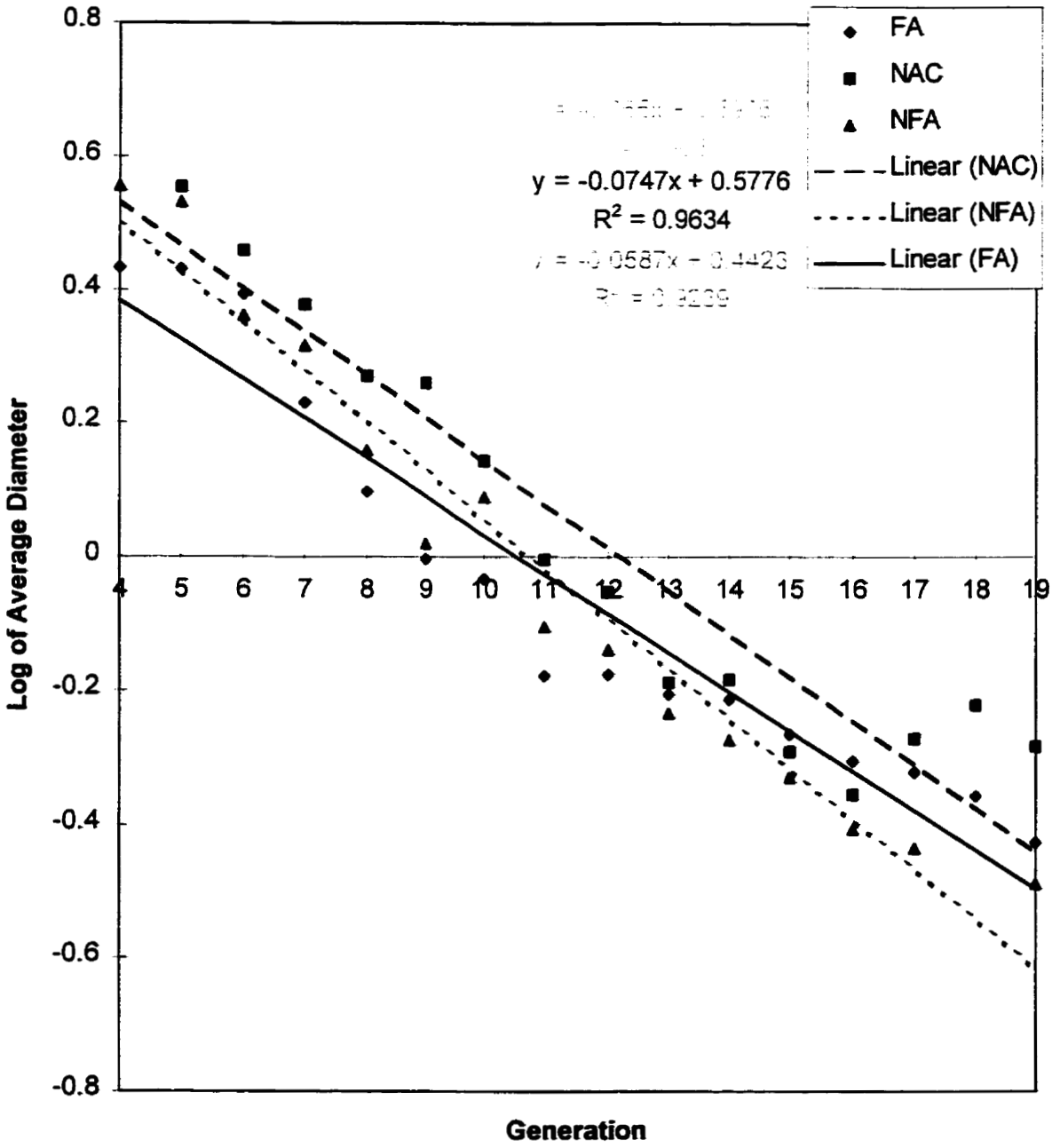

Figure 20B. Average change of minor daughter airway log diameter with increasing generation.

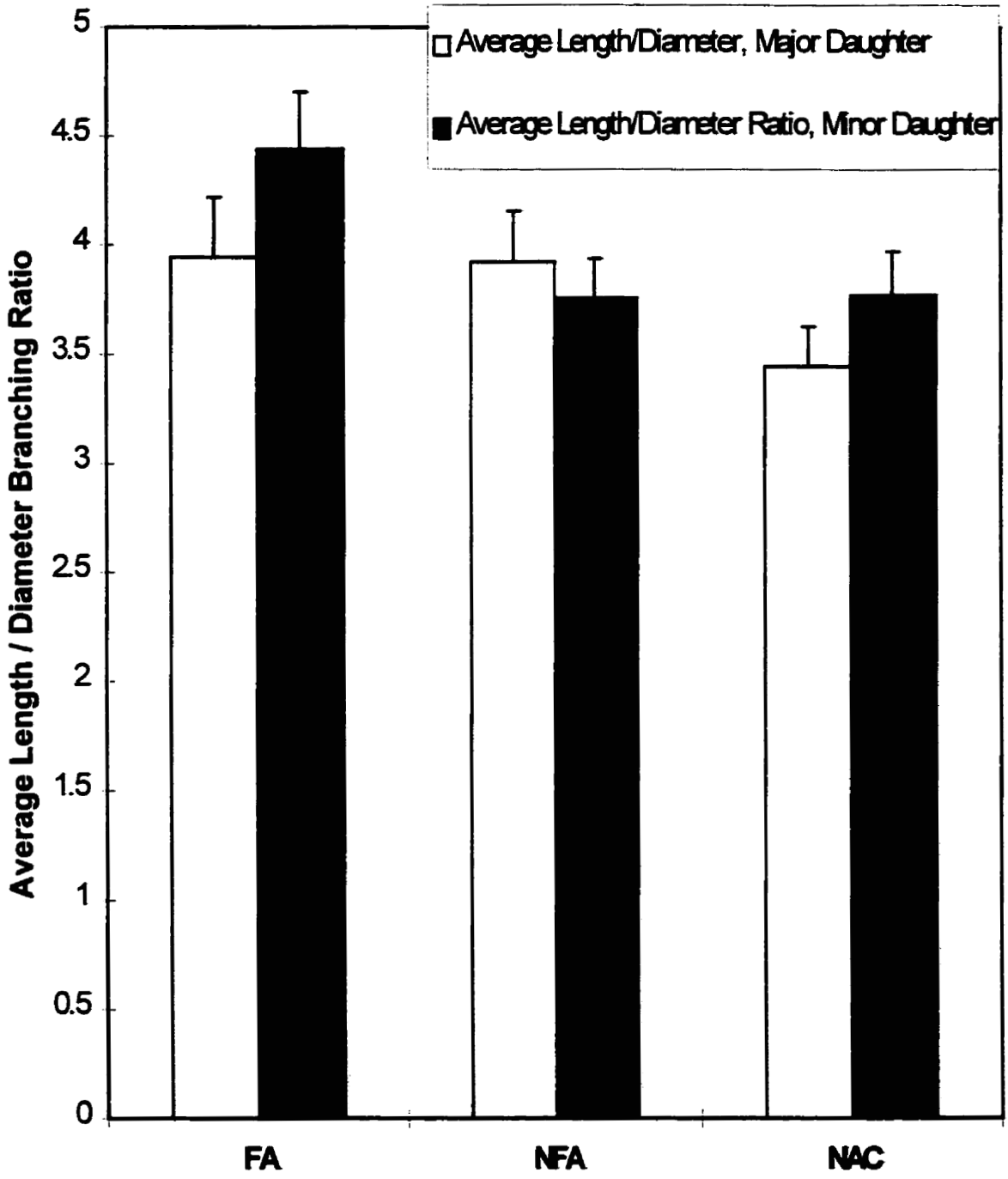

Figure 21. Average airway length / diameter ratio for both major daughter branches and minor daughter branches in all three groups of fatal asthma (FA), non-fatal asthma (NFA) and non-asthma control (NAC).

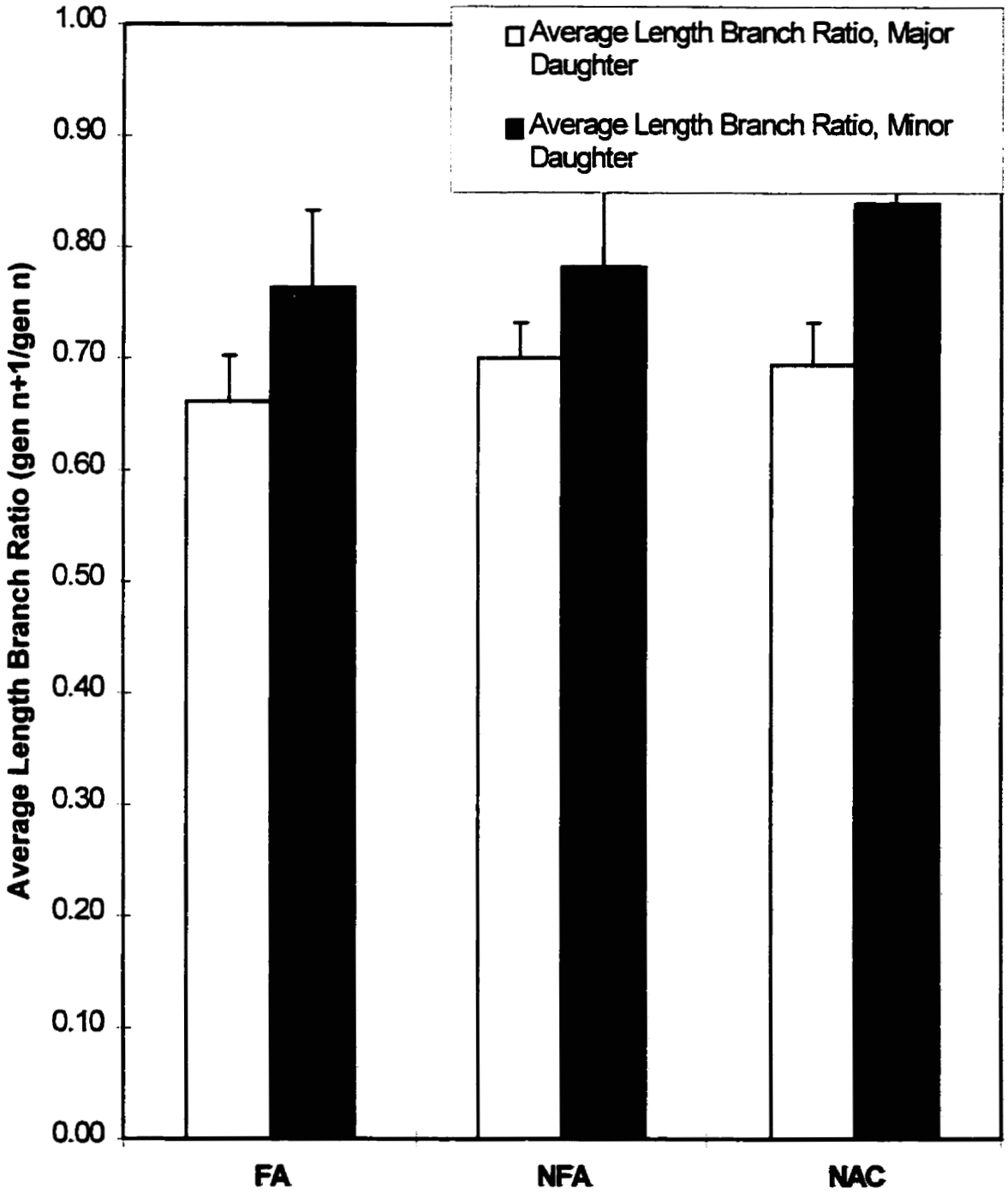

Figure 22. Average airway length branching ratio for both major daughter and minor daughter branches in all three groups of fatal asthma (FA), non-fatal asthma (NFA), and non-asthma control (NAC).

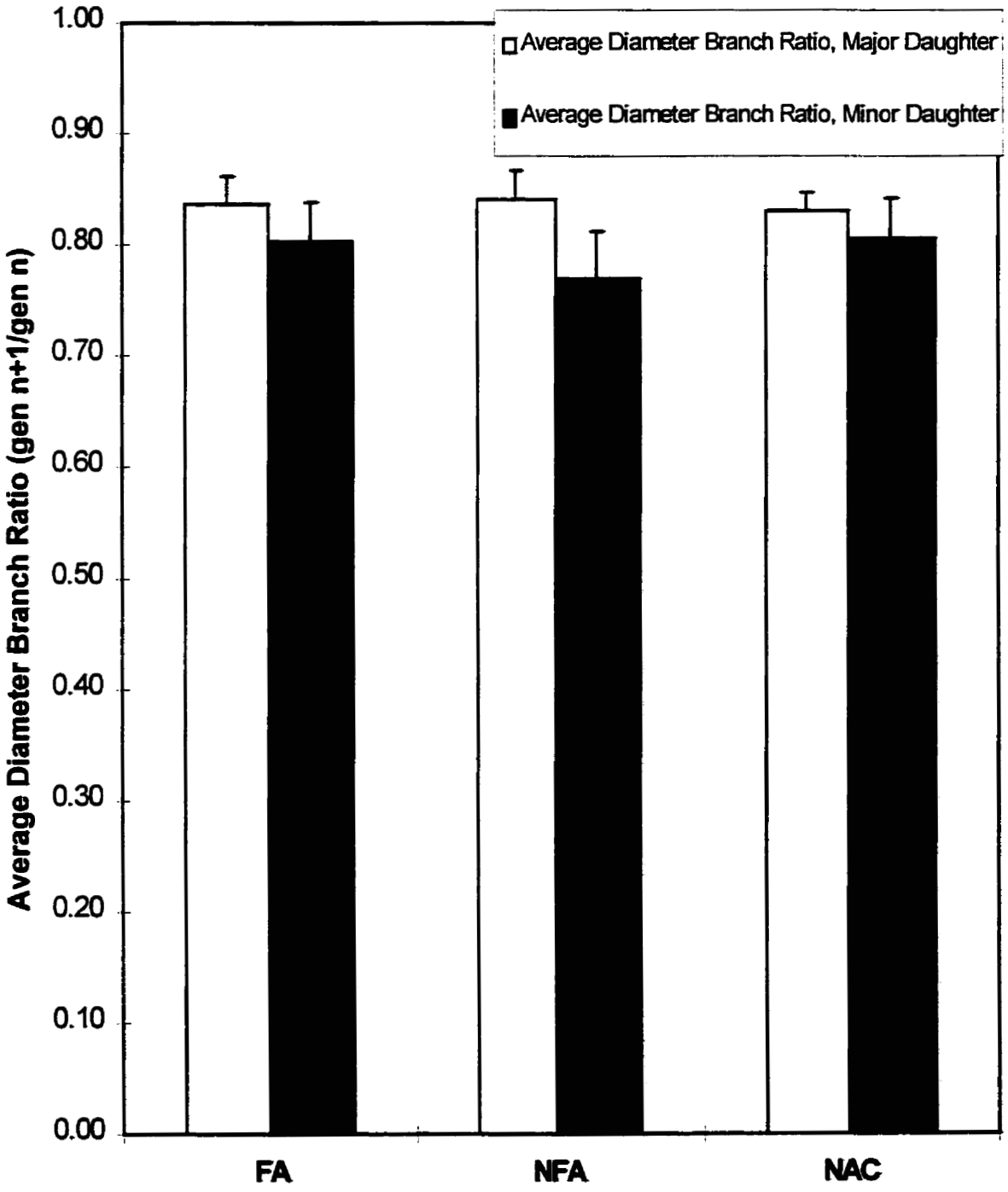

Figure 23. Average airway diameter branch ratio for both major and minor daughter branches in all three groups of fatal asthma (FA), non-fatal asthma (NFA) and non-asthma control (NAC).

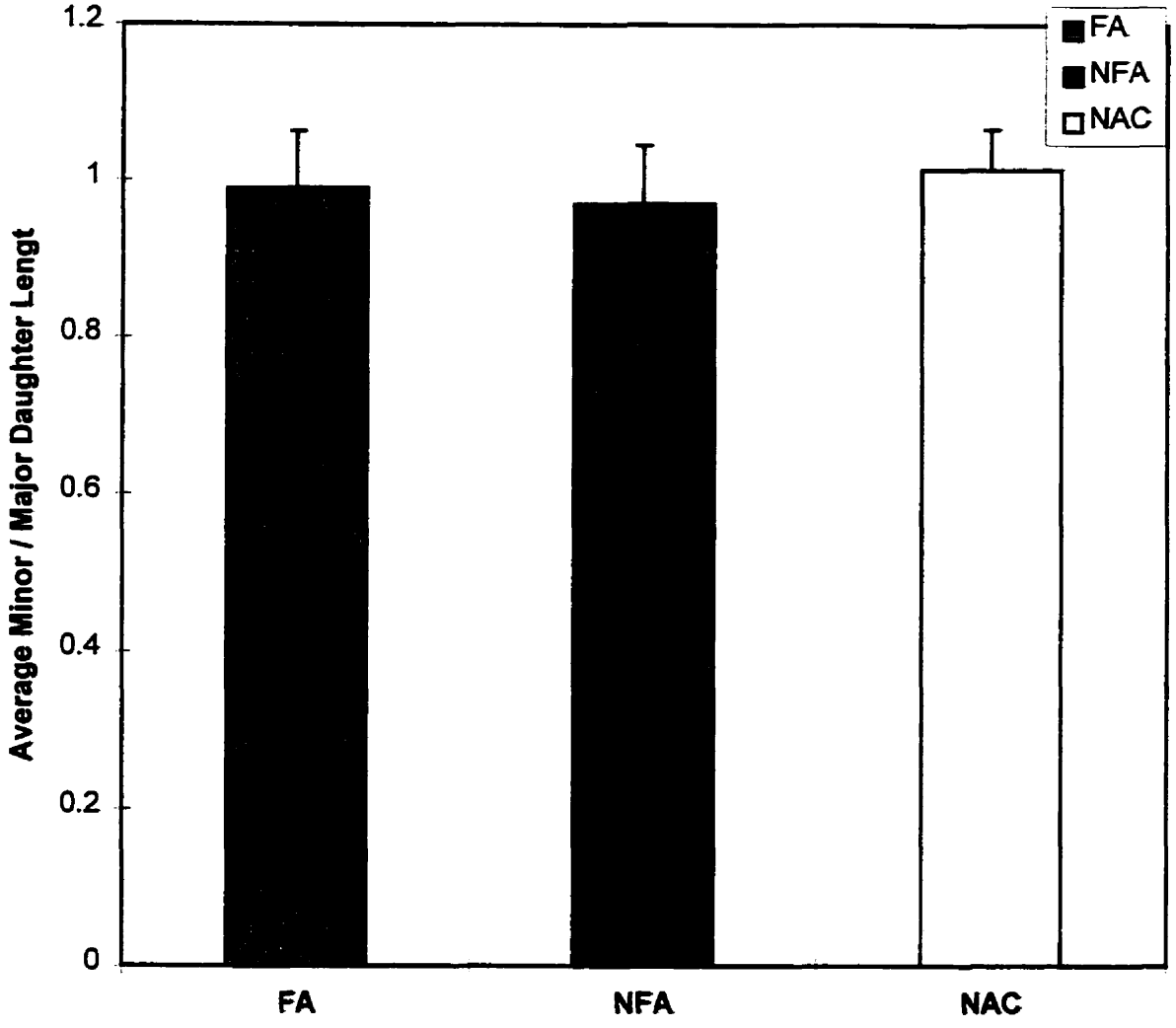

Figure 24. Average airway minor daughter / major daughter length in all three groups of fatal asthma (FA), non-fatal asthma (NFA) and non-asthma control (NAC).

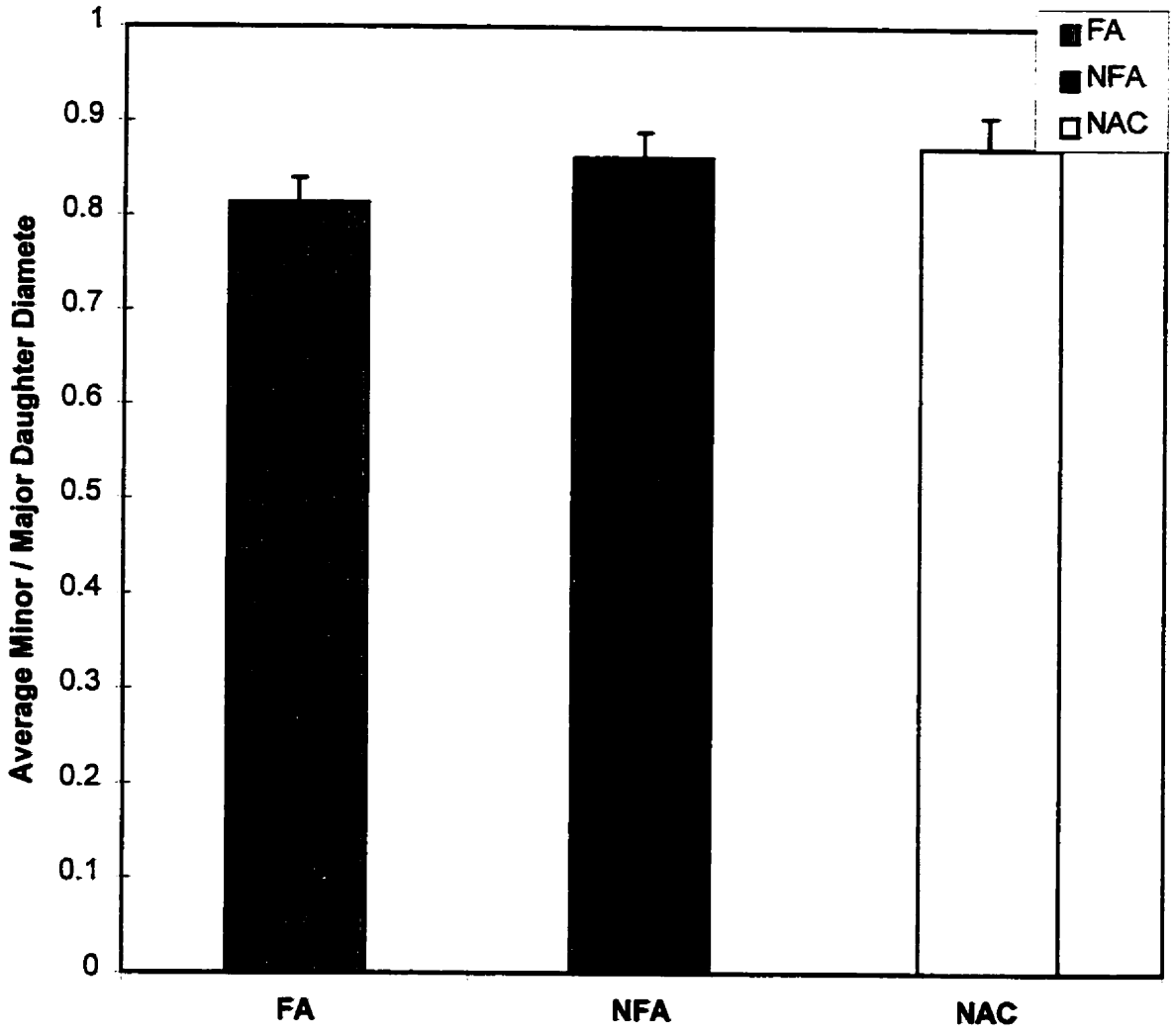

Figure 25. Average airway minor daughter / major daughter diameter in all three groups of fatal asthma (FA), non-fatal asthma (NFA), and non-asthma control (NAC).

Fractal Dimensions

No variation was found on ten repeated measures of a circle, square, Koch curve and 3 lung casts (Figure 26). In comparison to the known fractal dimension for these objects and the mean of ten measurements, coefficient of variability was found to be less than 1.4% (circle 0.21 %, square 1.39 %, Koch curve 0.56 %). The coefficient of variation for the fractal dimension of portions of a lung cast compared to the whole lung cast fractal dimension were 1.99%, 1.89% and 0.99% for a lung cast from each of FA, NFA and NAC respectively. Results for all of the tests 1-7 are shown in Table 5, including coefficient of variation (CV) for each test, and the p value from the paired t-test. In addition, no significant differences were found between D1 and D2 for each lung cast in each group ($p = 1.0$) (Table 6).

The average fractal dimension for each group is given in Figure 27. The fractal dimension was significantly different between FA and NAC ($p = 0.028$). The comparisons of small, medium and large box sizes for each group is shown in Figure 28. The fatal asthma group shows three distinct fractal dimensions, whereas the NAC group has two.

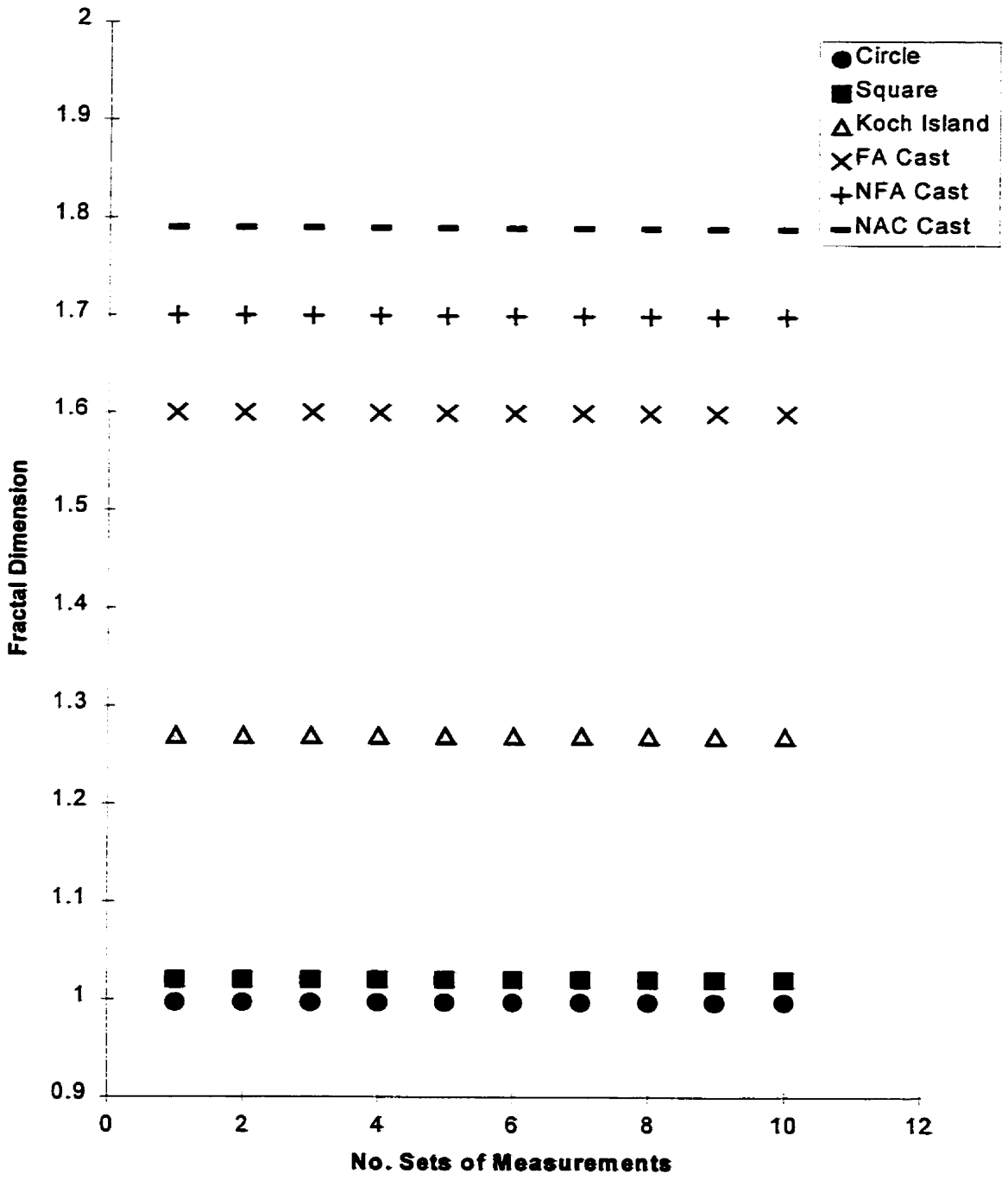

Figure 26. Cumulative mean plot for the measured fractal dimension of a circle, a square, a Koch island, and three lung casts from each group of fatal asthma (FA), non-fatal asthma (NFA) and non-asthma control (NAC), showing little variation between ten sets of measurements.

Table 5. Results of tests 1-7 to measure the reliability of the fractal method. See text for a description of each test.

Test	Coefficient of Variance (CV)	T-test (p value)
1	circle: 0.21% square: 1.39% koch: 0.56% FA: 0 NFA: 0 NAC: 0	
2	FA: 0.31% NFA: 1.37% NAC: 0.50%	0.9242
3	FA: 3.77% NFA: 0.25% NAC: 0.77%	0.9849
4	FA: 1.45% NFA: 1.21% NAC: 0.58%	0.0472
5	FA:3.74% NFA: 3.38 NAC: 1.37%	0.0074
6	0.42%	0.1934
7	FA: 1.99% NFA: 1.89% NAC:0.99%	

Table 6. Fractal dimension of casts on one side (D1) and the other (D2) in fatal asthmatic airway casts (FA) ,non-fatal asthma casts (NFA) and non-asthma control casts (NAC).

	FA	*NFA*	*NAC*
D1	1.773	1.662	1.617
D2	1.777	1.672	1.608

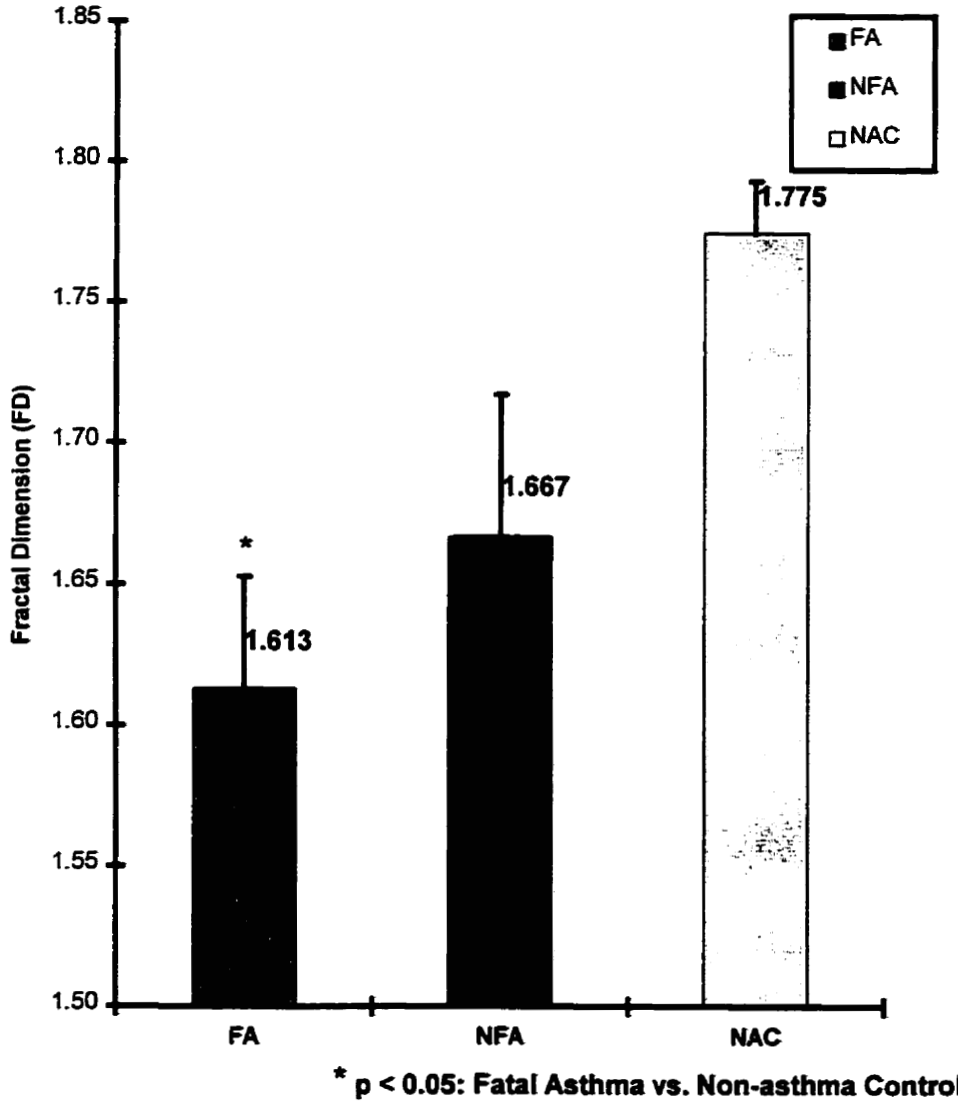

Figure 27. Average fractal dimension (D) in each of three groups of fatal asthma (FA), non-fatal asthma (NFA) and non-asthma control (NAC).

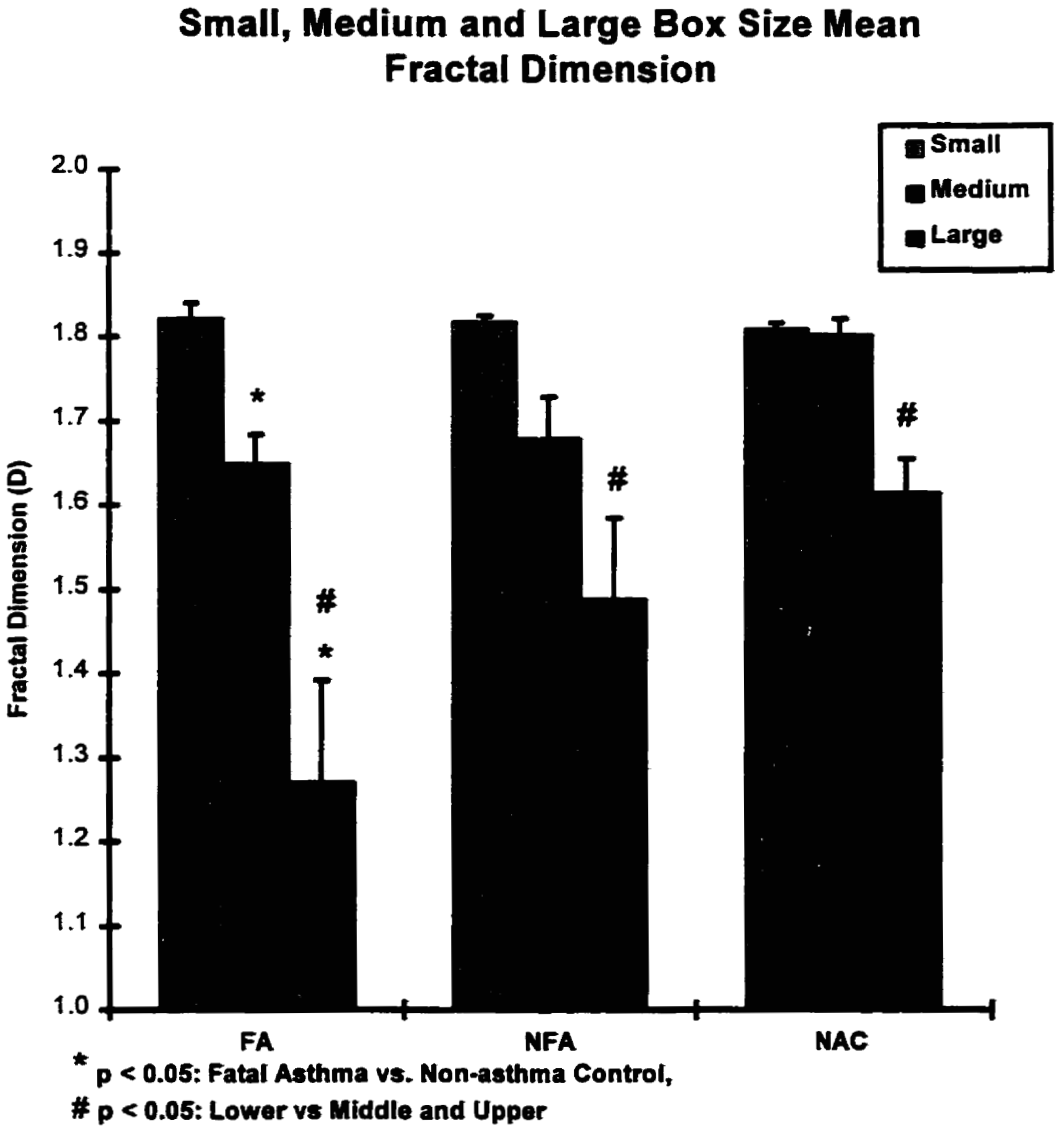

Figure 28. Fractal dimension (D) of all three groups of fatal asthma (FA), non-fatal asthma (NFA) and non-asthma control (NAC). The fractal dimension has been calculated for the small, medium and large box sizes, in order to determine if the lung casts are a composite of multiple fractal structures, each with their own fractal dimension.

Small Airway Disease in Asthma

Cases

Ten control, 11 non fatal and 10 fatal asthma cases were studied for the terminal bronchioles (TB). Seven cases in each group were studied for the respiratory bronchioles. Table 7 shows the patient characteristics for all airway types, followed by Table 8 which indicates cause of death for each case. The three groups did not differ in mean age or number of males and females. All of the cases were non-smokers, determined by histology and next of kin questionnaires. Generally, in the asthmatic cases, there was a long history of persistent asthma, and use of ß-Agonists, and inhaled or oral corticosteroids.

The mean basement membrane perimeters for each airway type are shown in Table 9, along with the number of airways measured. The interobserver (including grid variability)(Table 10) and intraobserver (including grid variability (Table 11), and not including grid variability (Table 12)) overall mean coefficient of variation was 16.1%, 20.7% and 3.8% respectively, which was averaged over all airway dimensions measured. Coefficients of variation for each individual dimension or parameter are given in Table 10, 11 and 12.

Table 7. Patient characteristics for the small airway study.

	Terminal Bronchioles			Respiratory Bronchioles		
	FA	NFA	NAC	FA	NFA	NAC
Age, yr						
Mean	30.6	29.3	33.8	31.4	24.4	32
Range	16-59	18-46	18-50	18-59	18-29	18-50
Sex, M/F	5/5	5/6	5/5	4/3	4/3	4/3
Asthma Duration, yr						
Mean	15.1	14.9	0	13.5	14.6	0
Range	6-26	2-31	0	6-26	2-31	0
Asthma Grade						
Overall	34	8	0	24	5	0
Average	3.4	0.89	0	3.4	0.83	0
Treatment, % of subjects						
B-Agonists	100	70	0	100	71.4	0
In-Steroids	50	50	0	42.9	42.9	0
Oral Steroids	40	10	0	28.6	14.3	0

Table 8. Subject cause of death and age for the small airway study. All subjects were used for the measurement of terminal bronchioles. Those with stars (*), were used for the measurement of respiratory bronchioles, generation 1-3.

Group	Case	Age	Cause of Death
FA*	H253	55	Asthma
FA*	H248	59	Asthma
FA*	H296	18	Asthma
FA*	H297	18	Asthma
FA*	H316	24	Asthma
FA*	H324	20	Asthma
FA	H245	24	Asthma
FA	H266	46	Asthma
FA	H323	16	Asthma
FA*	H260	26	Asthma
NFA*	H234	29	Intraventricular hemorrhage
NFA*	H235	33	Drug toxicity, obesity
NFA*	H236	21	Acute ethanol toxicity
NFA*	H269	23	Asphyxia, suffocation in avalanche
NFA*	H314	25	Morbid obesity, enlargement of heart and liver
NFA*	H334	18	Diabetic ketoacidosis
NFA	H279	25	Congenital heart disease
NFA	H308	45	Multiple drug toxicity, COPD, Obesity
NFA	H259	46	Pulmonary congestion, edema, Chronic heart disease
NFA*	H329	22	Epilepsy
NFA	H306	35	Acute myocardial infarction, atherosclerosis
NAC	H338	33	Pneumonia, Neural and musculoskeletal dev. disorder
NAC	H271	40	Hepatocellular carcinoma, marfan's syndrome
NAC*	H267	42	Primary dissecting aneurysm of left coronary artery
NAC	H339	41	Renal transplant rejection, CMV enteritis, pneumonia
NAC*	H288	50	Leukemia
NAC*	H330	21	Motor vehicle accident
NAC*	H331	18	Brainstem tumor, acute bronchopneumonia
NAC*	H332	33	Subarachnoid hemorrhage
NAC*	H340	29	Seizure disorder
NAC*	H343	31	Self inflicted gunshot wound to the head

Table 9. Mean basement membrane perimeter (mm) for terminal bronchioles (TB), respiratory bronchioles generation 1-3 (RB1,2,3), followed by the number of airways measured in each group (n). Values are mean ± standard deviation.

	TB	*RB1*	*RB2*	*RB3*
FA	2.34 ± 0.71	2.06 ± 1.38	1.23 ± 0.38	1.18 ± 0.50
	n = 30	n = 24	n = 24	n = 24
NFA	1.64 ± 0.63	1.68 ± 0.92	1.19 ± 0.53	0.92 ± 0.30
	n = 33	n = 24	n = 24	n = 24
NAC	1.80 ± 0.37	1.76 ± 0.87	1.16 ± 0.50	1.01 ± 0.32
	n = 30	n = 24	n = 24	n = 24

Table 10. Interobserver variability, including grid variability for all airway dimensions in terminal bronchioles (TB) and respiratory bronchioles generation 1-3 (RB1,2,3). Values are given as mean followed by range.

Coefficient of Variation (CV %)

Dimensions	TB	RB1	RB2	RB3	Average
Perimeter	3.4 (1.2-7.4)	5.1 (1.6-11.8)	15.7 (8.0-25.3)	19.0 (5.4-35.4)	10.8
Epithelium	9.7 (6.5-13.0)				9.7
Mucous Cells	10.4 (4.0-16.9)				10.4
Smooth Muscle	10.8 (5.8-19.5)	27.6 (7.2-48.5)	12.1 (3.1-19.1)	30.2 (15-54.4)	20.2
Blood Vessel	33.0 (16.8-68.8)	6.9 (4.6-11.8)	56.1 (10.5-141.4)	23.8 (5.4-41.0)	30.0
Interstitium	6.2 (2.3-13.4)	6.3 (0.8-20.0)	42.4 (12.6-87.6)	43.1 (5.2-141.0)	24.5
Total Wall Thickness	6.4 (2.1-14.2)	3.0 (0.3-7.2)	16.9 (0.3-27.2)	19.2 (14.8-28.3)	11.4
Lumen Free	7.7 (1.2-21.3)	11.6 (3.0-31.6)	19.0 (12.0-30.1)	17.7 (12.0-25.7)	14.0
Lumen Diameter	7.7 (1.2-21.3)	11.6 (3.0-31.6)	19.0 (12.0-30.1)	17.7 (12.0-25.7)	14.0
Alveolar Wall Perimeter		7.2 (1.9-11.8)	14.2 (1.2-28.3)	13.8 (7.3-27.0)	11.7
Alveolar Wall		27.7 (6.3-72.2)	21.3 (6.3-35.4)	14.1 (7.3-23.3)	21.0
Alveolar Wall Thickness		25.1 (6.3-62.2)	13.8 (1.2-29.3)	15.01 (0.3-35.0)	18.0
Alveolar Lumen		10.4 (0.9-26.3)	17.9 (7.8-43.6)	6.7 (2.7-9.4)	11.7
Alveolar Lumen Diameter		10.4 (0.9-26.4)	18.2 (7.8-44.9)	6.7 (2.6-9.4)	11.8
Average	10.6	12.7	22.2	18.9	**16.1**

Table 11. Intraobserver variability including grid variability for dimensions of terminal bronchioles (TB) and respiratory bronchioles generation 1-3 (RB1,2,3)

	Coefficient of Variation (CV %)				
Dimensions	**TB**	**RB1**	**RB2**	**RB3**	**Average**
Perimeter	8.3	5.5	23.2	15.9	13.2
Epithelium	29.1				29.1
Mucous Cells	37.1				37.1
Smooth Muscle	24.2	12.6	31.2	38.0	26.5
Blood Vessel	11.3	3.9	24.3	36.1	18.9
Interstitium	17.4	20.5	51.1	40.3	32.3
Inflammation	22.8	54.0			38.4
Wall Thickness	5.8	6.7	18.4	26.6	14.4
Lumen Free	11.5	7.2	13.8	8.5	10.2
Lumen Diameter	10.2	7.2	13.8	8.5	9.9
Alveolar Perimeter		13.8	4.4	3.4	7.2
Alveolar Wall		42.8	56.1	25.8	41.6
Alveolar Wall Thickness		30.0	37.8	23.6	30.5
Alveolar Lumen Free		27.7	14.4	5.2	15.8
Alveolar Lumen Diameter		27.7	14.4	5.2	15.8
Average	17.8	20.0	25.2	19.8	**20.7**

Table 12. Intraobserver variability not including grid variability (Feature identification), for all dimensions of terminal bronchioles (TB), and respiratory bronchioles generation 1-3 (RB1,2,3)

	Coefficient of Variation (CV %)				
Dimensions	**TB**	**RB1**	**RB2**	**RB3**	**Average**
Perimeter	2.1	1.6	2.5	1.9	2.0
Epithelium	5.3				5.3
Mucous Cells	24.3				24.3
Smooth Muscle	8.9	1.6	2.4	1.9	3.7
Blood Vessel	3.8	1.6	2.4	1.9	2.4
Interstitium	2.8	1.2	9.6	1.9	3.9
Inflammation	16.6	1.6			9.1
Wall Thickness	2.6	1.0	4.0	1.9	2.4
Lumen Free	4.7	1.6	3.7	2.6	3.2
Lumen Diameter	4.7	1.6	3.7	2.6	3.2
Alveolar Wall Perimeter		2.1	1.7	1.0	1.6
Alveolar Wall		2.2	1.7	5.8	3.2
Smooth Muscle Cell		2.2	1.7		2.0
Total Wall Thickness		2.2	1.7	5.8	3.2
Alveolar Lumen Free		2.2	3.5	1.0	2.2
Alveolar Lumen Diameter		2.2	3.5		2.8
Average	7.6	1.8	3.2	2.6	**3.8**

Airway Smooth Muscle Thickness and Distribution

The thickness of smooth muscle was significantly greater in cases of fatal asthma than in non-asthma control cases for all four small airway classes (TB, RB1, RB2 , RB3) (figure 29). Smooth muscle areas of NFA small airways were intermediate between the FA and NAC groups. None of the differences were statistically significant however, except for the TB in the NFA group, which were significantly different from NAC. In both FA and NFA, the thickness of smooth muscle was significantly greater in RB1 compared to RB3, whereas in NAC, there was no significant differences in smooth muscle content between the three generations of respiratory bronchioles.

For all four categories of airway (TB, RB1, RB2, RB3), and for all groups (FA, NFA, NAC), with one exception being TB in the FA group, the thickness of muscle was greater in the upper lobes compared to the lower lobes (Table 13).

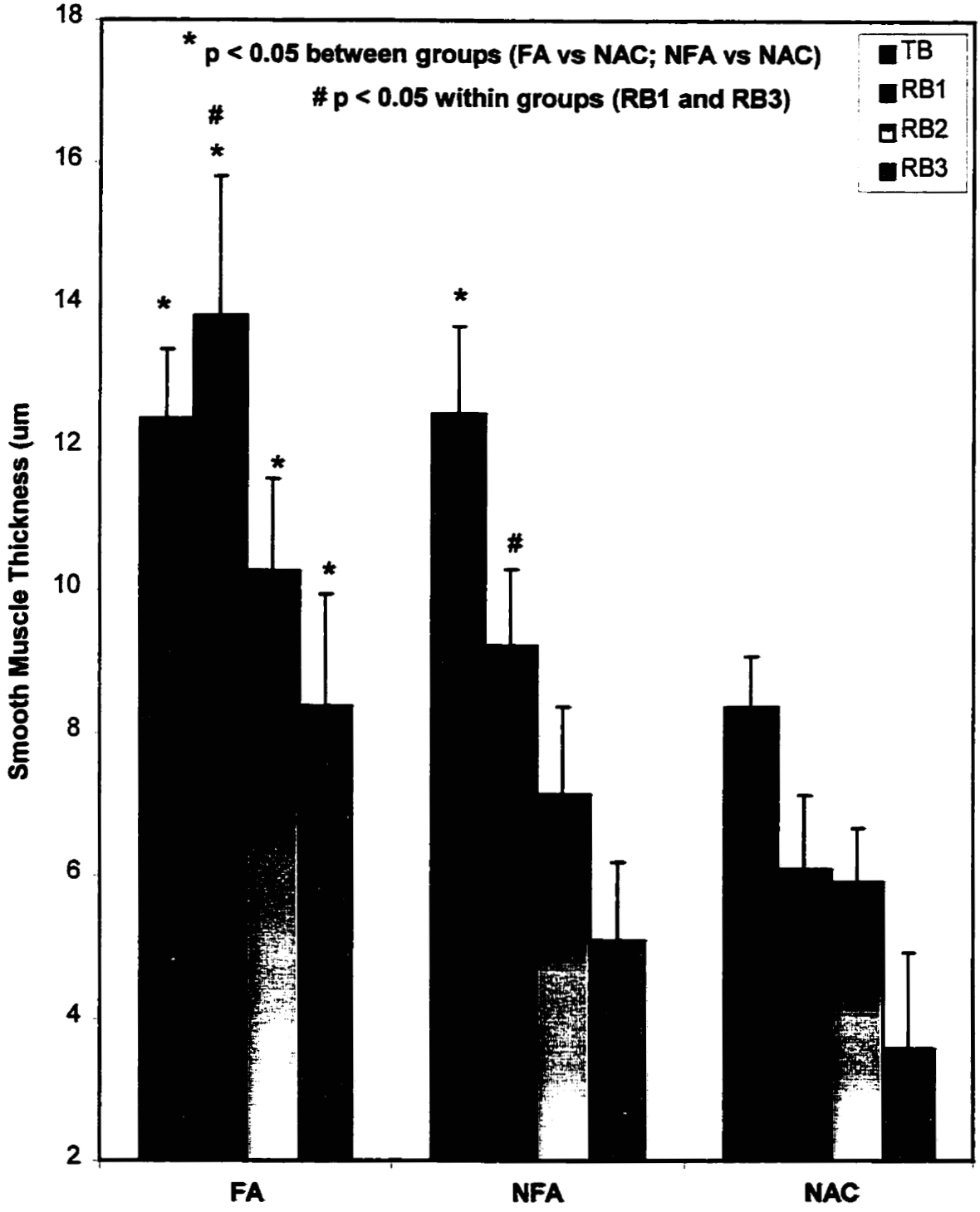

Figure 29. Overall smooth muscle thickness in the terminal bronchioles and respiratory bronchioles (generation 1-3), of fatal asthmatics (FA), non-fatal asthmatics (NFA) and non-asthma controls (NAC).

Table 13. Smooth muscle thickness distribution between upper and lower lobes in the small airways consisting of terminal bronchioles (TB) and respiratory bronchioles generation 1-3 (RB1,2,3) in fatal asthmatics (FA), non-fatal asthmatics (NFA) and non-asthma controls (NAC). Values are mean ± standard error.

Smooth Muscle Thickness (um)

	TB		RB1		RB2		RB3	
	upper	lower	upper	lower	upper	lower	upper	lower
FA	11.62 ± 1.82	12.40 ± 1.02 *	16.44 ± 3.85	12.81 ± 1.33 * **	12.86 ± 1.65 #	9.22 ± 0.88 *	11.97 ± 1.55 **#	6.29 ± 1.12 *
NFA	14.5 ± 1.35 ***	11.00 ± 1.19	10.94 ± 1.46	7.93 ± 1.60	8.29 ± 1.18	5.85 ± 1.48	4.79 ± 1.70	5.32 ± 1.37
NAC	8.88 ± 1.04	8.09 ± 0.99	8.15 ± 2.43	5.06 ± 0.74	7.15 ± 1.64	5.40 ± 1.08	7.28 ± 1.00 #	1.73 ± 0.83

* $p < 0.05$; FA vs NAC
** $p < 0.05$; FA vs NFA
*** $p < 0.05$: NFA vs NAC
\# $p < 0.05$; upper and lower lobes

Other Airway Features

In the terminal bronchiole, the only significant difference was found in the amount of mucous cells in the epithelium in asthma compared to NAC ($p = 0.0045$). Basement membrane thickness, inflammation or wall thickness were all increased in FA and NFA compared to NAC but none of the differences were statistically significant (Table 14). In the respiratory bronchioles a similar trend was seen. The only significant difference was found in the RB1 wall thickness between FA and both NFA and NAC ($p = 0.0066$) (Table 14). The measure of bronchoconstriction was significantly greater in the terminal bronchioles of fatal asthmatics compared to both non fatal asthmatics and non asthma controls ($p = 0.017$).

Table 14. Thickness of other airway features in μm in the terminal bronchioles (TB) and respiratory bronchioles generation 1-3 (RB1,2,3) in fatal asthmatics (FA), non-fatal asthmatics (NFA) and non-asthma controls (NAC). Values are ± standard error.

	Airway Features	FA	NFA	NAC
TB	Mucous Cells	2.18 ± 0.49 *	0.91 ± 0.1	0.0
	Basement Membrane	5.70 ± 1.23	5.65 ± 1.11	4.0 ± 0.5
	Inflammation	7.25 ± 1.45	5.76 ± 1.14	4.9 ± 0.74
	Wall Thickness	86.67 ± 9.1	81.7 ± 6.5	75.0 ± 5.4
RB1	Mucous Cells	2.1 ± 1.91	0.0	0.0
	Basement Membrane	5.02 ± 2.5	1.23 ± 0.62	1.22 ± 0.38
	Inflammation	6.06 ± 1.75	3.92 ± 1.07	3.2 ± 1.07
	Wall Thickness	70.28 ± 8.1 **	46.0 ± 5.0	45.0 ± 4.01
RB2	Inflammation	3.67 ± 0.92	4.28 ± 1.47	1.95 ± 0.49
	Wall Thickness	27.9 ± 1.36	24.6 ± 5.18	24.1 ± 2.59
RB3	Inflammation	1.58 ± 0.75	1.95 ± 0.38	0.92 ± 0.5
	Wall Thickness	18.37 ± 1.11	14.3 ± 1.91	13.4 ± 1.91

The Lung Parenchyma in Asthma

Cases

Subject characteristics (age, sex, duration of asthma, asthma grade and treatments), for the seven cases in each group are shown in Table 15 followed by Table 16, which indicates causes of death for each case. No differences in mean age or the number of males and females in each group were found. Overall, the asthma cases revealed a long history of persistent asthma, with the use of B-Agonists and inhaled or oral corticosteroids. All of the cases were non-smokers, ascertained by next of kin questionnaires and confirmed by histologic analysis of lung sections.

Table 15. Patient characteristics for the parenchymal study

	FA	NFA	NAC
Age, yr			
Mean	31.4	24.4	32.0
Range	18-59	18-29	18-50
Sex, M/F	4/3	4/3	4/3
Asthma Duration, yr			
Mean	13.5	14.6	0
Range	6-26	2-31	0
Asthma Grade			
Overall	24	5	0
Average	3.4	0.83	0
Treatment, % of subjects			
β-Agonists	100	71.4	0
In-Steroids	42.9	42.9	0
Oral Steroids	28.6	14.3	0

Table 16. Subject cause of death and age for the parenchymal study.

Group	Case	Age	Cause of Death
FA	H253	55	Asthma
FA	H248	59	Asthma
FA	H296	18	Asthma
FA	H297	18	Asthma
FA	H316	24	Asthma
FA	H324	20	Asthma
FA	H260	26	Asthma
NFA	H234	29	Intraventricular hemorrhage
NFA	H235	33	Drug toxicity, obesity
NFA	H236	21	Acute ethanol toxicity
NFA	H269	23	Asphyxia, suffocation in avalanche
NFA	H314	25	Morbid obesity, enlargement of heart and liver
NFA	H334	18	Diabetic ketoacidosis
NFA	H329	22	Epilepsy
NAC	H267	42	Primary dissecting aneurysm of left coronary artery
NAC	H288	50	Leukemia
NAC	H330	21	Motor vehicle accident
NAC	H331	18	Brainstem tumor, acute bronchopneumonia
NAC	H332	33	Subarachnoid hemorrhage
NAC	H340	29	Seizure disorder
NAC	H343	31	Self inflicted gunshot wound to the head

Parenchymal Smooth Muscle Thickness and Distribution

The mean alveolar wall perimeters for each group are shown in Table 17, along with the number of parenchymal areas measured. The interobserver (Table 18) and intraobserver (Table 19) mean coefficient of variation was 5.36 % and 2.55 % respectively, for all parenchymal dimensions measured.

Table 17. Alveolar wall perimeter in fatal asthmatics (FA), non-fatal asthmatics (NFA) and non-asthma controls (NAC). Values are mean ± standard deviation.

	PAR
FA	7.77 ± 2.52
	n = 24
NFA	5.73 ± 3.06
	n = 24
NAC	7.82 ± 2.09
	n = 24

Table 18. Interobserver variability in the parenchyma dimensions measured. Values are mean followed by range in brackets.

Coefficients of Variation (CV %)	
Dimensions	**Parenchyma**
Perimeter	2.3 (0.5-5.9)
Alveolar Duct Wall Smooth Muscle	11.9 (0.5-33.
Alveolar Wall Smooth Muscle	5.6 (1.3-9.9)
Blood Vessel Smooth Muscle	9.3 (0.5-29.7)
Other Wall Features	7.2 (0.3-12.2)
Lumen Free	2.0 (0.01-7.5)
Blood Vessel Lumen	2.6 (0.5-5.9)
Total Parenchymal Thickness	2.0 (0.08-5.9)
Average	**5.4**

Table 19. Intraobserver variability in the parenchyma dimensions measured

Coefficient of Variation (CV %)	
Dimensions	**Parenchyma**
Perimeter	0.9
Alveolar Duct Wall Smooth Muscle	0.9
Alveolar Wall Smooth Muscle	7.7
Blood Vessel Smooth Muscle	0.9
Other Wall Features	5.0
Lumen Free	1.7
Blood Vessel Lumen	
Total Parenchymal Thickness	0.9
Average	**2.6**

The thickness of smooth muscle in both alveolar duct wall and alveolar wall was significantly greater in cases of fatal asthma than in control cases (Figure 30). This was also found to be the case in non-fatal asthma in comparison to non-asthma controls. There were no significant differences between the fatal asthma and non-fatal asthma groups.

The thickness of smooth muscle in the alveolar duct wall was significantly greater in cases of fatal asthma than in control cases in both the upper and lower lobes (Table 20). In addition, the non-fatal asthma group had significantly greater smooth muscle in the lower lobe compared to the non-asthma control group. Alveolar duct smooth muscle was greater in the upper lobes compared to lower lobes for all three groups; however none of these differences were statistically significant.

In the alveolar wall, the thickness of smooth muscle was significantly greater in cases of fatal and non-fatal asthma compared to control cases for the upper lobe (Table 20). There were no significant differences for alveolar wall smooth muscle between fatal asthma and non-fatal asthma. Both the fatal asthma and the non-fatal asthma groups had significantly more smooth muscle in alveolar walls taken from the upper lobes compared to the lower lobes. This lobar effect was not seen in the non-asthma control group.

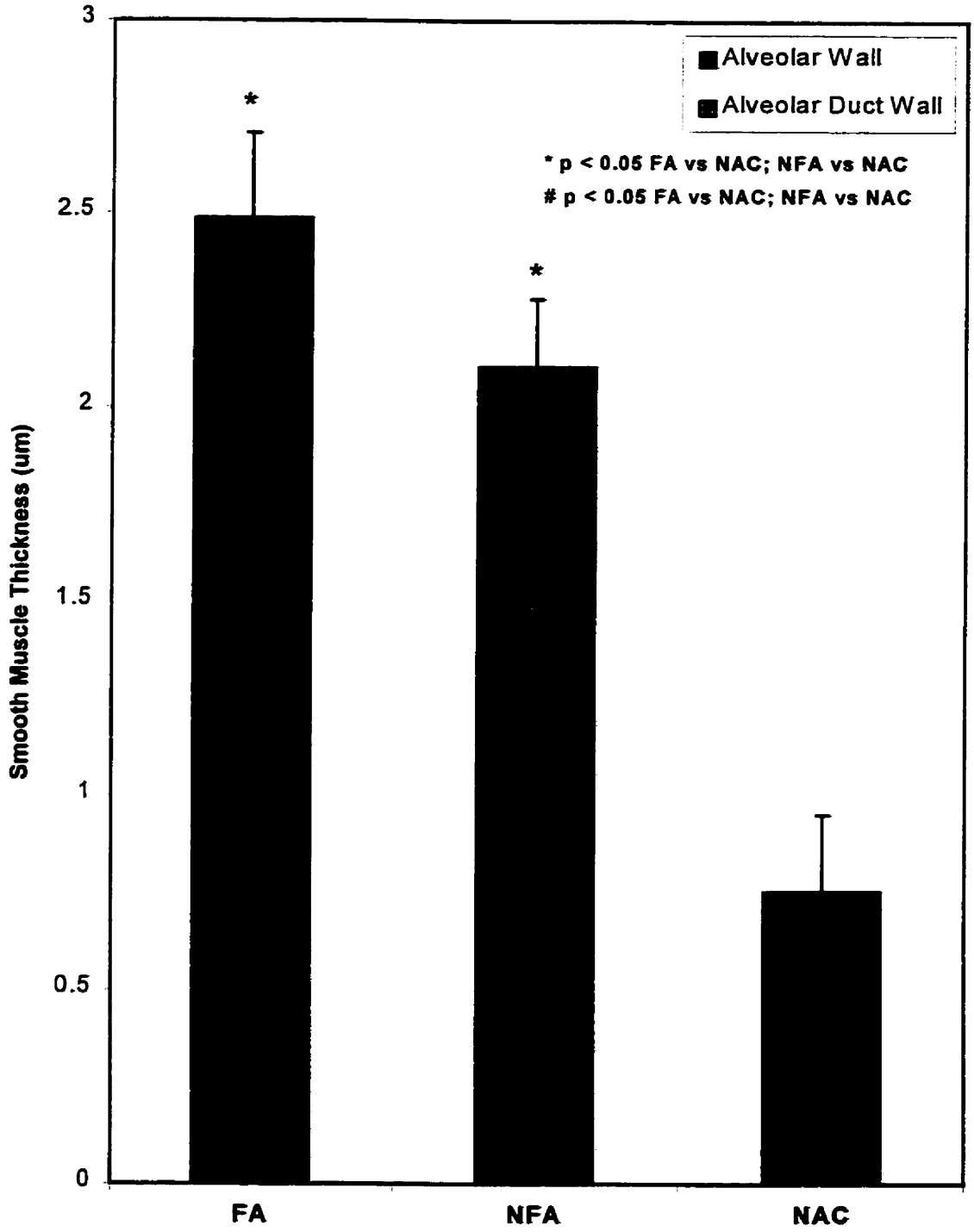

Figure 30. Overall smooth muscle thickness in both the alveolar duct (septal) wall and the alveolar wall in three groups of fatal asthma (FA), non-fatal asthma (NFA) and non-asthma control (NAC).

Table 20. Alveolar duct wall and alveolar wall smooth muscle thickness (um) in the upper and lower lobes in fatal asthmatics (FA), non-fatal asthmatics (NFA), and non-asthma controls (NAC). Values are mean ± standard error.

	Alveolar Duct		**Alveolar Wall**	
	upper	lower	upper	lower
FA	1.31 ± 0.33 †	0.82 ± 0.15 †	2.52 ± 0.56 †#	1.00 ± 0.25
NFA	0.82 ± 0.12	0.62 ± 0.15 ‡	1.97 ± 0.23 ‡#	0.85 ± 0.22
NAC	0.16 ± 0.12	0.14 ± 0.06	0.67 ± 0.18	0.57 ± 0.17

† $p < 0.01$; FA vs NAC
‡ $p < 0.01$; NFA vs NAC
# $p < 0.01$; upper and lower lobes

Other Parenchymal Features

The other parenchymal features measured were blood vessel smooth muscle, and parenchymal wall thickness. The blood vessel smooth muscle showed no significant difference between fatal asthma and control, whereas the parenchymal wall thickness was significantly thicker in cases of FA compared to NAC (Table 21).

Table 21. Parenchymal blood vessel smooth muscle thickness and total wall thickness in fatal asthmatics (FA), non-fatal asthmatics (NFA) and non-asthma controls (NAC). Values are mean ± standard error.

Thickness (μm)

Parenchymal Dimensions	FA	NFA	NAC
Blood Vessel Smooth Muscle	0.69 ± 0.14	0.55 ± 0.14	0.31 ± 0.10
Total Wall Thickness	10.70 ± 0.76*	10.41 ± 0.43	8.56 ± 0.60

* $p < 0.05$; FA vs NAC

Chapter 4: Discussion

Lung Casting

The purpose of this initial study was to determine if lung casting from patients with diseases associated with airway obstruction produces an accurate replica of the bronchial tree. The lungs casted were from persons who smoked, non smokers and a case of bronchiectasis. The technique is rapid, with the time from fixation of the lung to finished cast being 3-4 days. This is much quicker than using enzymatic digestion and KOH maceration as in other studies (Nettum, 1993).

Dow-Corning 734 RTV diluted by 10% (v/v) with low-viscosity silicone oil and introduced at –10 kPa negative pressure produces casts of the human bronchial tree that are well suited for research purposes. The injection mass fills airways only down to the level of the alveolar ducts, which eliminates the need for excessive trimming of the casts. The bronchiectasis case (Figure 11) illustrates the advantages of the negative pressure injection technique, as the silicone enters into distorted airways closed by mucous plugs and ectatic mucous gland ducts. Both of these features are characteristic of the disease. In addition, the small amount of shrinkage of the elastomer makes these preparations suitable for quantitative studies of airway dimensions and for modeling aerosol deposition. The preservation of surface irregularities also make it suitable for fractal analysis (Cross et.al, 1994).

In conclusion, under the conditions of this new technique of negative pressure injection, the silicone is able to penetrate to the level of the respiratory bronchioles and alveolar ducts without causing overdistention. Since the elastomer is introduced under a negative pressure, it is able to penetrate into noncollapsible, obstructed airways and even into the very small openings of ectatic mucous gland ducts and alveolar sacs of the proximal respiratory bronchioles. As a result, this method can be very useful in studying chronic obstructive airway diseases such as asthma, as well as for producing casts suitable for aerosol deposition modeling studies.

Euclidean and Fractal Analysis of the Airways

The method used in this study was very reliable in that there was 100% accuracy on ten repeated measures of a circle, square, Koch curve, and three lung casts, with less than 1.4% coefficient of variation between known fractal dimensions and the average of ten repeated measures. For all of the other tests of method accuracy (1-7), including position of the cast, lighting, and grid rotation, the coefficient of variation ranged from 0.25 – 3.77% (Table 5). T-tests were also used to analyze these tests, and the only two that showed any significant differences were the positioning test, where the airways were compared when placed close together, and then spread out on the cast ($p = 0.05$), as well as the trimming of the cast ($p = 0.01$). As a result of these differences, the casts were only analyzed with their airways spread apart as much as possible when photographed, and only trimmed casts were used in the overall analysis between groups.

The fractal dimension varied less then 2% between portions of the lung casts that were measured and compared to the whole lung cast. Similar results were found in a study by Kitaoka et.al, using a 3D reconstruction of a normal lung. In this study the fractal dimension was very similar between portions of the entire 3D reconstruction of the airways ($D = 1.74, 1.73, 1.74$), with each portion containing varying numbers of generations and different airway volumes (Kitaoka et.al, 1994). This has important implications for casting of asthmatic lungs due to the presence of mucous plugging which prevents complete cast filling of the

airways. Consequently, only portions of the airways can be measured. Yet, despite the possibility of having a cast with differing numbers of branching generations or volume density, the fractal dimension remains constant and gives an integrated description of the spatial distribution of the airways.

Euclidean geometry, on the other hand, is very dependent on branching generations in order to calculate branching patterns of the lung. These calculations revealed no significant differences between the asthmatics versus controls. In addition, the slopes of the graphs of (log) lengths and (log) diameters versus generation were not very different. This is an indication that perhaps euclidean geometry is not well suited to measure roughened surfaces or irregularities, which are often encountered in histological studies (Sanders et.al, 1993) and indeed which are seen in the lung casts of fatal and non-fatal asthmatics. This is also proven by the fact that the only euclidean measure which did show a difference was that of the variability (CV) in diameter in each generation in the FA group as compared to the NAC group (Table 4). Yet, despite these differences or irregularities in each generation, it could not measure an overall difference in the FA group as compared to the NAC group for all measures of branching pattern.

In addition, euclidean geometry must be performed under very precise conditions of magnification, where the measure would depend on the size of the measuring instrument. As the ruler becomes infinitesimally smaller, the value becomes infinitely longer. Indeed, this has been happening to measurements of

the lung. As they become more precise, alveolar surface area, for example, increases (Rigaut, 1984). At the subcellular level as well, the perimeter of organelles seem to continually grow, as more accurate measurements are made (Paumgartner et.al, 1980). As a result of this, euclidean values of length and diameter are becoming increasingly ambiguous as they are very dependent on the scale at which they are measured (McNamee, 1991). Fractal geometry, on the other hand, remains constant at all scales in a structure exhibiting self-similarity, and is therefore a more useful descriptor of these structures.

The fractal dimension of an object as it may be encountered in nature would lie between 1 and 2, the fractal dimension of a straight line being 1, and that of a two dimensional plane being 2. As the dimension increases between 1 and 2, so does the complexity and irregularity of the object. The fractal dimension of models of normal airways have been measured by other investigators with a mean values of 1.75 (Kitaoka et.al, 1994; Meakin, 1987), which is very similar to our value for normal airways (D = 1.775). The results in this study indicate that the airway branching patterns are fractal in nature, in that they are different from both 1 and 2, and that this value can change in the presence of disease. The FA group had a significantly lower fractal dimension (D = 1.66) in comparison to the NAC group (D = 1.775). The consequences of the airways being fractal are important from a physiological perspective in that due to their large area-volume ratio, they are well suited for the task of diffusional exchange (Mandelbrot, 1982). The decrease in fractal dimension in fatal asthmatics indicates a loss of

complexity and space filling capacity in these airways, and therefore a loss in their diffusion ability. This overall fractal dimension, though, may not be describing the entire structure of the airway casts as accurately as we may think.

The fractal dimension of the whole lung cast may only be an average of a number of fractal dimensions for numerous fractal structures found within the cast of the airways. It is well known that mathematical objects are created that possess a similar self-similarity pattern and complexity at all box sizes. Yet, in natural structures, such as the lung, objects are constrained by the materials that make them, as well as the space that limits them (Mandelbrot, 1983; Weibel, 1991). Consequently, natural structures can have different fractal dimensions at different scales of magnification. In the lung, there are different structures that are responsible for forming irregularities in the airways at different resolutions. As you increase resolution in the airways, you first see the branched tubular airways themselves, followed by the alveoli as pouches in these tube walls, followed by capillary imprints on the alveolar walls, and finally, the membrane folds over these capillary ridges (Weibel, 1991). The lung casts may not reveal such detailed structure as capillary imprints, but alveolar pouches are visible on these casts, even to the naked eye. In addition, structures such as longitudinal ridges, smooth muscle constrictions and mucous gland ducts are also visible. Therefore, it seems possible that more than one fractal dimension may result, representing multiple fractal structures present in the lung casts.

As a result, we divided the log-log curves plotted to calculate fractal dimension for each lung cast into three portions. Each portion corresponded to different ranges of box sizes. The first range of box sizes corresponded to 1-7 pixels in width (0.6 mm-4.2mm), the second range to 7-55 pixels (4.2mm-33mm), and the third range to 55-240 pixels (33mm-144mm). In terms of a normal lung cast the literature cites the mean diameter as 0.65 mm for an alveolar sac and 0.69 mm for an alveolar duct/respiratory bronchiole (Haefeli-Bleuer et.al, 1987). Therefore, in our study, a single pixel, being approximately 0.6 X 0.5mm, and having a area of 0.3mm^2 is able to include a structure such as an alveolus which has a mean diameter of 0.65 mm and a rough calculated circular area of 0.33 mm^2.

With this in mind, our study found three distinct fractal dimensions in both the FA and NFA group as compared to the NAC group. In the medium and large box sizes, there was a significant decrease in the fractal dimension in the FA group compared to NAC, which points to a loss of complexity in the structures falling within these areas of the lung cast. The greatest loss of complexity in FA is seen in the region measured by the largest boxes. When comparing the small box size fractal dimension between groups, there were no significant differences. This may indicate no change in this area of the lung, but it is possible that structural changes at this level require a system with higher resolution in order to detect changes.

There is also a chance that a higher resolution system may be able to detect more fractal structures in the lung than were revealed in this study. The remodeling that occurs in the airways in asthma may lead to the development of additional fractal structures within the lung, and this may be a unique characteristic of fatal asthmatics. The decrease in fractal dimension or complexity seen in fatal asthmatics has also been discovered in other disease processes. The normal heart beat, for example, is irregular to a degree, but becomes very regular preceding cardiac arrest (Goldberger et.al, 1990).

In conclusion we have shown that the fractal dimensions of asthmatic airways differ significantly from normal airways. By constrast, the euclidean description of geometry revealed no significant differences. Visually it is apparent that asthmatic airways are markedly abnormal. The fact that fractal geometry was able to measure a difference in asthmatic airways at all, whereas euclidean geometry could not, may indicate the benefits of using this type of a model. Consequently, this method should be considered when quantitating other biological structures with fractal features. Further work is required to determine which abnormal feature of the asthmatic airway is being detected by the fractal method.

Small Airway and Parenchymal Remodelling

Our findings show an increase in smooth muscle in all of the small airways (terminal bronchioles and respiratory bronchioles generations 1-3) in fatal asthma compared to non-asthma controls. These data are consistent with studies that included small airways, specifically terminal bronchioles (Carrol et.al, 1993; Kuwano et.al, 1993). Smoking was a confounding factor in these studies as it has been shown that the site of chronic inflammation and obstruction to airflow in heavy smokers is located in the terminal and respiratory bronchioles (Bosken et.al, 1990; Wright et.al, 1992). Consequently, only non-smokers were used in this study in order to better attribute abnormal airway structure to asthma alone.

Each subject was critically evaluated through the use of pathology grading in order to confirm the presence or absence of asthma. In many analyses the diagnosis of asthma has been based on information gathered by law enforcement officers or legal professionals, who may have little knowledge of respiratory disease. In addition, a simple review of a patients medications does not rule out chronic bronchitis, as similar medications are used for both conditions (Roche, 1998). Next of kin questionnaires also gave additional information as to asthmatic status.

In order to compare features between groups, it is important to match for airway size. Analysis revealed that airways of similar size were compared between groups, as well as between lobes and no terminal bronchioles larger than 1.2 mm in diameter were measured.

In this study we found that the interobserver and intraobserver variability were relatively low. In general, the intraobserver variability (with changing grid position) was greater than the interobserver variability (with changing grid position), which was greater than the intraobserver variability (with no change in grid position). It is important to note that the interobserver variability (16.1%) was well within the range of the intraobserver variability using different grid positions (20.7%), meaning that both observers were able to identify the same features. It is the coefficient of variation (CV = standard deviation / mean * 100%) that was used in this study as an index of variability. It is disproportionately affected by the magnitude of the numerator and denominator used in its calculations, and as a result, when the mean observed is a very small number the CV derived from this may not necessarily reflect the true variation in the measurement. For example, if the amount of smooth muscle measured in a normal airway by two different observers were 0 and 1, then the CV would be 141%. This suggests marked variation in this measure when in fact they are very similar. This is a recurrent issue when dealing with very small airways as in this study, due to the fact that the number of points landing on specific features, even at higher magnifications, are still very small. Consequently, there is a fairly large range of variations for specific features. Other studies have reported variability's within a range of 5%-13% for intraobserver error and 19%-21% for intraairway measurements (Azzawi, 1992), which is similar to the mean coefficients of variation in this study.

Other airway features including inflammation, basement membrane thickness, epithelial mucous cells and total wall thickness were all increased in asthmatic subjects. The FA airways showed a significantly increased overall thickness compared to NAC, in addition to a greater variability. Other studies have found significant differences in FA in these structures compared to controls (Carroll et.al, 1993; Kuwano et.al, 1993), yet these studies did not specifically examine small airways. It is important to consider that the measures in this study were taken using a stain specific for smooth muscle only, and that identification of other features may not be as accurate as measurements made using stains specific for these structures.

In addition to finding increased smooth muscle in the small airways of asthmatics compared to controls we also observed lobar differences. The overall amount of smooth muscle in the upper lobe was greater than the lower lobe for all types of airways. In RB2 and RB3, there was a significant difference between the upper and lower lobes in FA, which could suggest that there is a greater tendency for smooth muscle hypertrophy/hyperplasia in this area of the lung. This may be why there is more variability in the upper lobe smooth muscle thickness, as compared to the lower lobe. Studies using Technegas® by King et.al, in press, have looked at inhomogeneity between large and small airways in individuals with asthma, rather than differences in the upper and lower lobes. Perhaps future studies will reveal more detailed sites of airway closure in the

lung. This would better indicate if differences in smooth muscle content in the upper and lower lobe leads to regional heterogeneity in small airway closure.

It is not yet known if the increase in airway smooth muscle is accompanied by an increase in force generation (Seow et.al, 1998). Proliferation of smooth muscle cells can produce non-contractile cells in vitro (Halayko et.al, 1996). Yet, this proliferation will have an effect on the thickness of the airway wall, consequently leading to excessive airway narrowing. On the other hand, if the force of smooth muscle contraction is increased after hypertrophy/hyperplasia, there will be an even greater impact on airway narrowing (Seow et.al., 1998). Lambert and colleagues (Lambert et.al, 1993) attempted to determine how important an increase in smooth muscle could be as a contributor to increased airway narrowing compared to an increase in airway mucosal (wall) thickening. Results indicated that mucosal thickening could increase maximal airway narrowing by two to ten fold, whereas smooth muscle thickening has a potential to increase airway narrowing by two orders of magnitude. This indicates that an increase in smooth muscle, if it also increases in contractility, is the most important abnormality in asthma (Lambert et.al, 1993).

It is not completely understood if small airway smooth muscle even behaves in the same manner as in proximal airways. The innervation of small airways is sparse compared to large airways (Barnes, 1998). In addition, human small airways have a different distribution of receptors. For example, tachykinin receptors are prominent in the small airways, whereas vasoactive intestinal

peptide has little effect in this area (Carstairs et.al, 1986; Palmer et.al, 1986; Carstairs et.al, 1986; Frossard et.al, 1991). In addition, β2-Receptors, are not located beyond the terminal bronchioles (Carstairs et.al, 1985). This has very important implications when considering targeting drug therapies to this region of the lung, as β2-agonists may have little or no effect on respiratory bronchioles and parenchyma.

Recently with the realization of the importance of small airways, new inhalant devices are being developed that are able to target this area of the lung. The majority of the drugs being studied, though, are bronchodilators (β2-agonists), which are able to provide a rapid response (Mitchell et.al, 1987; Johnson et.al, 1989; Zainudin et.al, 1988; Zainudin et.al, 1993; Clay et.al, 1986). Consequently, anti-inflammatory therapy in this region of the lung has largely been ignored due to the difficulties in determining the optimal measure of response (Howarth, 1998).

Anti-inflammatory therapy in the small airways could be of great importance as airway smooth muscle has been found to produce numerous cytokines and chemokines, which are all involved in recruitment of inflammatory cells (Saunders et.al, 1997; John et.al, 1997; John et.al, 1998). As a result, the increase in smooth muscle in asthma could contribute to the chronic inflammation in asthma. Certain TH2-type cytokines are expressed at a higher level in the small airways and the parenchyma as compared to the large airways in asthmatics (Minshall et.al, 1998).

Studies have shown that the small airways are the main site of obstruction in asthma (Yanai et.al, 1992). Small airway histamine challenge showed a much greater response in asthmatics as compared to controls (Wagner et.al, 1998). Our data shows that the greatest overall % increase of smooth muscle in FA was found in the alveolar ducts, indicating structural alterations in the smallest airways in asthma. It is this alveolar duct smooth muscle, as well as the 'contractile interstitial cell' or myofibroblasts in the alveolar wall that are thought to play a part in regulation of ventilation and perfusion (Kapanci et.al, 1974; Stephens, 1987). The impact on gas exchange efficiency could be serious if the increased number of myofibroblasts in asthma also have an increased contractile ability.

The distribution of parenchymal smooth muscle in the alveolar ducts by group was similar to that of the other small airways measured (TB, RB1, RB2, RB3). There was an overall increase in smooth muscle in the upper lobe of all three groups compared to the lower lobes. This lobar effect was greatest in the FA group and points to an even greater involvement of the upper lobe parenchymal region in fatal asthma.

The increase in parenchymal myofibroblasts in the asthmatic groups was also greatest in the upper lobes with relative sparing of the lower lobe. We propose that the marked increase in parenchymal myofibroblasts in FA and NFA acts as a protective mechanism by tethering the small airways with greater force, thus preventing their collapse during changes in lung volume. Brown et.al, 1997,

found that with induced airway smooth muscle constriction, the parenchymal attachments could no longer distend the airways with increased lung volume. Hyperplasia of interstitial contractile cells thus might be an adaptive response that serves to limit small airway closure during an asthma attack. Studies done by Dolhnikoff et.al, 1998, have shown that lung parenchymal strips contract with acetylcholine challenge and that small airways are not required for this response. In addition, Ludwig et.al, found a parenchymal response to histamine-induced constriction in canines (Ludwig et.al., 1991), again proving that there are contractile elements in the parenchymal tissue.

In summary, the presence of significant increases of smooth muscle in the small airways, including the terminal bronchioles, respiratory bronchioles, generation 1-3 and the alveolar ducts indicate severe remodeling at this level in the lung. There also appears to be a significant difference in the distribution of this smooth muscle between the upper and lower lobes, with the most smooth muscle found in the upper lobes. The increase in myofibroblasts found in the parenchymal alveolar walls could act as a tethering device to distend the smaller airways; preventing them from collapsing due to constriction of airway smooth muscle. If our hypothesis is correct, then B-agonists or similar drugs will need to be developed that relax small airway smooth muscle and at the same time have a stimulatory effect on the contractile interstitial cells.

References

ATS (American Thoracic Society). The role of small airways in asthma: a review and key questions. Am J Respir Crit Care Med 1998; 157.

Azzawi M, Johnston PW, Majumdar S, Kay AB, Jeffery PK. T lymphocyte and activated eosinophils in airway mucosa in fatal asthma and cystic fibrosis. Am Rev Respir Dis 1992; 145: 1477-1482.

Barnes PJ. Pharmacology of airway smooth muscle. Am J Respir Crit Care Med 1998; 158: S123-S132.

Bosken CH, Wiggs BR, Pare PD, Hogg JC. Small airway dimensions in smokers with obstruction to airflow. Am Rev Respir Dis 1990; 142: 563-570.

Brown RH, Mitzner W, Bulut Y, Wagner EM. Effect of lung inflation in vivo on airways with smooth muscle tone or edema. J Appl Physiol 1997; 82(2): 491-499.

Brown PJ, Greville HW, Finucane KE. Asthma and irreversible airflow obstruction. Thorax 1984; 39: 131-136.

Bullen SS. Correlation of clinical and autopsy findings in 176 cases of asthma. J Allergy 1952; 23: 193-203.

Carroll N, Cooke C, James A. The distribution of eosinophils and lymphocytes in the large and small airways of asthmatics. Eur Respir J 1997; 10: 292-300.

Carroll N, Carello S, Cooke C, James A. Airway structure and inflammatory cells in fatal attacks of asthma. Eur Respir J 1996; 9: 709-715.

Carroll N, Elliot J, Morton A, James A. The structure of large and small airways in nonfatal and fatal asthma. Am Rev Respir Dis 1993; 147: 405-410.

Carstairs JR, Barnes PJ. Autoradiographic mapping of substance P receptors in lung. Eur J Pharmacol 1986; 127: 295-296.

Carstairs JR, Barnes PJ. Visualization of vasoactive intestinal peptide receptors in human and guinea pig lung. J Pharmacol Exp Ther 1986; 239: 249-255.

Carstairs JR, Nimmo AJ, Barnes RJ. Autoradiographic visualization of B-adrenoreceptor subtypes in human lung. Am Rev Respir Dis 1985; 132: 541-547.

Clay MM, Pavia D, Clarke SW. Effect of aerosol particle size on bronchodilatation with nebulised terbutaline in asthmatic subjects. Thorax 1986; 41: 364-368.

Cross SS, Cotton DWK, Underwood JCE. Measuring fractal dimensions, sensitivity to edge-processing functions. Analyt Quant Cytol Histol 1994; 16: 375-379.

Cutz E, Levison H, Cooper DM. Ultrastructure of airways in children with asthma. Histopathology 1978; 2: 407-421.

Despas PJ, Leroux M, Macklem PT. Site of airway obstruction in asthma as determined by measuring maximal expiratory flow breathing air and a helium-oxygen mixture. J Clin Invest 1972; 51(12): 3235-3243.

Dolhnikoff M, Morin J, Ludwig MS. Human lung parenchyma responds to contractile stimulation. Am J Respir Crit Care Med 1998; 158: 1607-1612.

Duncker H-R, Haufe E, Schluter O. Die darstellung der lungen und luftsacke der bogel, teil I. Praparator 1964; 10(1): 9-16.

Duncker H-R, Schluter O. Die darstellung der lungen und luftsacke der vogel, teil II. Praparator 1964; 10(2): 49-60.

Dunnill MS, Massarella GR, Anderson JA. A comparison of the quantitative anatomy of the bronchi in normal subjects, in status asthmaticus, in chronic bronchitis and in emphysema. Thorax 1969; 24: 176-179.

Dunnill MS. The pathology of asthma with special reference to changes in the bronchial mucosa. J Clin Pathol 1960; 13: 27-33.

Ebina M, Yaegashi H, Chiba R, Takahashi T, Motomiya M, Tanemura M. Hyperreactive site in the airway tree of asthmatic patients revealed by thickening of bronchial muscles. Am Rev Respir Dis 1990; 141: 1327-1332.

Editorial. Fractals and medicine. Lancet 1991; 338: 1425-1426.

Frank NR, Yoder RE. A method of making a flexible cast of the lung. J Appl Physiol 1966; 21: 1925-1926.

Frossard N, Barnes PJ. Effect of tachykinins on small human airways. Neuropeptides 1991; 19: 157-162.

Glynn AA, Michaels L. Bronchial biopsy in chronic bronchitis and asthma. Thorax 1960; 15: 142-153.

Goldberger AL, West BJ. Chaos and order in the human body. M.D. Computing 1992; 9(1): 25-34.

Goldberger AL, Rigney DR, West BJ. Choas and fractals in human physiology. Sci Am 1990; 262: 42-49.

Green FHY, Harji S, Butt JC, Li F, Ruff M, Karkhanis A, Hessel P, Perry S. Regional distribution of airway smooth muscle in asthma. 1995 ISAM International Congress, Hamilton, Ontario, May 1995.

Haefeli-Bleuer B, Weibel ER. Morphometry of the human pulmonary acinus. Anat Rec 1988; 220: 401-414.

Halayko AJ, Ma X, Stephens NL. Markers of airway smooth muscle cell phenotype. Am J Physiol 1996; 270: L1040-L1051.

Heard BE, Hossain S. Hyperplasia of bronchial smooth muscle in asthma. J Pathol 1972; 110: 319-331.

Hogg W, Brunton J, Kryger M, Brown R, Macklem PT. Gas diffusion across collateral channels. J Appl Physiol 1972; 33(5): 568-575.

Hoppin FG. Parenchymal mechanics and asthma. Chest 1995; 107(3): 140S-144S.

Horsfield K. Methods for casting airways. In: Models of disease: Microscopy and structural methods 1990; 265-277. Marcel Dekker, Inc, New York.

Horsfield K, Gordon WI, Kemp W, Phillips S. Growth of the bronchial tree in man. Thorax 1987; 42: 383-388.

Horsfield K, Relea FG, Cumming G. Diameter, length and branching ratios in the bronchial tree. Respir Phsyiol 1976; 26: 351-356.

Hossain S. Quantitative measurements of bronchial smooth muscl ein men with asthma. Am Rev Respir Dis 1973; 107: 99-109.

Houston JC, De Naavasquex S, Trounce JR. A clinical and pathological study of fatal cases of status asthmaticus. Thorax 1953; 8: 207-213.

Howarth PH. Small airways and asthma; An important therapeutic target? Am J Respir Crit Care Med 1998; 157: S173.

Ingram RH. Relationship among airway-parenchymal interactions, lung responsiveness, and inflammation in asthma. Chest 1995; 107(suppl): 148S-151S.

James AL, Pare PD, Hogg JC. The mechanics of airway narrowing in asthma. Am Rev Respir Dis 1989; 139: 242-246.

Jeffery PK, Wardlaw AJ, Nelson FC, collins JV, Kay AB. Bronchial biopsies in asthma: an ultrastructural, quantitative study and correlation with hyperreactivity. Am Rev Respir Dis 1989; 140: 1745-1753.

John M, Jose PJ, Lim S, Saunders MA, Barnes PJ, Mitchell JA, Belvisi MG, Chung KF. Expression and release of interleukin-8 by human airway smooth muscle cells: inhibition by Th2 cytokines and corticosteroids. Am J Respir Cell Mol Biol 1998; 18: 84-90.

John M, Hirst SJ, Jose P, Robichaud A, Wilt C, Twort C, Berkman N, Barnes PJ, Chung KF. Human airway smooth muscle cells express and release RANTES in response to Th1 cytokines: regulation by Th2 cytokines. J Immunol 1997; 158: 1841-1847.

Johnson MA, Newman SP, Bloom N, Talaee N, Clarke SW. Delivery of albuterol and ipratropium bromide from two nebuliser systems in chronic stable asthma. Chest 1989; 96; 6-10.

Kapanci Y, Assimacopoulos A, Irle C, Kwahlen A, Gabbiani G. "Contractile interstitial cells" in pulmonary alveolar septa: a possible regulator of ventilation / perfusion ratio? Ultrastractural, immunofluorescence and in vitro studies. J Cell Biol 1974; 60: 375-392.

King G, Eberl S, Salome CM, Young IH, Woolcock AJ. Differences in airway closure between normals and asthmatics measured by SPECT and Technegas. Am J Respir Crit Care Med, in press.

Kitaoka H, Takahashi T. Relationship between the branching pattern of airways and the spatial arrangement of pulmonary acini- A re-examination from a fractal point of view. In: Fractals in Biology and Medicine. Editors: Nonnenmacher TF, Losa GA, Weibel ER. 1994, pp. 116-131. Birkhauser Verlag, Basel, Switzerland.

Kuwano K, Bosken CH, Pare PD, Bai TR, Wiggs BR, Hogg JC. Small airways dimensions in asthma and in chronic obstructive pulmonary disease. Am Rev Respir Dis 1993; 148: 1220-1225.

Lambert RK, Wiggs BR, Kuwano K, Hogg JC, Pare PD. Functional significance of increased airway smooth muscle in asthma and COPD. J Appl Physiol 1993; 74: 2771-2781.

Ludwig MS, Robatto FM, Sly PD, Browman M, Bates JHT, Romero PV. Histamine-induced constriction of canine peripheral lung: an airway or tissue response? J Appl Physiol 1991; 71(1): 287-293.

Ludwig MS, Romero PV, Bates JHT. A comparison of the dose-response behavior of canine airways and parenchyma. J Appl Physiol 1989; 67: 1220-1225.

Macklem PT. The physiology of small airways. Am J Resp Crit Care Med 1998; 157: S181-S183.

Macklem PTD, Proctor DF, Hogg JC. The stability of peripheral airways. Respir Physiol 1970; 8(2): 191-203.

Mandelbrot, B. The fractal geometry of nature. 1983. W.H. Freeman and Company, New York.

McFadden ER, Lyons HA. Airway resistance and uneven ventilation in bronchial asthma. J Appl Physiol 1968; 25: 365-370.

McNamee JE. Fractal perspectives in pulmonary physiology. J Appl Physiol 1991; 71(1): 1-8.

Meakin P. Diffusion-limited cluster-cluster aggregation. In: Phase Transitions and Critical Phenomena. Editors: Domb C, Lebowitz JL. 1987; pp. 432-439. Academic Press, New York.

Messer J, Peters GA, Bennet WA. Cause of death and pathological findings in 304 cases of bronchial asthma. Dis Chest 1960; 38: 616-24.

Minshall EM, Hogg JC, Hamid QA. Cytokine mRNA expression in asthma is not restricted to the large airways. J Allergy Clin Immunol 1998; 101(3): 386-390.

Mitchell DM, Soloman MA, Tolfree EJ, Short M, Spiro SG. Effect of particle size of bronchodilator aerosols on lung distribution and pulmonary function in patients with chronic asthma. Thorax 1987; 42: 457-461.

Moreno RH, Hogg JC, Pare PD. Mechanics of airway narrowing. Am Rev Respir Dis 1986; 133: 1171-1180.

Nelson TR. Fractals, physiologic complexity, scaling, and opportunities for imaging. Invest Radiol 1990; 25: 1140-1148.

Nettum JA. Bronchoalveolar casting using formalin fixed canine lungs and a low viscosity silicone rubber. Anat Rec 1993; 235: 408-410.

Palmer JBD, Cuss FMC, Barnes PJ. VIP and PHM and their role in nonadrenergic inhibitory responses in isolated human airways. J Appl Physiol 1986; 61: 1322-1328.

Patel PD, Mukai D, Wilson AF. Dose-response effects of two sizes of monodispersed isoproterenol in mild asthma. Am Rev Respir Dis 1990; 141: 357-360.

Paumgartner D, Losa G, Weibel ER. Resolution effect on the stereological estimation of surface and volume and its interpretation in terms of fractal dimensions. J Microsc 1981; 121: 51-63.

Perry SF, Purohit AM, Boser S, Mitchell I, Green FHY. Bronchial casts of human lungs using negative pressure injection. Experimental Lung Research 1999; in press.

Phalen RF, Yeh H-C, Rabbe OG, Velasquez DH. Casting the lungs in situ. Anat Rec 1973; 177: 255-264.

Phillips C, Kaye S, Schroter R. A diameter-based reconstruction of the branching pattern of the human bronchial tree. Part I. Description and application. Respir Physiol 1994; 98: 193-217.

Phillips C, Kaye S, Schroter R. A diameter-based reconstruction of the branching pattern of the human bronchial tree. Part II. Mathematical formulation. Respir Physiol 1994; 98: 219-226.

Redington AE, Howarth PH. Airway wall remodelling in asthma. Thorax 1997; 52(4): 310-312.

Rigaut JP. An empirical formulation relating boundary lengths to resolution in specimens showing "non-ideally fractal" dimensions. J Microsc 1984; 133: 41-54.

Roche WR. Inflammatory and structural changes in the small airways in bronchial asthma. Am J Respir Crit Care Med 1998; 157: S191-S194.

Roche, et.al. Subepithelial fibrosis in the bronchi of asthmatics. Lancet 1989; 1: 520-524.

Saetta M, Di Stefano A, Rosina C, Thiene G, Fabbri LM. Quantitatiive structural analysis of peripheral airways and arteries in sudden fatal asthma. Am Rev Respir Dis 1991; 143: 138-143.

Sakae RS, Martins MA, Criado PMP, Zin WA, Saldiva PHN. In vivo evaluation of airway and pulmonary tissue response to inhaled methacholine in the rat. J Appl Physiol 1997; 82(5): 1479-1487.

Salvato G. Some histological changes in chronic bronchitis and asthma. Thorax 1968; 23: 168-172.

Sanders H, Crocker J. A simple technique for the measurement of fractal dimensions in histopathological specimens. J Pathol 1993; 169: 383-385.

Saunders MA, Mitchell JA, Seldon PM, Barnes PJ, Giembycz MA, Belvisi MG. Release of granulocyt-macrophage colony-simulating factor by human cultured airway smooth muscle cells; suppression by dexamethasone. Br J Pharmacol 1997; 120: 545-546.

Schlesinger RB, MdFadden LA. Comparative morphometry of the upper bronchial tree in six mammalian species. The Anatomical Record 1981; 199: 99-108.

Seow CH, Schellenberg R, Pare PD. Structural and functional changes in the airway smooth muscle of asthmatic subjects. Am J Respir Crit Care Med 1998; 158: S179-S186.

Smith BJ, Holladay SD, Hudson LC. A simplified method of casting the macroscopic airways of lungs. Acta Anat 1990; 137: 109-113.

Stephens NL. Airway smooth muscle. Am Rev Respir Dis 1987; 135:960-975.

Takizawa T, Thurlbeck WM. Muscle and mucous size in the major bronchi of patheints with chronic bronchitis, asthma, and asthmatic bronchitis. American Review of Respiratory Disease 1971; 104: 331-336.

Tough SC, Green FH, Paul JE, Wigle DT, Butt JC. Sudden death from asthma in 108 children and young adults. J Asthma 1996; 33:3, 179-188.

Unger L. Pathology of bronchial asthma. South Med J. 1945; 38: 513-522.

Wagner EM, Bleecker ER, Permutt S, Liu MC. Direct assessment of small airways reactivity in human subjects. Am J Respir Crit Care Med 1998; 157(2): 447-452.

Wagner EM, Liu MC, Weinmann GG, Permutt S, Bleecker ER. Peripheral lung resistance in normal and asthmatic subjects. Am Rev Respir Dis 1990; 141: 584-588.

Wang PM, Kraman SS. Construction of a flexible airway model for teaching. Anat Rec 1988; 221: 780-781.

Weibel ER. Fractal geometry: a design principle for living organisms. Am J Physiol 1991; 261 (Lung Cell Mol Physiol 5): L361-L369.

Weibel ER. Morphometry of the human lung. 1963. Heidelberg, Springer-Verlag; New York, Academic Press.

Weibel ER, Gomez DM. Architecture of the human lung. Science 1962; 137: 577-585.

Woolcock AJ. Effects of drugs on small airways. Am J Respir Crit Care Med 1998; 157: S203-S207.

Woolcock AJ, Peat JK. Evidence for the increase in asthma worldwide. Ciba Found Symp. 1997; 206: 122-134; discussion 134-139, 157-159.

Wright JL, Cagle P, Churg A, Colby TV, Myers J. State of the art: diseases of the small airways. Am Rev Respir Dis 1992; 146: 240-262.

Yanai M, Sekizawa K, Ohrui T, Sasaki H, Takishima T. Site of airway obstruction in pulmonary disease: direct measurement of intrabronchial pressure. J Appl Physiol 1992; 72(3); 1016-1023.

Yeh HC, Schum GM. Models of human lung airways and their application to inhaled particle deposition. Bull Math Biol 1980; 42: 461-480.

Yeh HC, Schum GM, Duggan MT. Anatomic models of the tracheobronchial and pulmonary regions of the rat. Anat Rec 1979; 195: 483-492.

Zainudin BMZ, Biddiscombe M, Tolfree SEJ, Short M, Spiro SG. Comparison of bronchodilator response and deposition patterns of salbutamol inhaled from a pressurised aerosol metered dose inhaler, as a dry powder and as a nebulised solution. Thorax 1993; 45: 469-473.

Zainudin BMZ, Tolfree SEJ, Short M, Spiro SG. Influence of breathing pattern on lung deposition and bronchodilator response to nebulised salbutamol in patients with stable asthma. Thorax 1988; 43: 987-991.